Modelling of the contact mechanics of thin films using analytical linear elastic approaches

Von der Fakultät für Naturwissenschaften der Technischen Universität Chemnitz genehmigte

Habilitationsschrift

zur Erlangung des akademischen Grades

doctor rerum naturalium habilitatus

(Dr. rer. nat. habil.)

von

Dr. Norbert Schwarzer

geboren am 7. Januar 1966 in Eilenburg

Preface

This habilitation thesis collects and summarizes original research on mechanical contact for the case of layered materials, which the author performed in the years 1998 to 2002.

The thesis consists of two parts. The first part is intended to give an introduction and figurative understanding of those parts of the original research being collected in the second part. In addition it gives extensions and applications of the latter in order to demonstrate the principle potential of these approaches. It is organized as follows. First, in the introduction part a rough overview of the "state of the art" concerning the external and internal mechanical loading of layered materials is given. Then a manly figurative or verbal presentation of the theoretical approaches crucial for this work is presented. Here the method of "image loads" for the modelling of mechanical contact problems for layered materials and two extensions of this method are presented together with an approach allowing the complete three dimensional modelling of intrinsic stresses for coating-substrate systems. In chapter three a selection of examples for the application of the above approaches is given. Finally, chapter 4 is devoted to a short summary and outlook.

The second part of the thesis is a selection of reprints of original publications in refereed journals, which are crucial for this work. All references available there will be addressed with the capital letter "C" before their number throughout this thesis. To give an example, the paper being addressed with [C2] can be found as the second paper within the reprint-selection-part of this work. All these publications might differ in few details from the journal-printed versions and are only intended to deliver a convenient insight into the content of the paper. However, the reader is referred to the original publication. Only the most important papers containing some of the cumbersome and long evaluations necessary for this work are made available as reprints. So the number of reprints was restricted to three. However during this Habilitation time, the author has also published 6 yet unrefereed contributions as well as 14 further refereed articles, which are treating additional applications or extensions of the reprints. But because the immense volume of this work and its relatively broad field of possible applications these publications have not been reproduced here. In addition there are five software and computer video packages, which resulted directly from this work. Their references are listed after the table of contents.

The work presented here would have been impossible without the contribution of many friends and colleagues. I am thus grateful to Prof. F. Richter and Prof. G. Hecht from the Technical University of Chemnitz for their continuing support and the uncountable number of interesting and helpful discussions. I am furthermore greatly indebted to Prof. M. Swain from

the University of Sydney and Prof. G. Pharr from the University of Tennessee who both happened to be greats host during my stays in their institutes and who managed to provide a fruitful mixture of guidance and motivation for my work. Particular thanks are given to Dr. T. Chudoba from the company ASMEC who not only developed an easy to use software package using some of my results but also achieved amazingly impressive experimental results in applying my theoretical approaches that in some cases even the author would never have imagined as being possible. The record in measuring the Young's modulus of an only 4.3nm thin coating using spherical indentation definitively belongs to this kind of positive surprises. Over the course of this work, many other colleagues have contributed ideas and suggestions for which I am thankful.

Contents

Refereed papers:

T. Chudoba, N. Schwarzer, F. Richter: ”New Possibilities of Mechanical Surface Characterization with Spherical Indenters by Comparison of Experimental and Theoretical Results”, San Diego Conference ICMCTF 1999, Metallurgical Coatings and Thin Films Vol. II, Elsevier, pp. 284-289 and Thin Solid Films 355-356 (1999), 284-289

T. Chudoba, N. Schwarzer, F. Richter: "Determination of Elastic Properties of Thin Films by Indentation Measurements with a Spherical Indenter", J. of Surface & Coatings Technology 127 (2000) 9-17

N. Schwarzer: "Coating Design due to Analytical Modelling of Mechanical Contact Problems on Multilayer Systems", proceedings of the ICMCTF 2000, San Diego, USA, April 2000, 397 - 402, in addition: Surface and Coatings Technology 133 –134 (2000) 397 - 402

T. Chdoba, N. Schwarzer, F. Richter, U. Beck: "Determination of mechanical film properties of a bilayer system due to elastic indentation measurements with a spherical indenter", proceedings of the ICMCTF 2000, San Diego, USA, April 2000, 366 – 372, in addition: Thin Solid Films 377 – 378 (2000) 366 - 372

N. Schwarzer, D. Heuer, Th. Chudoba: ”Application of modern approaches in mechanics to adhesion problems in dentistry”, proceedings of the EURADH 2000, Lyon, France, September 2000, Edition SFV, 19 rue du Renard, 75004 Paris, 377-382

N. Schwarzer, F. Richter: ”Adhesion Modelling in Layered Materials Using Analytical Solutions of Crack Problems”, proceedings of the EURADH 2000, Lyon, France, September 2000, Edition SFV, 19 rue du Renard, 75004 Paris, 586-591

F. Richter, T. Chudoba, N. Schwarzer, G. Hecht: “Neue Möglichkeiten zur Charakterisierung dünner Schichten mit Indentermethoden - Novel Possibilities for Thin Film Characterisation Using Indentation Methods”, Materialwissenschaften und Werkstofftechnik 32 (2001) 621-627

O. Wändstrand, N. Schwarzer, T. Chudoba, Å. Kassman-Rudiphi: ”Load-carrying capacitity of Ni-plated media in spherical indentation: experimental and theoretical results”, Surface Engineering Vol. 18 (2002) No. 2, 98 - 104

T. Chudoba, N. Schwarzer, F. Richter: ”Steps towards a mechanical modeling of layered systems”, Surface and Coatings Technology 154 (2002) 140 - 151

INDICOAT (1999): “Determination of hardness and modulus of thin films and coatings by nanoindentation”, final report (European community, project no. SMT4-CT98-2249), May 2001, ISSN 1473-2734

V. Linss, N. Schwarzer, I. Hermann, U. Kreissig, F. Richter: “The B-C-N triangle - a suitable system for the production of thin films with high load carrying capacity”, proceedings of the ICMCTF 2002, San Diego, USA, April/Mai 2002

A. Faulkner, K.C. Tang, N. Schwarzer, R.D. Arnell, F. Richter: "Comparison between an Elastic-Perfectly Plastic FE Model and a Purely Elastic Analytical Model for a Spherical Indenter on a Layered Substrate", Thin Solid Films 300 (1997) 177

N. Schwarzer, I. Hermann, T. Chudoba, F. Richter: ”Contact Modelling in the Vicinity of an Edge”, Surface and Coatings Technology 146-147 (2001) 371-377

N. Schwarzer, F. Richter: "A Simple Biaxial Bending Technique for Coated Materials - Theory and Application", proceedings to the workshop "Mechanical Behaviour of PVD Coated Materials", 13.-17.10.1997 in Holzhau, Germany, edited by H. Oettel, S. Hogmark, J. v. Stebut, published in "Freiburger Forschungshefte", B 287, 1998, pp. 93 - 100

N. Schwarzer, F. Richter, B. Michel: ”Penny shaped interface crack under uniform pressure and shear loading”, in ”Modeling and Simulation Based Engineering”, Vol. II, Ed. S. N. Atluri, P. E. O'Donoghue, Atlanta, USA (1998), Tech Science Press

Not, respectively not yet refereed papers:

N. Schwarzer, F. Richter: Short note: On the determination of film stress from substrate bending using Stoney´s formula, Thin Solid Films, submitted January 2002

I. Hermann, T. Chudoba, V. Linss, N. Schwarzer, F. Richter: „Improving the load carrying capacity of a layered system due to the design of a film stack with an optimized modulus variation”, poster presentation at the ICMCTF 2002, San Diego, USA, April/Mai 2002

F. Richter, N. Schwarzer, V. Linss, I. Hermann, T. Chudoba: “Depth-depending Young´s modulus of thin films for increased load carrying capacity”, oral presentation at the ICMCTF 2002, San Diego, USA, April/Mai 2002

N. Schwarzer: „About the theory of thin coated plates”, published in the internet at: http://archiv.tu-chemnitz.de/pub/2002/0006/index.html

N. Schwarzer: “Arbitrary load distribution on inhomogeneous isotropic half spaces”, Int. J. of Solids and Structures, submitted February 2003

N. Schwarzer: “Justification for the use of the Hertzian load model on layered materials”, J. of Surface & Coatings Technology, submitted October 2002

Software- and tutor-packages resulted from this work:

T. Chudoba and N. Schwarzer: ELASTICA, software demonstration package, available in the internet at: http://www.asmec.de

P. Heuer, N. Schwarzer, T. Chudoba: „Avoiding of plastic deformation – an ELASTICA presentation“, computer video, published in the internet at: http://www.tu-chemnitz.de/physik/PHFK/abstracts/mechanic

P. Heuer, N. Schwarzer: „Glass protection by coatings – an ELASTICA presentation“, computer video (15 minutes), available from http://www.asmec.de

P. Heuer, N. Schwarzer: „Steel protection by coatings – an ELASTICA presentation“, computer video (20 minutes), available from http://www.asmec.de

P. Heuer, N. Schwarzer: „Learning Contact Mechanics by Doing – a html-Help-Document for the Software Package ELASTICA“, available from http://www.asmec.de

Part I

To the modelling of the external and internal mechanical laoding of layered materials

1. Introduction

The utilisation of thin films in numerous different fields of practical daily life has dramatically increased in the recent years. A considerable number of companies is providing a variety of coatings for such different fields like e.g. the automotive and aircraft industry, high energy applications and even medical devices and implants. The spectrum of goals being pursued with the trend of utilisation thin films appears to be amazingly broad. So plans for example the truck building industry to increase the use of coatings in order to obtain improvements in the following areas [1]:

- power increase,
- mileage increase from 1,2 up to 2Mkm,
- weight reduction,
- emission reduction.

But looking behind the curtains and asking for the technical problems one has to solve to contribute to the above mentioned points one gets the following answers [1]:

- increasing of the load bearing resistance,
- reduction of friction (thus reduction of internal losses),
- wear reduction,
- higher service temperatures
- solving heat transfer problems.

The first three of the technical problems are directly related to the field of mechanical contact problems. So one easily comes to the conclusion that product improvement using thin films needs in quite a lot practical applications considerations of the problem of mechanical loads on layered materials. And this does not hold for the automotive industry only. There are many other examples of applications of thin films where a mechanical contact of the coated body with a counterpart is formed and the mechanical interaction is unavoidable (e.g.: thin films intended to provide good electrical contact in switches and plugs, coated tools like drills and punches, or optical thin films on surfaces which are additionally exposed to mechanical contact). In all these cases, the lifetime and reliability of the coated item is determined to a certain extent (and in many cases completely) by the mechanical interaction (Figure 1). In addition the intrinsic stresses (or more accurate the intrinsic elastic field) remaining from the deposition process have to be taken into account. In this context, knowledge of stress and strain fields arising in the film-substrate system due to the mechanical contact and the

intrinsic field would be very useful, for instance for failure analysis or for the optimum design of film systems with improved durability.

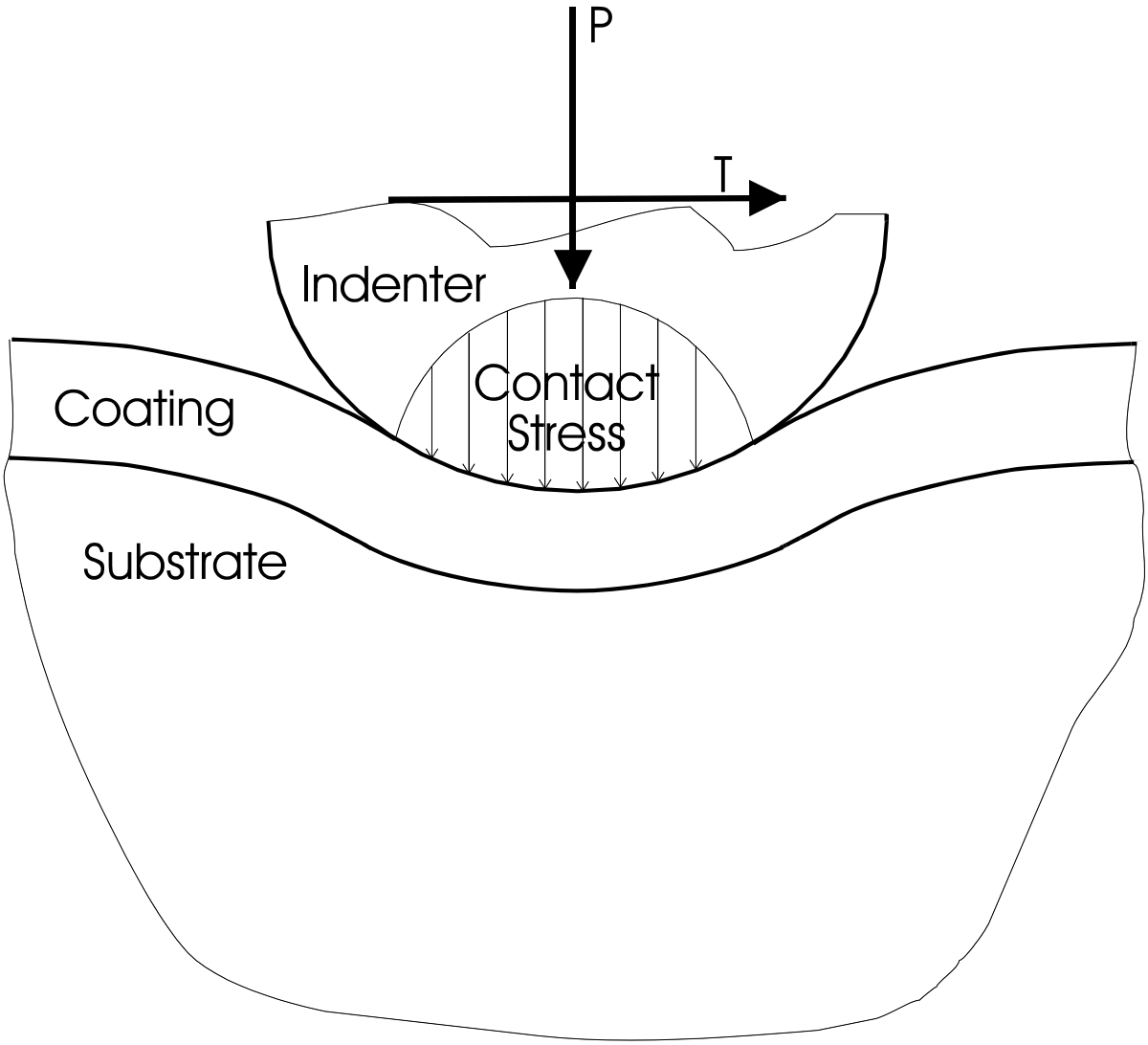

Figure 1: **Schematic figure for the contact between a coated body and an indenter, which acts with a normal P and a tangential force component T.**

In this work the author presents simulation procedures (mathematical models) with the aim to help determining and analysing the mechanical properties of coating-substrate-systems and finding an "optimal" coating structure which should protect the compound from inelastic deformation under a given range of load conditions. Such procedures may be used as a tool to minimise the search field for experimental work. For this purpose one would need a mathematical model which allows one to calculate the complete elastic field with all its displacement and stress components within a multilayer film on a substrate under given mechanical loading and intrinsic stress conditions.

1.1. External mechanical loading of layered materials – "state of the art"

State of the art does not mean that the author here gives a comprehensive overview of all publications and works being related to this topic but only the most important ones for the later considerations within this work will be mentioned and discussed.

Several approaches from other authors are known which investigate the above mentioned problem of loads on layered materials with integral transform, perturbation or semi-empirical methods. Doerner and Nix [2] have published an approach which deals with effective material constants for the Young's modulus and the Poisson's ratio of coating and film (single layer) to describe the elastic behaviour of the compound. The resulting effective constants are suitable combinations of the material parameters of both constituents. Using integral transform methods, Gupta and Wallowit [3] have found a solution for the contact problem of two cylinders in contact, where one of them is assumed to be coated with an elastic layer. Later, three dimensional problems were treated utilising this method (see e.g. the paper of Stone [4] where both completely and transversely isotropic materials were considered). The advantage of the integral transform method lays in the relatively high number of layers which can be treated, while the necessity of the integral transformation may be taken as a disadvantage. Alternatively, perturbation methods to solve contact problems for layered materials were used for example by Gao, Chiu and Lee [5] as well as Gao and Wu [6]. Here, the coating was taken as the perturbation of the substrate in a first approximation. Looking closely at the evaluation in the papers [5] and [6] one could get the impression that the "perturbation" as claimed by the authors is very similar to the first step of the image-load-method as proposed here. That's why the author would call the method in [5] and [6] an incomplete image-load rather than a perturbation-method. At least it would be mathematically equivalent. A complete analytical approach for contact problems with materials of varying Young's modulus that may be expressed as $E=E_m*z^m$ (E_m=constant, z – co-ordinate in the direction of the axis of indentation and m an arbitrary parameter in the range $0\leq m<1$) was given by Popov [7] (see in addition [8], pp. 182). The method applied there is based on the results of Rostovtsev [9]. Unfortunately, it cannot be extended to describe multilayer structures as proposed here. Finally, there have been numerous numerical solutions to the contact problem using the finite element method and the boundary element method (see e.g. [10-12]). These techniques do have some advantages for treating the nonlinear elastic-plastic problem.

In this work, the final solution of any contact problem for the layered half space will be developed from that of the homogeneous half-space by an uncompromising use of the method of image charges of potential theory [C1], well known from electrodynamics. This method

provides complete analytical solutions that can be expressed in elementary functions and closed form, as long as the solution of the corresponding contact problem for the homogenous half space is known and elementary. Many such "homogeneous" solutions for various contact problems have been published in recent years (e.g. [13 – 20]). The main advantage of the method described here is the opportunity to find the complete analytical solution of the problem of a load acting on a layered body by extending the corresponding "homogeneous" solution utilising a straightforward mathematical procedure. Meanwhile various experimental proofs and applications of the method have been published [22-28]. In addition the reader can find an easy to use software package, which allows to calculate the complete elastic field for different load problems on layered half spaces [21]. The disadvantage is the relatively low number of layers (<6) which can be treated within an acceptable calculation time. While the evaluation of the elastic field of a one layer contact problem using ELASTICA needs only a few seconds on a usual PC (CPU: Pentium 450MHz, 256MB RAM) a 3-layer system already requires about 1 minute. Here, only solutions for the Hertzian contact problem using circular [16] and elliptical [20] contact shapes will be used for the contact modelling as they are of practical relevance. In addition in order to treat more complex contact shapes the superposition of load dots is applied.

1.2. Internal mechanical loading of layered materials – "state of the art"

Intrinsic stresses within thin film-substrate compounds are mainly caused by atomic mismatch at the interface between substrate and coating, thermal stresses resulting from the difference between deposition and room or service temperature and other effects like for example ion bombardment coming from the deposition process itself. Apart from finite element calculations dealing with the problem of intrinsic stresses (see e.g. [32]) and very few somewhat more general approaches (e.g. [33], [34]) the problem of intrinsic stresses has mostly been considered using the so called "thin plate simplification", which neglects all stress components pointing in the direction of the plates normal axis. A plate-like form of the film-substrate-compound means that the total thickness, h_{tot}, is constant and small in comparison to its lateral dimensions. So, if one takes for example the z-axis as the normal axis of the coating-substrate-system one has to set:

$$\sigma_{xz} = \sigma_{yz} = \sigma_{zz} = 0\,. \tag{1}$$

A first consideration of the effect of intrinsic stresses came from STONEY [35] who has published a simple formula describing the bending of a coated bar in dependence on the intrinsic stress within the film. This internal stress in the film on a bar or also on a plate-like

substrate causes the film-substrate compound to warp until mechanical equilibrium is reached, i.e. until both net force and bending moment are zero. From the curvature of the elastically deformed coated substrate the average film stress, σ^f, can be calculated. This method is very popular since the curvature of the bent substrate can easily be measured and no information on the elastic parameters of the film material is necessary. As substrate material often silicon is used since its mechanical properties are well defined and well known. If necessary, small beams (cantilevers) can be made of single-crystal silicon using micromechanical technology [36] which allows to apply the method also to very thin films. When the thickness of the film, h_f, is small compared to that of the substrate, the above mentioned simple formula of STONEY [35] holds. It can be given as follows:

$$\sigma_{zz}^{f} \approx -E_s \frac{h_s^2}{6h_f} \frac{1}{R}, \tag{2}$$

with R - radius of curvature and E_s - YOUNG´s modulus of the substrate. In those cases, where the film is not thin compared to the substrate this formula has to be modified [47]. In its original form, the STONEY formula is valid only for a narrow coated beam. The index "zz" denotes the stress component in direction of the length side of the beam which we chose to be along the z-axis.

When measuring thin films deposited on plate-like substrates, the corresponding biaxial deformation has to be taken into account [37] by using the biaxial modulus, $E_{b,s}$, of the substrate rather than the YOUNG´s modulus alone:

$$E_s \rightarrow E_{b,s} = E_s / (1 - \nu_s) \tag{3}$$

with ν_s - POISSON´s ratio of the substrate. This corresponds to the cap or bowl-like deformation of a circular substrate under the influence of intrinsic film stress. Since many solid materials have POISSON´s ratios between 0.2 and 0.3, using the biaxial modulus instead of E_s yields a modification in the calculated σ_f values by 25 to 43 %.

For practical reasons, instead of a circular substrate often an elongated rectangular substrate is used, either as a "macroscopic" strip having a length in the centimetre range, or as a micromechanical cantilever typically few 100 µm in length. It was argued [38] that such a substrate rather curls into an approximately cylindrical shape instead of bowl or cap-like deformation. Therefore, in STONEY´s formula E_s should be replaced in this case by the plate modulus, $E_{p,s}$, rather than by the bipolar modulus of the substrate:

$$E_s \rightarrow E_{p,s} = E_s / (1 - \nu_s^2). \tag{4}$$

In the meantime, this apparently plausible argumentation was repeatedly followed in the literature [39]. Considering transverse contraction in this manner modifies σ^f only by 4 to 9 % when typical ν_s values between 0.2 and 0.3 are assumed. But it has been shown in [40] that in the case of plate-like coating-substrate-compounds the assumption of a cylindrical bending shape as outlined in [38] is wrong. Provided that

- $h_s << b$ ($b<a$ with a and b denoting the two sides of the rectangular substrate) , i.e. provided the plate approximation (1) is valid and
- the film thickness h_f is small compared to the substrate thickness h_s, thereby assuring a constant film stress over the whole substrate,

the coated substrate gets a constant curvature everywhere on its surface. In particular, even for an elongated, strip-like substrate a cap or bowl-shaped deformation is formed, as far as the smaller side of the strip is large in comparison to the substrate thickness. This is the case for many substrates, both macroscopic strips and micromechanical cantilevers used in laboratories for stress measurement. Then, the YOUNG´s modulus in STONEY´s equation (2) has to be replaced by the biaxial modulus rather than by the plate modulus. Otherwise, the stress values determined would be too big by a factor of

$$(1 - \nu_s^2) / (1 - \nu_s) = 1 + \nu_s,$$

i.e. by 20...30 % for typical ν_s values of 0.2...0.3. This insight is of great importance for the further considerations within this work. Because here the effect of intrinsic stresses on the resulting stress fields of external loads shall be discussed and consequently only correct assumptions for the intrinsic stresses can guarantee sufficiently correct resulting elastic fields of the combined internal and external loading. At the end of paragraph 2.2 of this work we will discuss the possibility of a complete analytical prove to the argumentation brought in [40] applying the existing mathematical approaches.

An investigation of the boundary conditions for the validity of the plate-approximation as well as a very useful collection of formulae concerning its application in the case of layered materials can be found in [47].

2. About the Theory

In order to avoid cumbersome and boring evaluations within this more general survey all complex derivations absolutely necessary to repeat the calculations leading to the results presented here are embedded in separate papers specialised in the topic of question. These

papers are either mentioned in the reference part or – in the case of crucial contributions – printed in full in the reprint-part. Here we will therefore concentrate on a more "verbal understanding" of the models and methods developed and used by the author. Only so far unpublished results need to be elaborated in more detail.

2.1. Arbitrary load distribution on inhomogeneous half spaces

This problem can easily be treated by the method of image loads. In addition to the already mentioned paper concerning the usage of this method in order to solve mechanical contact problems in layered elastic spaces [C1] the interested reader may find useful procedures and results in the following publications [C2, C3, 22 - 31]. The mathematical principle is rather simple: All interfaces and the surface will be treated as boundaries at which special conditions for the elastic field have to be satisfied. Starting with the known "homogeneous" solution for the load conditions in question, one has to add potential functions to the existing solution which will satisfy the additional boundary conditions at the interfaces. One may readily illustrate the resulting structure of the final solution as follows. We consider a layered or "coated" half space and investigate the elastic field within the area $0 \leq |z| < h$ (here, $z=-h$: position of the interface). An observer in this zone may consider the resulting elastic field as a product of an arbitrary contact on a non-homogeneous (in this case layered) half space. Alternatively, one may consider the complete space as homogeneous and interpret the sets of additional potentials as additional loads which act from the positions $z=2h$, $z=-2h$, $z=4h$, $z=-4h$..., and so on (Figure 2).

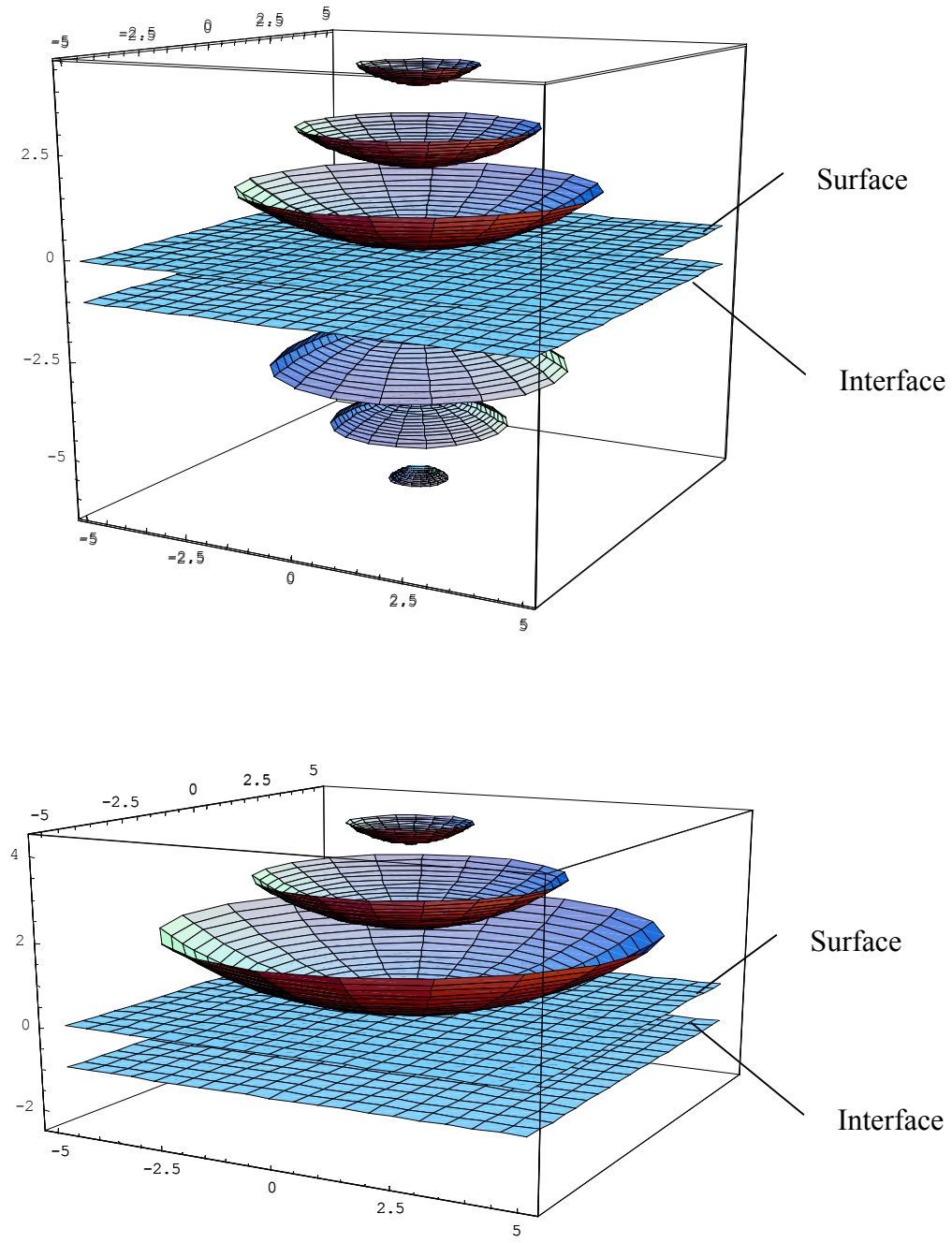

Figure 2: **Figurative presentation of the mathematical method used in this paper for a hypothetical contact (see text). Units in directions x, y and z are normalised to the thickness of the coating h.**

In the same manner the observer would interpret the elastic field in the $|z|\geq h$ zone as one of a homogeneous infinite space with the original contact force at $z=0$ and additional loads from the positions $z=2h$, $z=4h$, $z=6h$,... and so on corresponding with the added potential functions. Within this work the von Mises stress σ_M will be considered intensively. It is given as:

$$\sigma_M = \sqrt{\frac{1}{2}\left(\left(\sigma_{xx}-\sigma_{yy}\right)^2+\left(\sigma_{zz}-\sigma_{yy}\right)^2+\left(\sigma_{xx}-\sigma_{zz}\right)^2+6*\left(\tau_{xy}^2+\tau_{xz}^2+\tau_{zy}^2\right)\right)}\,.$$

2.1.1. Extensions

2.1.1.1. Arbitrarily shaped interfaces

The method can be extended to arbitrarily shaped interfaces [49]. This extension is of great importance because it offers the opportunity to investigate curved interfaces occurring for example in the case of relatively rough substrate surfaces. An example, the "overfilled trench", is given in [49]. But because the mathematical method requires relatively complex and voluminous elaborations, which would completely burst this work we will here neither consider the theoretical approach nor give any application. The interested reader is referred to the above-mentioned publication, being directly available from the author.

2.1.1.2. Gradient coatings

Furthermore an extension to gradient coatings is possible in those cases where the Poisson's ratio does not vary within the coating but only the Young's modulus. One comes to an approximated solution of this problem by a simple superposition of the elastic fields for varying positions of interfaces. This becomes clear if one considers the following different forms of representation of a linear decreasing Young's modulus dropping from its maximum value E_{max} at the surface z=0 to the substrate value E_S at the interface z=h:

$$E(z) = E_{\max} - \frac{E_{\max}-E_S}{h} * z = E_{\max} - \lim_{n\to\infty}\left[\sum_{i=1}^{n}\frac{E_{\max}-E_S}{n}\Phi\left(i*\frac{h}{n}\right)\right], \tag{5}$$

with

$$\Phi(h) = \begin{cases} 0 \; for \; z \le h \\ 1 \; for \; z > h \end{cases} \tag{6}$$

giving the so called Heaviside function. On the right hand side of equation (5) the gradient transition between the Young's modulus E_{max} and E_S over the thickness h has been represented as an infinite sum of abrupt transitions (jumps) E_{max} to E_S at various positions $0 \leqq z \leqq h$. But because it is exactly the abrupt transition of the Young's modulus we are able to model applying the method of image loads we simply need to build up a sum of a sufficiently large number of suitable one-layer-solutions with varying interface positions to come to an approximated description of the gradient-layer-problem. The reader might have realised that

this holds for all forms of E(z) as long as they are monotonic, because for these types of functions one can find a representation similar to that given on the right hand side of (5). This more general approach would take the form:

$$E(z) = E_0 + \frac{E_1}{n} * \left(\lim_{n \to \infty} \left[\sum_{i=1}^{n} \Phi\left(\Delta h_i\right) \right] \right) \tag{7}$$

or as for any function f(z) within a range $[z_0, z_0+h]$:

$$f\left(z\right) = c_1 + \frac{f\left(z_0 + h\right) - f(z_0)}{n} * \left(\lim_{n \to \infty} \left[\sum_{i=1}^{n} \Phi\left(f^{-1}\left(\left\{ f\left(z_0 + h\right) - f(z_0) \right\} \frac{i}{n} + c_2 \right) \right) \right] \right), \tag{8}$$

where $f^{-1}(z)$ defines the inverse function to f(z). For example, we can give a quadratic function $f(z)=z^2$ in the following Heaviside description:

$$z^2 = \frac{h^2}{n} * \left(\lim_{n \to \infty} \left[\sum_{i=1}^{n} \Phi\left(h * \sqrt{\frac{i}{n}} \right) \right] \right). \tag{9}$$

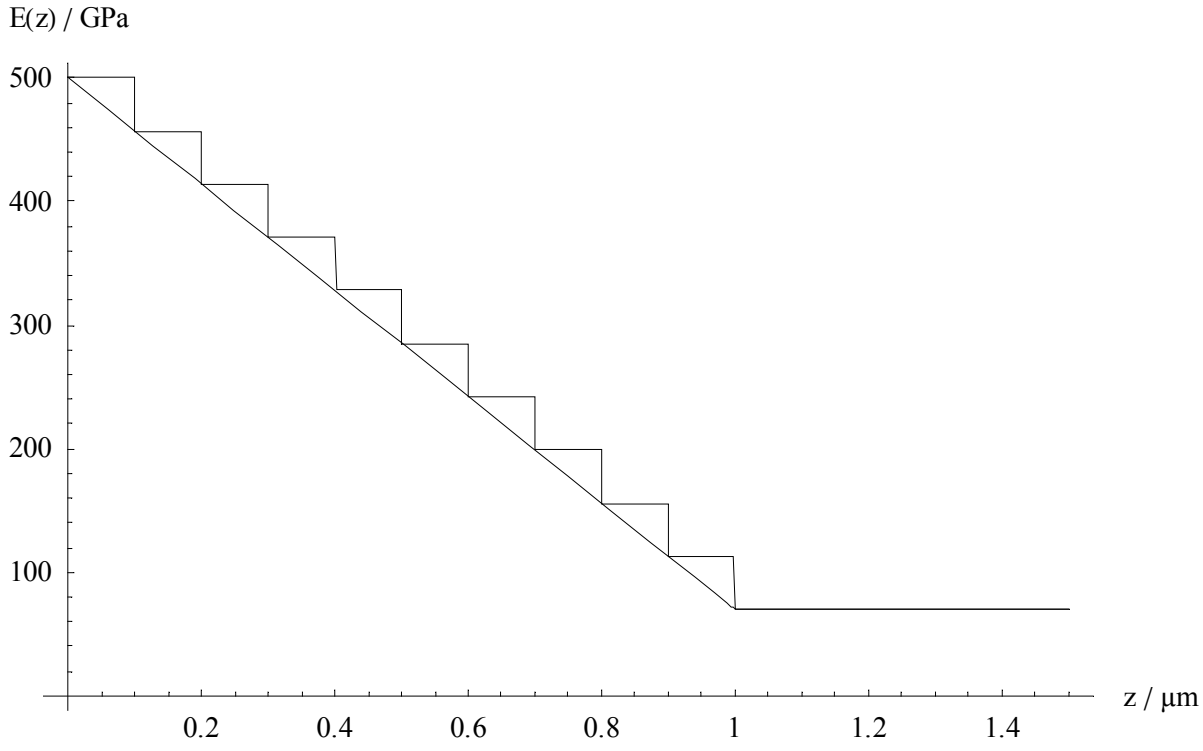

Figure 3: **Approximation of linear decreasing Young's modulus (straight line) using a representation with Heaviside function (zig-zag-line: here only 10 Heaviside functions have been used in order to make the approximation visible).**

In addition it should be noted, that the following generalisations/extensions to the gradient approach are possible:

1. This approach is also valid for a parameter combination of Young's modulus and Poisson's ratio as one simply writes (7) in the form:

$$E(z) = E_0 f(z); \nu(z) = \nu_0 f(z); f(z) = k_0 + \frac{k_1}{n} * \left(\lim_{n \to \infty} \left[\sum_{i=1}^{n} \Phi\left(\Delta h_i\right) \right] \right), \qquad (10)$$

meaning, that within a given range both, the Young's modulus and the Poisson's ratio, are being varied from a starting value E_{start} and ν_{start} to an end value E_{end} and ν_{end} with a z-dependence proportional to the function f(z). Figure 3 shows an example of a linear decreasing Young's modulus.

2. For not simply monotonic functions, for example first decreasing and later increasing E-modulus and ν-functions the approach (10) (or any proper combination of terms of this kind) could be combined with the multilayer approach of [C1] and thus very complex parameter functions like e.g. $E(z)=E_0 + E_1 \sin(z)$ and $\nu(z)=\nu_0 + \nu_1 \sin(z)$ could be treated, where only for each change of monotony a new layer has to be modelled. So, applying the new gradient-approach to a three-layer solution one could mathematically describe the above assumed trigonometric approach within a range of two ranges of monotonic values and therefore e.g. from $z = -\frac{\pi}{2}$ until $z = \frac{5\pi}{2}$. Figure 4 shows an example for such a periodic parameter function. It has the concrete form $E(z)=300GPa+200GPa*\sin(z-\pi/2)$.

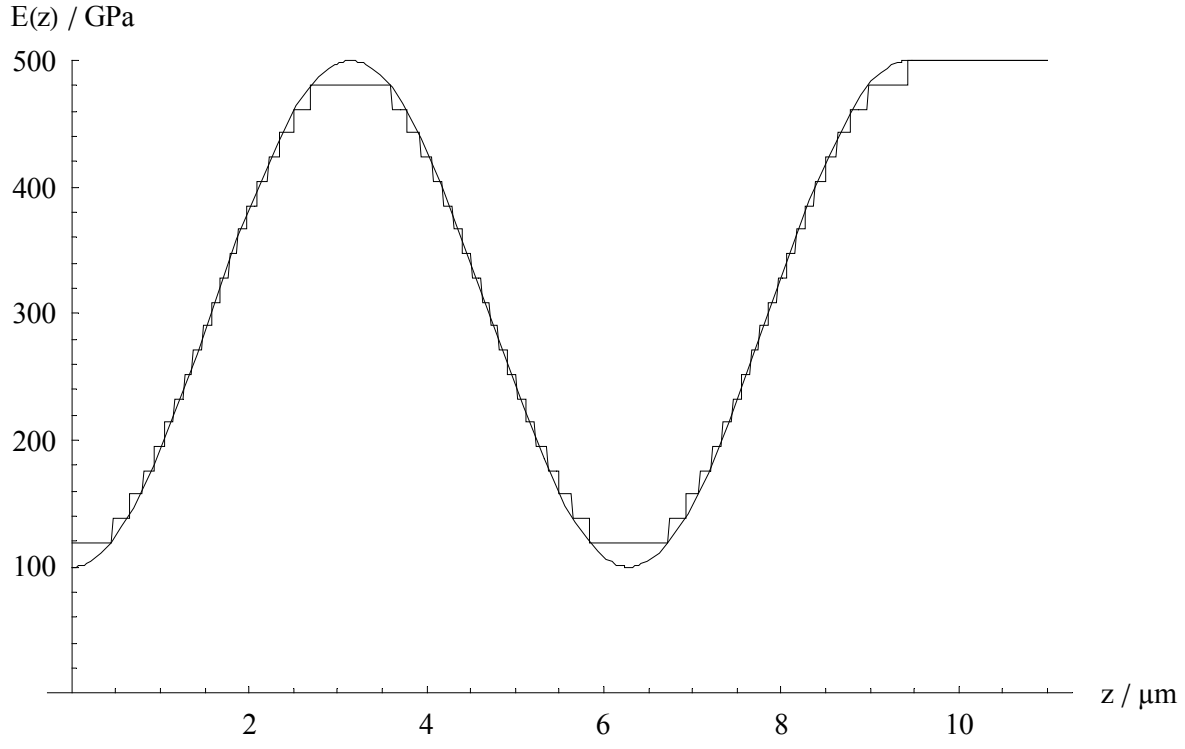

Figure 4: Approximation of a periodic Young's modulus (straight line) using a representation with Heaviside functions (zig-zag-line: here 63 Heaviside functions have been used).

If $P(h_i)$ gives the potential function for the solution of a one-coating-half-space with coating thickness h_i we construct the final approach for a gradient coating in the form:

$$\sum_{\forall i} w_i P(h_i) \cong G\,, \tag{11}$$

with w_i and G denoting suitable constants and the correct solution, respectively. Even if the w_i have to be determined using a less approximated solution (e.g. a multi-layer solution applying the integral method) the final advantage in the calculation time justifies the usage of this gradient approach. For example, applying the integral and the approximate gradient method to a 10-layer system the gradient method calculates the complete elastic field about 6500 times faster with a deviation from the integral approach nowhere bigger than 0.3%. In Figure 5 the displacement w is shown as a function of the depth for an example of a 11-layer-"gradient" (calculation parameters: load p=1N, deviation from the axis of symmetry x=0.1µm, radius of contact a=1µm, Poisson's ratio 0.3, Young's modulus {3, 2.8, 2.6, 2.4, 2.2, 2, 1.8, 1.6, 1.4, 1.2, 1, 0.8}*100GPa – from top layer to substrate, thickness see gridlines in Figure 5).

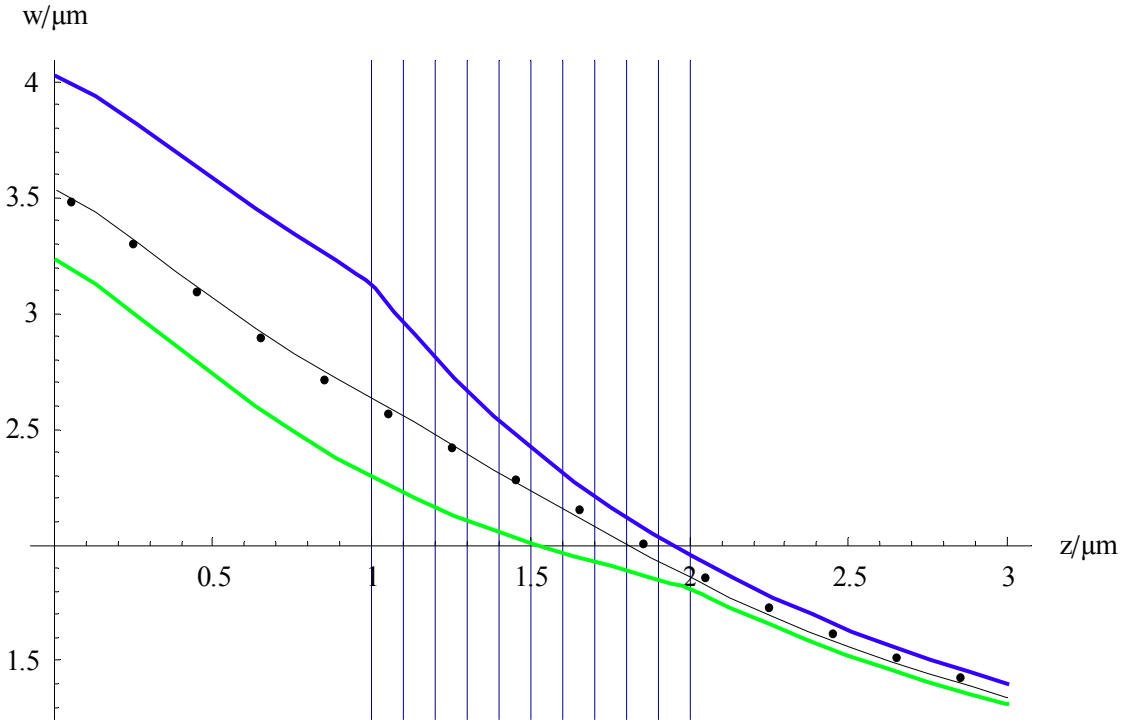

Figure 5: **Displacement w as a function of depth for a 11-layer-system using the gradient approach (black line) and the integral approach (dots). The gridlines give the positions of the interfaces. In addition the single-layer solutions for systems with a 300GPa-coating on a 80GPa-substrate with interfaces at 1µm (blue) and 2µm (green) are shown.**

2.2. The intrinsic stresses

In those cases, where the coating-substrate-compound can be considered as plate-like and the film thickness is small compared to the substrate thickness the following two assumptions can be made [37, 40]:

- the thin plate approximation is valid,
- the film-stress can be considered as being independent from the distance of the interface (here the z-axis shall be parallel to the plate's normal).

This automatically yields a linear z-dependant stress within the substrate [47] and we obtain a very simple stress distribution where only the stress tensor components σ_{xx}, σ_{yy}, $\tau_{xy}=\sigma_{xy}$ are of importance. If we in addition assume to have isotropic or transversely isotropic (with the c-axis parallel to the substrate normal) substrate materials of symmetry of revolution and homogeneous deposition conditions over the whole substrate surface we result in only one governing stress value σ_{rr}, which is the radial stress[1]. While this stress is widely assumed [37] to be homogeneous within the film it follows a linear z-dependant function within the substrate. This principle distribution of the σ_{rr} stress component occurs only under the above mentioned conditions.

Unfortunately for most cases, like coated tools, car components or massive lenses, the assumption of a plate-like film-substrate-compound is not valid and thus the stress distribution might be completely different from that one described above. This holds especially for the substrate. For the film however we still can assume, that $\sigma_{zz}=0$ is valid and the biaxial stress is homogeneous over the film thickness as long as the film is thin and there is no significant displacement, phase transition or other inelastic effect of any of the parts of

---

[1] One can evaluate this by combining the thin plate approximation (1) with the isotropy condition for material properties and deposition process ($\sigma_{xx}=\sigma_{yy}$, $\sigma_{xy}=0$) and the following transformation rules:

$$\sigma_{rr} = \cos^2\varphi\,\sigma_{xx} + \sin 2\varphi\,\sigma_{xy} + \sin^2\varphi\,\sigma_{yy} = \sigma_{xx},$$

$$\sigma_{\varphi\varphi} = \cos^2\varphi\,\sigma_{yy} - 2\cos\varphi\sin\varphi\,\sigma_{xy} + \sin^2\varphi\,\sigma_{xx} = \sigma_{xx},$$

$$\sigma_{r\varphi} = \cos 2\varphi\,\sigma_{xy} - \sin 2\varphi\,(\sigma_{xx} - \sigma_{yy})/2 = 0,$$

yielding:

$$\sigma_{ij} = \begin{pmatrix} \sigma_{rr} & 0 & 0 \\ 0 & \sigma_{rr} & 0 \\ 0 & 0 & 0 \end{pmatrix}.$$

the film causing local stress releases. This becomes clear if one notices that the linear z-dependant stress distribution within the substrate is caused by the bending of the compound but in all cases of non-plate-like substrates this is not possible. So the question arises: If we can still assume a constant σ_{rr}^{f} stress distribution for the coating, how could we come to a suitable stress description for the substrate?

To answer this question we assume the coating as to be separated from the substrate and pressed at its rim such, that exactly the bi-axial intrinsic stress state with σ_{xx} and σ_{yy} appears. This pre-stressed coating is now "stuck" on the substrate. The external forces Fx and Fy producing the pre-stress-state are removed allowing the coating-substrate-system to find its equivalency. The former forces acting on the rim of the coating must be now taken on by the elastic stiffness of the substrate. They, the forces, couple into the substrate as shearing forces Sx and Sy via its surface. In order to simplify the calculation we consider a substrate of square geometry with the side length s. We do not know yet the distribution of this shearing stress on the substrate surface so we start with a general solution of the problem, which can be given due to the following displacements:

$$\vec{u}=\sum_{\forall i,k} c_{ik}\begin{pmatrix} au\left(\left(A+B+Buz\right)e^{uz}-\left(D-F+Fuz\right)e^{-uz}\right)\sin\left[ax\right]\cos\left[by\right] \\ bu\left(\left(A+B+Buz\right)e^{uz}-\left(D-F+Fuz\right)e^{-uz}\right)\cos\left[ax\right]\sin\left[by\right] \\ u^{2}\left(\left(-A+\left(2-4\nu-uz\right)B\right)e^{uz}-\left(D+\left(2-4\nu+uz\right)F\right)e^{-uz}\right)\cos\left[ax\right]\cos\left[by\right] \end{pmatrix} \quad (12)$$

with $u^2=a^2+b^2$ and $a=\frac{i\pi}{s}$, $b=\frac{k\pi}{s}$ and i,k=1,3,5,7…, which assures the normal stresses σ_{xx} and σ_{yy} being zero at the substrate rim. The shearing stress σ_{xy} should be also zero there, but this condition can not be satisfied with the approach suggested in equation (12) as easy as the normal stress boundary conditions. In this case a suitable Fourier series would be necessary. However, because we will here only concentrate on the elastic field at the centre of the plate the influence of a non-zero σ_{xy} at the rim of the plate can be considered as being small. It can be shown that (12) satisfies the equation for equilibrium for an isotropic elastic medium (see e.g. [4]). The further boundary conditions:

$$\sigma_{zz}\big|_{z=0}=\sigma_{zz}\big|_{z=h_s}=\sigma_{xz}\big|_{z=h_s}=\sigma_{yz}\big|_{z=h_s}=0,\quad \sigma_{xz}\big|_{z=h_s}=\sigma_{yz}\big|_{z=h_s}=f\left(x,y\right),$$

$$Fx=Fy=\sigma_{rr}^{f}hs=Sx=Sy=\int_{-s/2}^{s/2}\int_{0}^{s/2}\sigma_{xz}dxdy=\int_{-s/2}^{s/2}\int_{0}^{s/2}\sigma_{yz}dydx$$

give the equations necessary to determine all constants including the coefficients c_{ik}.

In the case of thin films and plate-like substrates this new approach should agree with the results given by the equation of Stoney [47]. To test this we apply a very simple first order

approach of the general formulae (12) with i=k=1 and all c_{ik} for i,k>1 being 0 on the following system:

Table 1: Mechanical parameters for a system of a 1µm TiN-coating on silicon

	Young's modulus	Poisson's ratio	Thickness
coating	450 GPa	0.25	1µm
substrate	164.4 GPa	0.224	h_s = 200µm

Assuming now an intrinsic stress of $\sigma_{xx}=\sigma_{yy}$= -1GPa we vary the side length of our square substrate from relatively plate-like 3000µm (15*h_s) down to 20µm.

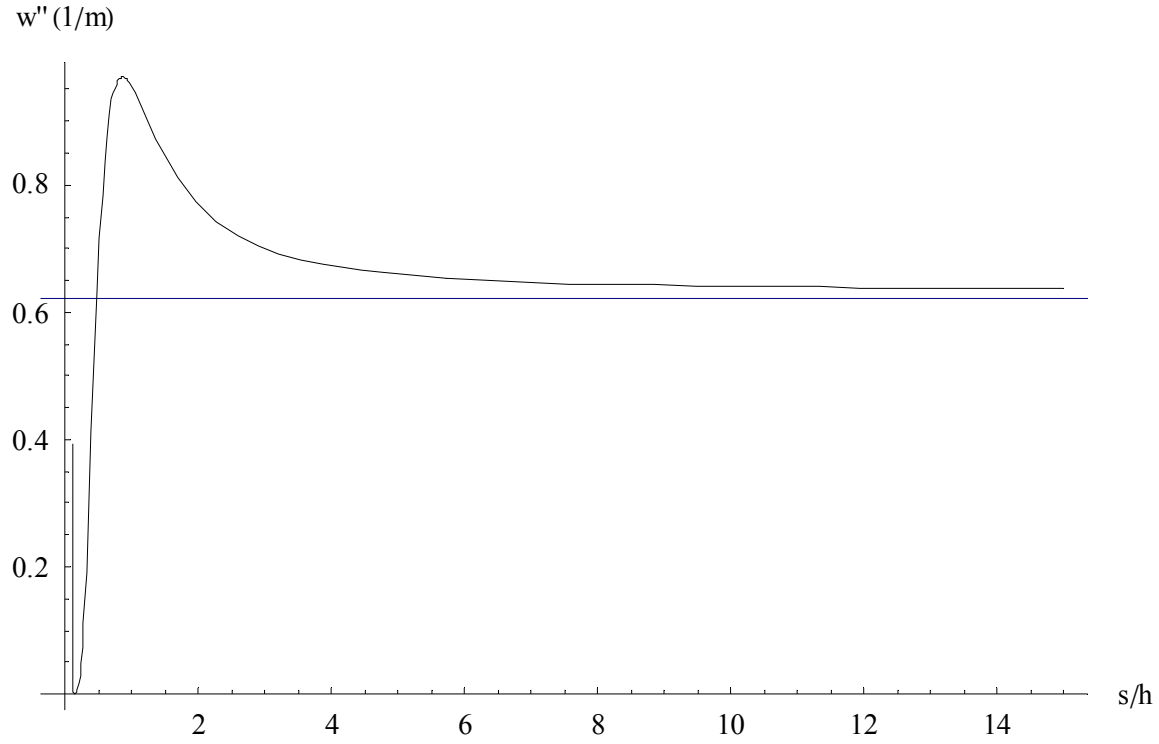

Figure 6: **Curvature of the system given in Table 1 (vertical axis) for various side length s assuming a bi-axial coating stress of –1GPa. The horizontal line gives the corresponding value of the Stoney equation.**

Figure 6 gives the values for the curvature (approximately the inverse of the radius of curvature) of the bent substrate at its centre position (x=y=0, z=h_s/2). We see, that from a side length of about s=10*h_s upwards the curve has reached its asymptotic value with a deviation of only 1%. The agreement with the result given by the Stoney equation is quite excellent (only 2% deviation). This is especially remarkable because of the very simple first order approach we have chosen for the shearing stress distribution on the substrate surface. However more accurate calculations should be performed if one wants to apply the general

approach (12) to analyse experimental data. But in this case a more critical discussion about the principle shape of the shearing stress distribution resulting from the deposition process seems necessary.

Unfortunately the approach (12) can not be extended to the general case of rectangular substrates. The reason lays in the properties of the approach, which can not satisfy independent boundary conditions for both the σ_{xz} and the σ_{yz} stress on the substrate surface. Such an approach would be very helpful in order to give complete analytical prove to the principle argumentation in [40] (see 1.2.) but so far the author was unable to find a more general solution.

3. Application of the theoretical models

In the papers [21-31] a number of different applications of the theoretical modelling described above are given. Among them we have:

- the realisation of an easy to use software package allowing the calculation of the elastic field for Hertzian load and contact problems (normal and tangential load) for coating-substrate-systems with up to three layers [21],
- analysis of experimental data of nanoindenter experiments of one-layer-substrate-compounds [22, 23, 29,31],
- analysis of experimental data of nanoindenter experiments of 2-layer-substrate-cpmpounds [25],
- application in dentistry [26] and
- in fracture mechanics [27],
- general modelling of coated systems and questions of coating optimisation [24, 28, 30].

Here we will concentrate on the following three problems:

- the increase of the load carrying capacity of multilayer-compounds for mixed load conditions (normal and tangential loads) with very high friction coefficients,
- the superposition of Hertzian loads on coating-substrate-compounds as a method to describe relatively complex load distributions and
- how to measure the intrinsic stress using nanoindentation methods

3.1. Coating design for mixed load conditions with very high friction coefficients

Due to the availability of software packages like ELASTICA [21], the problem of finding a proper protective 1-layer coating for a mechanical application within the linear elastic regime has been reduced to a relatively simple evaluation of a variety of different parameter combinations. Future versions of this software will provide highly automized procedures in order to simplify this process for the user. In [48] a good animated demonstration is presented showing the principle steps for such an optimisation process using the existing version of ELASTICA. However especially in cases of mixed load conditions or practical restrictions of the coating thickness and its mechanical parameters, single-layer coatings can often not provide a sufficient protection and thus more layers or even gradient coatings must be considered. A demonstration for two examples will be given in this section.

The author has used circular and elliptical Hertzian load distribution to describe the effect of the indenter. The mechanical parameters of the different compounds are given in Table 2.

Table 2: A variety of single and 3-layers coatings on a "steel"-substrate

Name of the compound	Layer 1 E^a(GPa)/ν^b/t^c(μm)	Layer 2 E (GPa)/ν/t(μm)	Layer 3 E (GPa)/ν/t(μm)	Substrate E (GPa)/ν
System 1	450/0.25/1	-	-	200/0.3
System 2	300/0.25/1	-	-	200/0.3
System 3	400/0.25/1	-	-	200/0.3
System 4	500/0.25/1	-	-	200/0.3
System 5	500/0.25/0.3	400/0.23/0.4	200/0.21/0.3	200/0.3
System 6	250/0.25/0.3	400/0.23/0.4	300/0.21/0.3	200/0.3

[a] Young's modulus

[b] Poisson's ratio: variation of this parameter has no significant effect

[c] layer thickness

The corresponding "homogeneous" solutions for the case of circular and elliptical contact regions may be found in the papers of Hanson [16, 20]. Unfortunately, the solution for the elliptical contact shape is not complete concerning their practical applicability. Hence, partly

numerical calculations were necessary and only the single layer case under normal load was considered. As an example we consider the von Mises stress σ_M for system 1 under elliptical Hertzian load. Figure 7 shows the stress distribution for a ratio a/b=1.6 with a (along the x axis) and b (along the y axis) as the main half axes of the contact ellipse. The average normal pressure within the contact zone is 1GPa. Repeating the calculation for various ratios a/b in the vicinity of the circular case a=b one finds that the maximum value as well as the principal distribution of the von Mises stress varies only marginally under a moderate variation of the shape of the contact region.

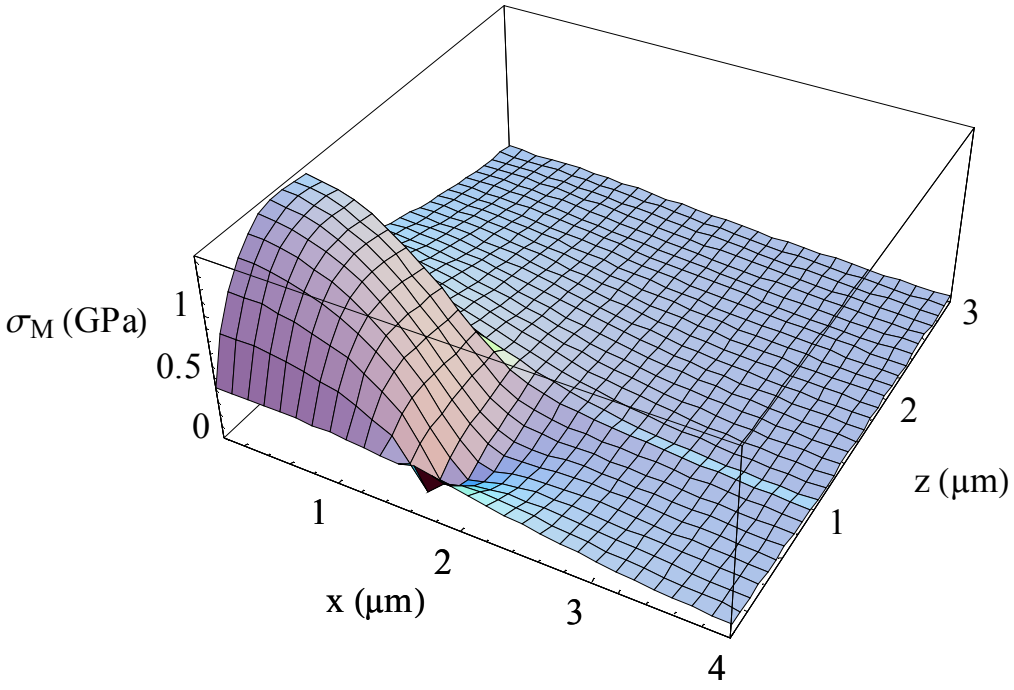

Figure 7: **v. Mises stress of an elliptical Hertzian load with half axes a=1.6μm and b=1μm within the x-z-plane (z≥0 decribes the coated elastic half space)**

In contrast to the elliptical contact, no time consuming numerical integration procedures are necessary if one investigates circular Hertzian load. The loads P, applied to the surfaces (z=0) of our hypothetical compounds, shall be of the technically "worst case" kind, with a very high portion of shear loading in x direction (friction coefficient μ=1), an average normal stress within the contact zone of 1GPa and contact radius, a, in the range of the total film thickness, h:

$$\sigma_{zz}\big|_{z=0} = \frac{3P}{2\pi a^2}\sqrt{a^2 - r^2}; \quad \tau_{xz}\big|_{z=0} = \frac{3(T = \mu P)}{2\pi a^2}\sqrt{a^2 - r^2}; \quad r^2 = x^2 + y^2 .$$

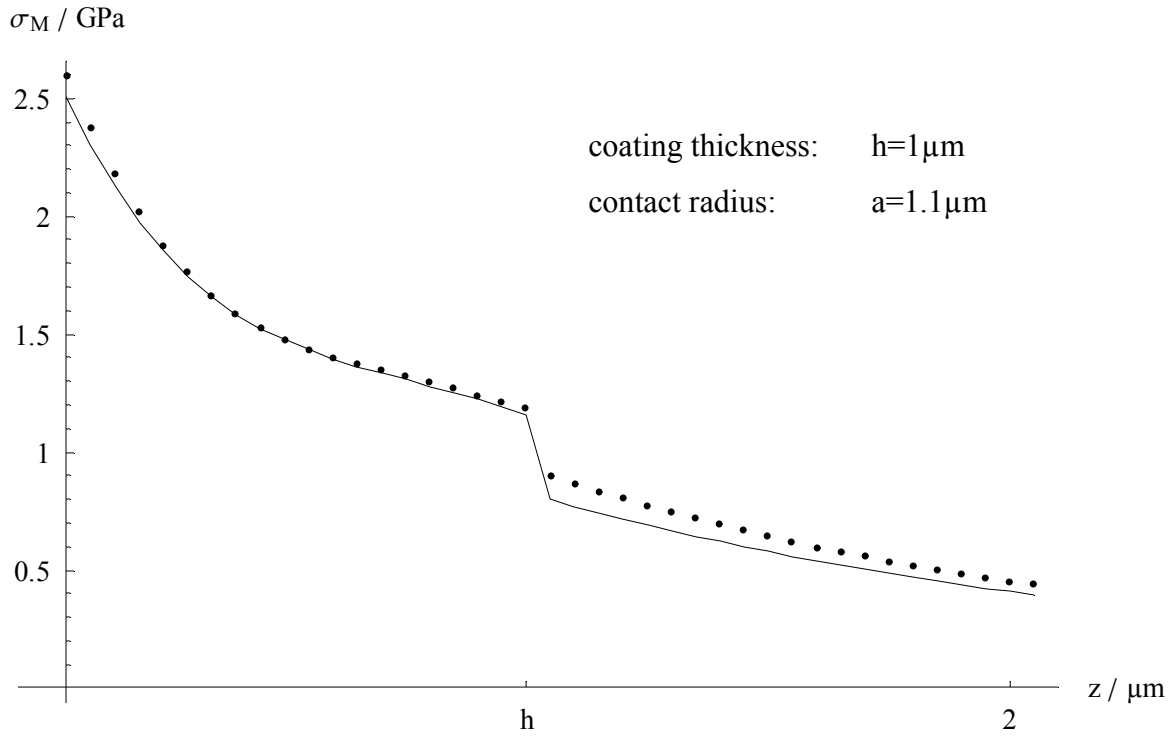

Figure 8: **Comparison between the maximum values of the v. Mises stress (points) and those ones along the z-axis (solid line) for system 3. The deviation is caused by the symmetry braking shear load.**

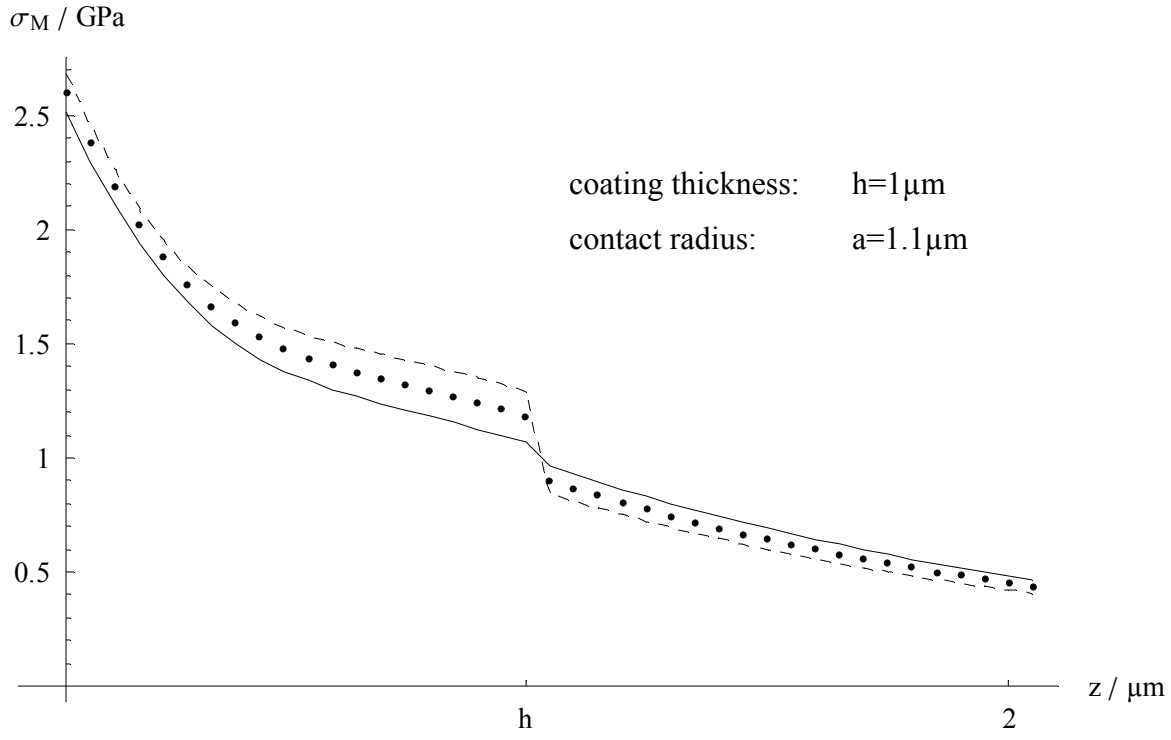

Figure 9: **Maximum values of the v. Mises stress at different depths for system 2 (solid line), 3 (points) and 4 (dashed line)**

We first consider the von Mises stress as given above for system 3 and compare the stress values along the z-axis and the corresponding maximum values at the same depth but different x,y-positions. As one can see clearly from Figure 8, these values differ significantly because the shear load breaks the symmetry. Thus, in the following only maximum values of the von Mises stress will be compared. In Figure 9 the maximum values of the von Mises stress for different single layers are shown. If we assume now to have a critical value of about 700MPa von Mises stress for the beginning of plastic deformation within the substrate we should strictly avoid generating such stress values in the vicinity of the interface region. But as we see in Figure 9 in all 3 single layer systems the critical von Mises stress is exceeded at the interface. In addition our load conditions cause relatively high tensile stresses at the surface (Figure 10) and in the case of the system 4 at the interface (Figure 11) which could lead to cracks ("Hertzian cone" and "star cracks", respectively) and subsequently to film delamination. This interface fracture initialisation mechanism in the case of relatively hard coatings on pliant substrate materials is know as the "egg-shell-effect".

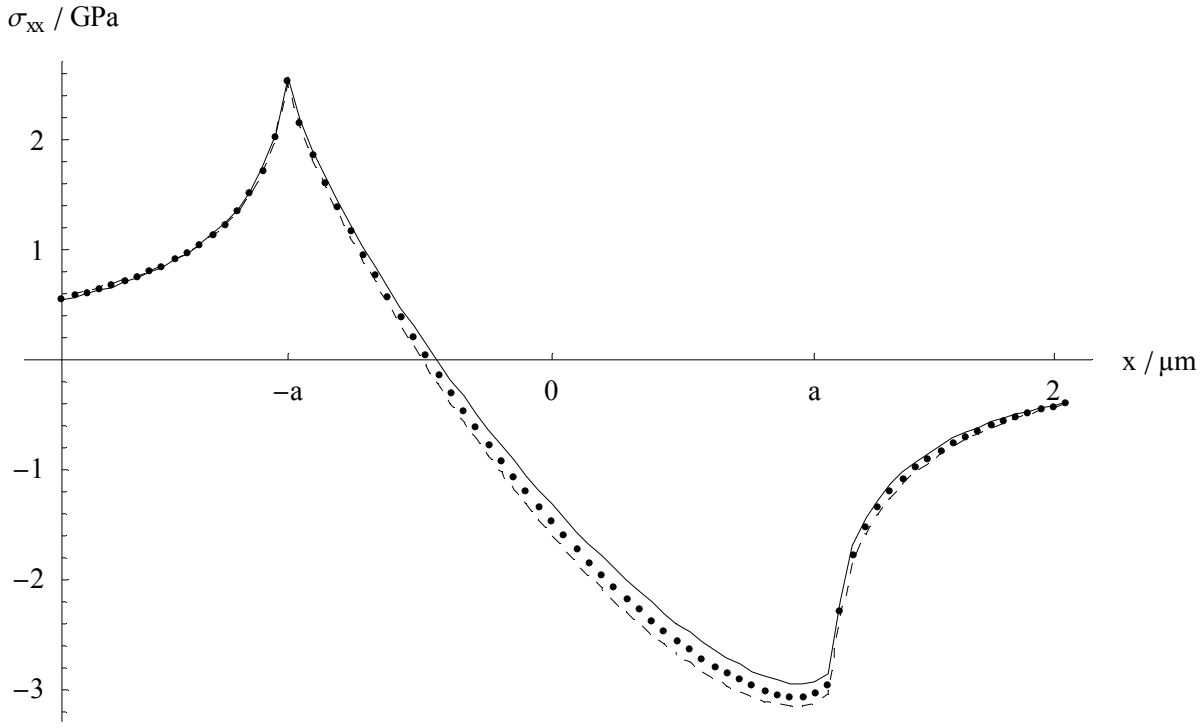

Figure 10: **σ_{xx} at the surface (z=0) for system 2 (solid line), 3 (points) and 4 (dashed line)**

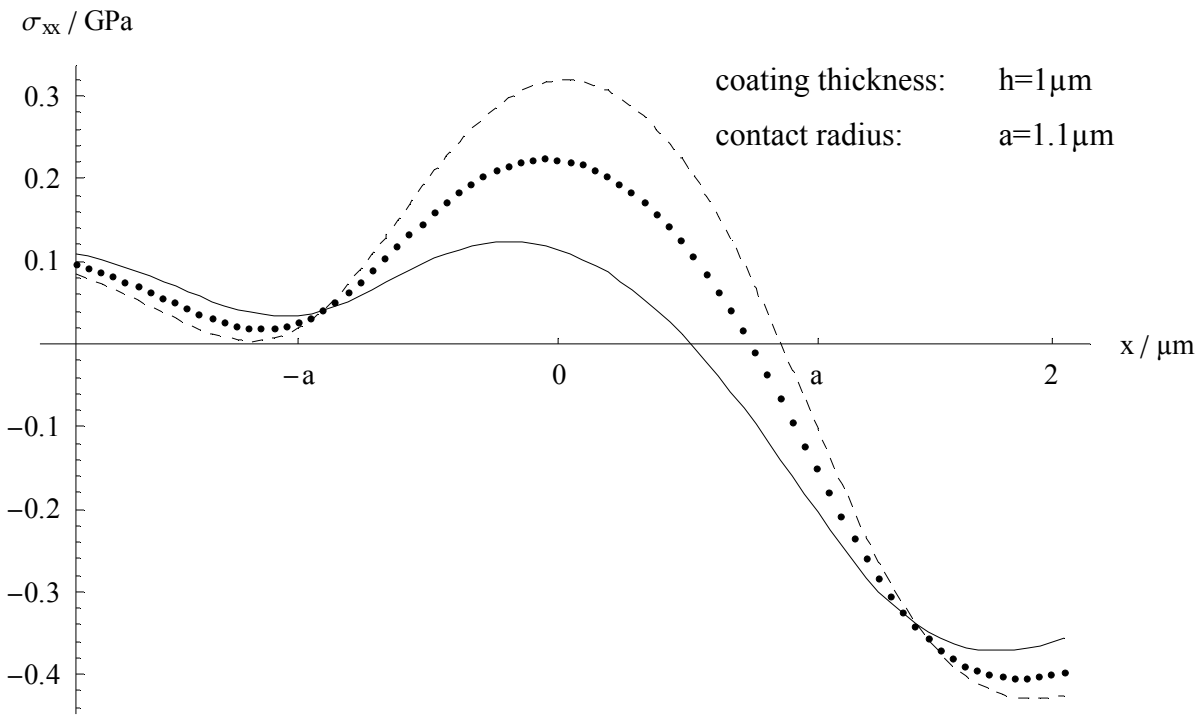

Figure 11: **σ_{xx} at the interface within the coating (z=h-10nm) for system 2 (solid line), 3 (points) and 4 (dashed line)**

The task is now to design a multilayer coating which first reduces the maximum von Mises stresses at the interface as well as decreases the tensile stresses within the film material. Comparison of Figure 9 and Figure 12 shows that a multilayer coating with a gradually increased Young's modulus in contrast to a single layer with its rather abrupt material transition indeed reduces the von Mises stress as well as generates sufficiently low tensile stresses at the interface (dashed lines in Figure 13). However, the tensile stress at the surface of system 5 is not decreased (points in Figure 13). This tensile stress can be reduced by adding a cover layer of somewhat lower Young's modulus as chosen in system 6. Further work should investigate this fact in more detail and with higher numbers of layers. Finally, to give the reader at least an idea of the influence of the friction coefficient µ on the stress distribution the author has in addition calculated the σ_{xx}-stress of system 2 and 4 for two different values of µ (Figure 14 and Figure 15).

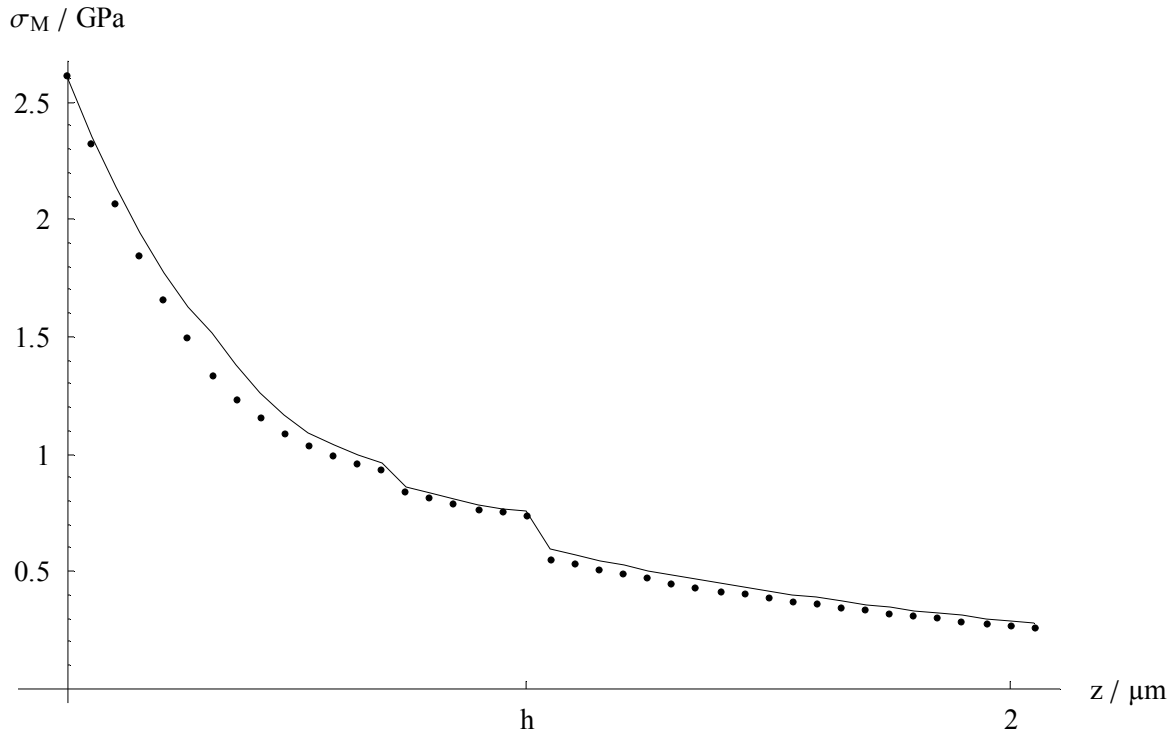

Figure 12: **Maximum values of the v. Mises stress at different depths for system 5 (points) and 6 (solid line)**

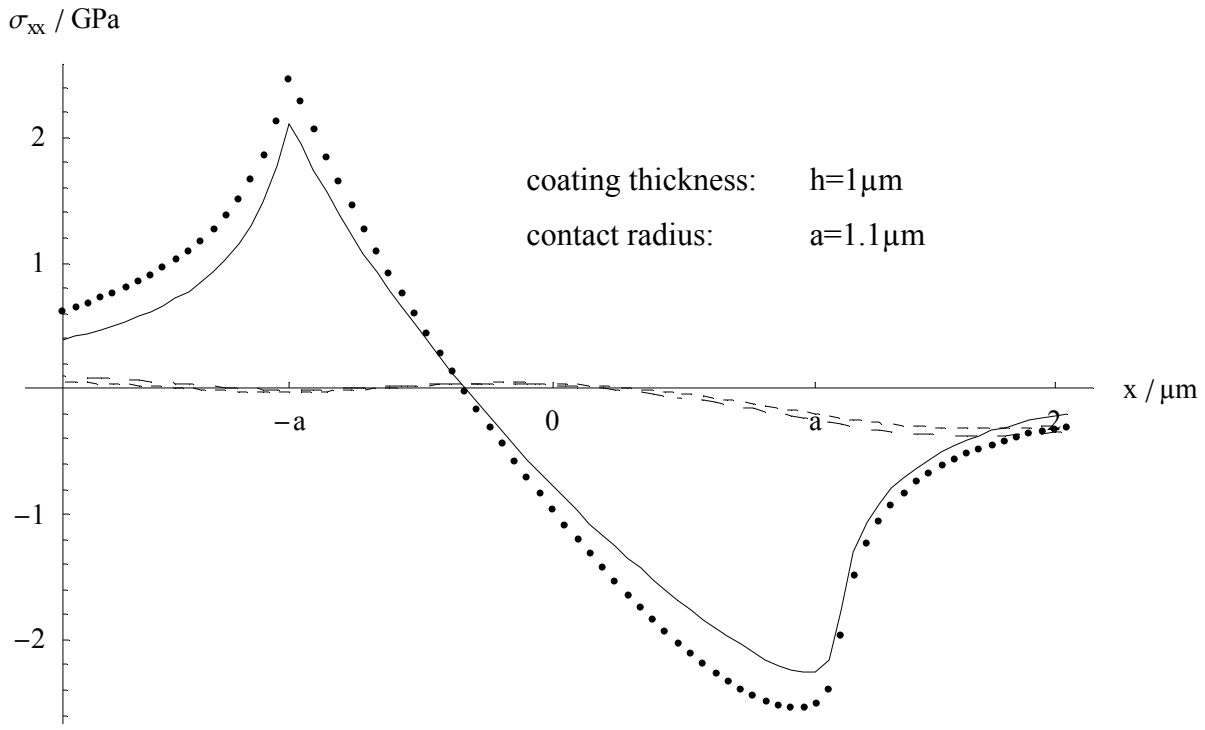

Figure 13: **σ_{xx} at surface and interface (z=h-10nm) for system 5 (points, small dashes) and 6 (solid line and long dashes)**

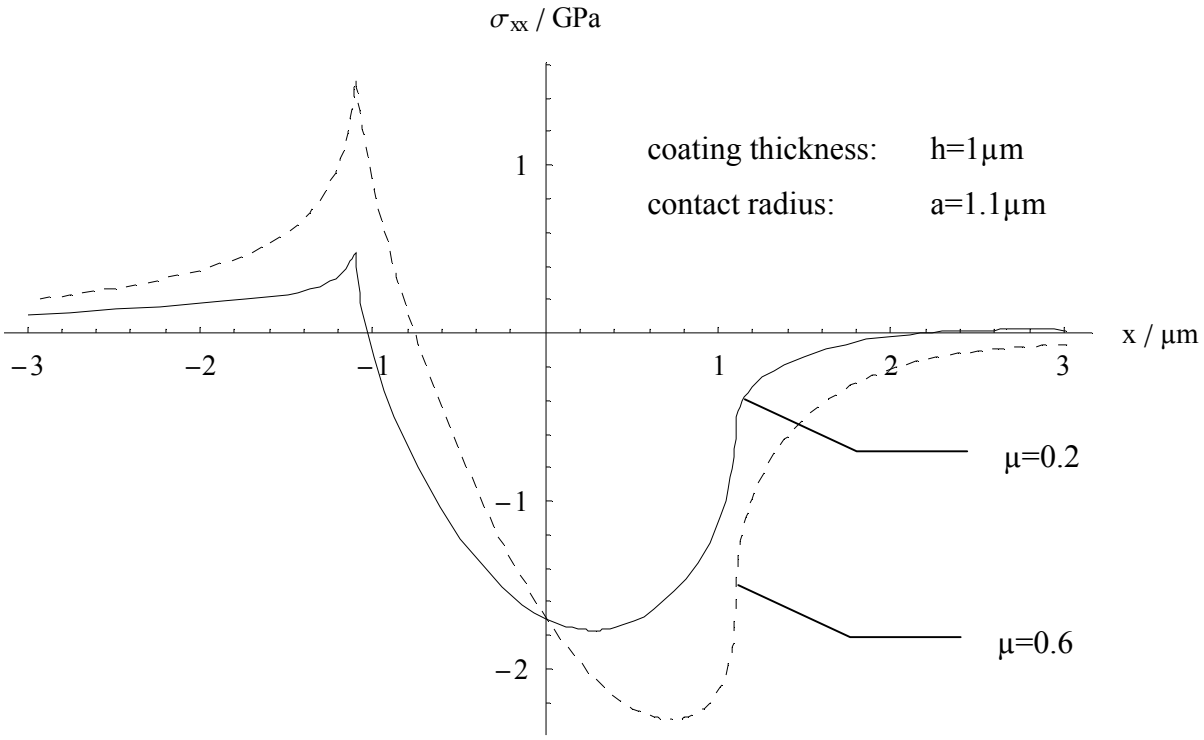

Figure 14: σ_{xx} **at the surface (z=0) for system 4 and different friction coefficients μ**

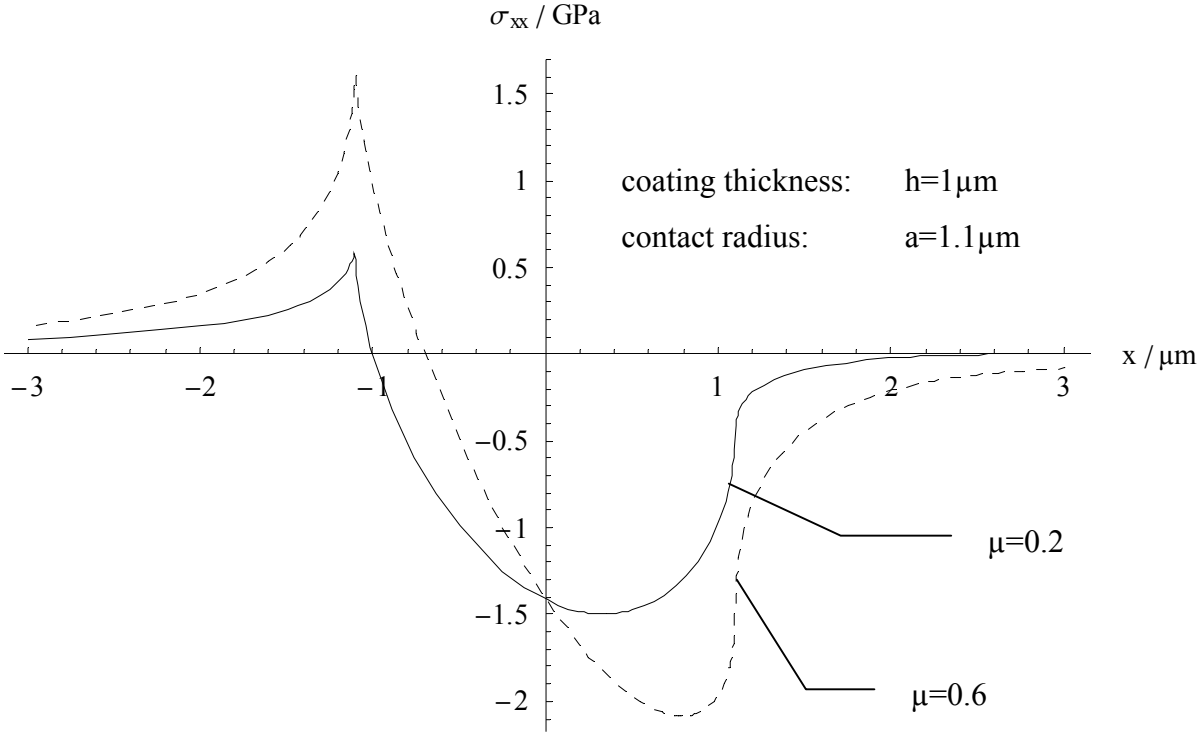

Figure 15: σ_{xx} **at the surface (z=0) for system 2 and different friction coefficients μ**

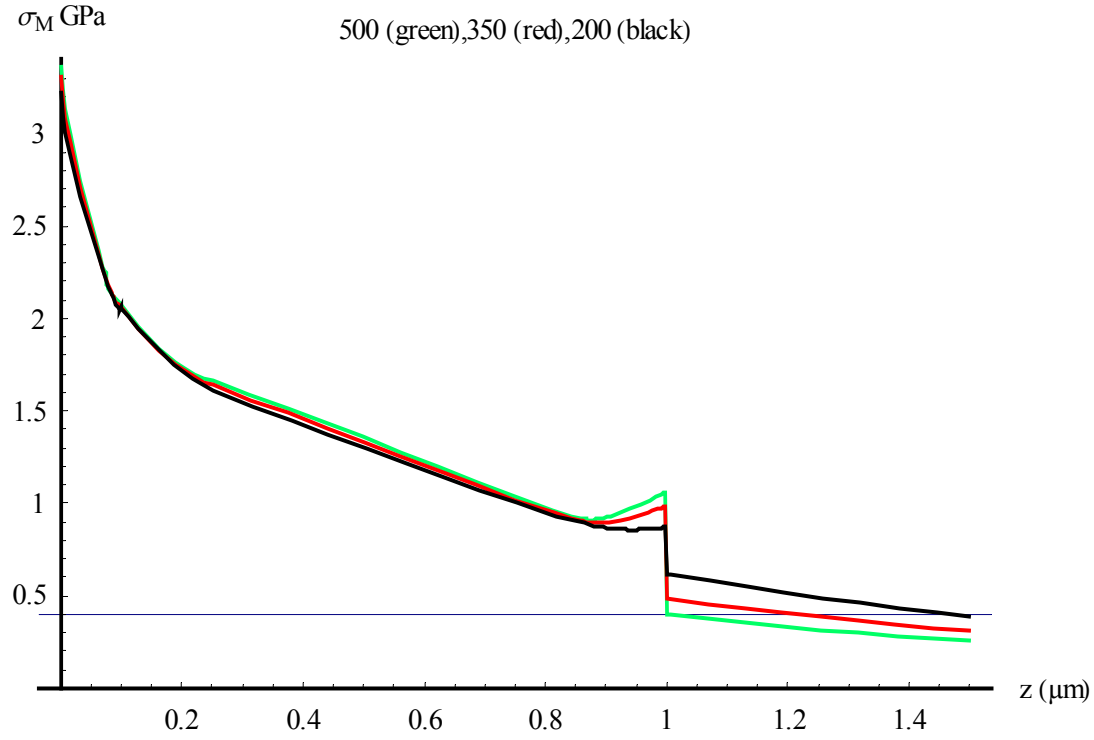

Figure 16: **Maximum values of the v. Mises stress at different depths for systems 7 (green), 8 (red) and 9 (black). The thin horizontal „grid-line“ at 400MPa marks the yield strength of the Al-alloy.**

Similar results concerning the structure of an “optimal” coating design were obtained for other substrates (e.g. Aluminium and Polymer), but with other parameters (depending on the substrate properties and the load conditions of the proposed application). Here we only present the results obtained for an Aluminium alloy with the following boundary conditions concerning the selectable coating material and contact conditions:

- Coating: Young’s modulus = 200-500 GPa,
  yield strength 3 GPa,
  thickness = 1μm,
  critical tensile stress: 2GPa
- Substrate: Al-alloy, Young’s modulus = 70 GPa, yield strength = 400 MPa,
- load conditions: the coated system must survive a contact pressure of 1 GPa with a friction coefficient of μ=1.

The systems investigated are given in Table 3.

Table 3: A variety of single, 3- and gradient-layer-coatings an “Al-alloy”

Name of the compound	Layer 1 E^a(GPa)/ν^b/t^c(μm)	Layer 2 E (GPa)/ν/t(μm)	Layer 3 E (GPa)/ν/t(μm)	Substrate E (GPa)/ν

System 7	500/0.25/1	-	-	70/0.35
System 8	350/0.25/1	-	-	70/0.35
System 9	200/0.25/1	-	-	70/0.35
System 10	gradient layer with: 500-70 (linear z-dependant[d])/0.25-0.35/1			70/0.35
System 11	200/0.25/0.1	500/0.23/0.6	200/0.21/0.3	70/0.35

[a] Young's modulus

[b] Poisson's ratio: variation of this parameter has no significant effect

[c] layer thickness

[d] Figure 3 gives the shape of the Young's modulus and the Haeviside-approximation, but in contrary to the figure a number of 101 Heaviside function have been used during the evaluation of the v. Mises and the σ_{xx} stress

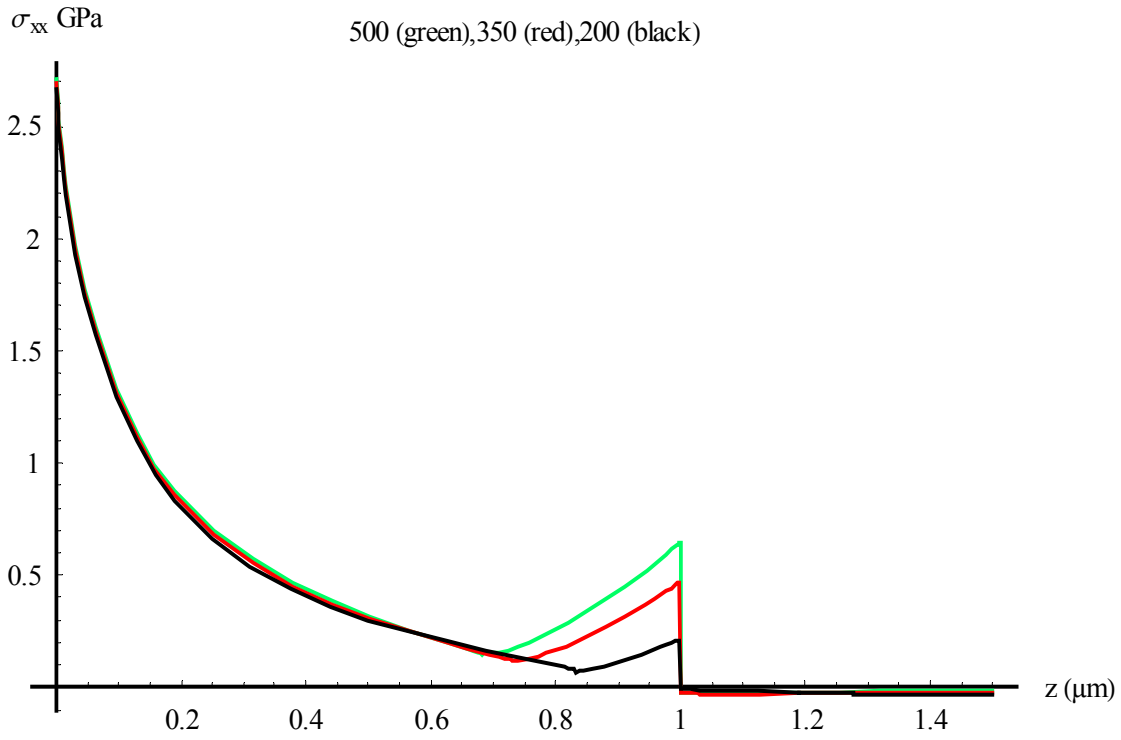

Figure 17: Maximum values of the σ_{xx} stress at different depths for the systems 7 (green), 8 (red) and 9 (black)

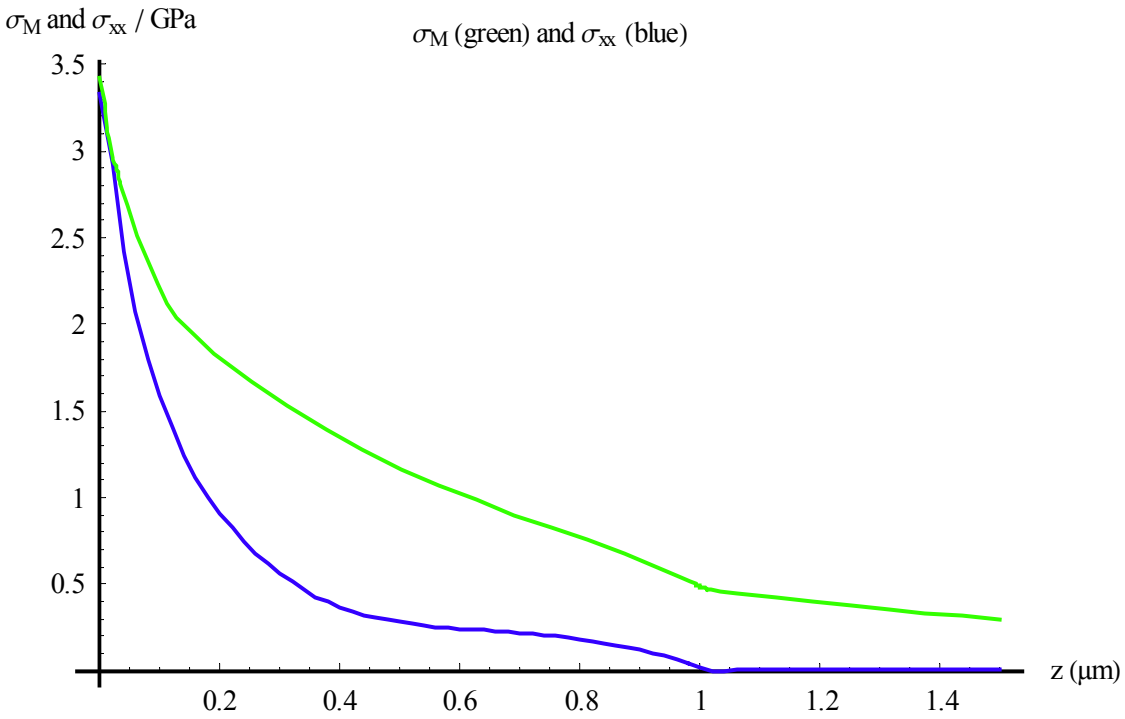

Figure 18: **Maximum values of the σ_{xx} (blue) and the v. Mises stresses (green) at different depths for the system 10.**

So, in Figure 16, Figure 17 and Figure 18 the Mises stress and the tangential stress σ_{xx} are shown for the three single layer systems and the gradient layer. We notice that none of the systems would survive the "worst contact case" with an contact radius in the range of the layer thickness (a=1μm) and a high friction coefficient of μ=1 (average normal pressure: 1GPa).

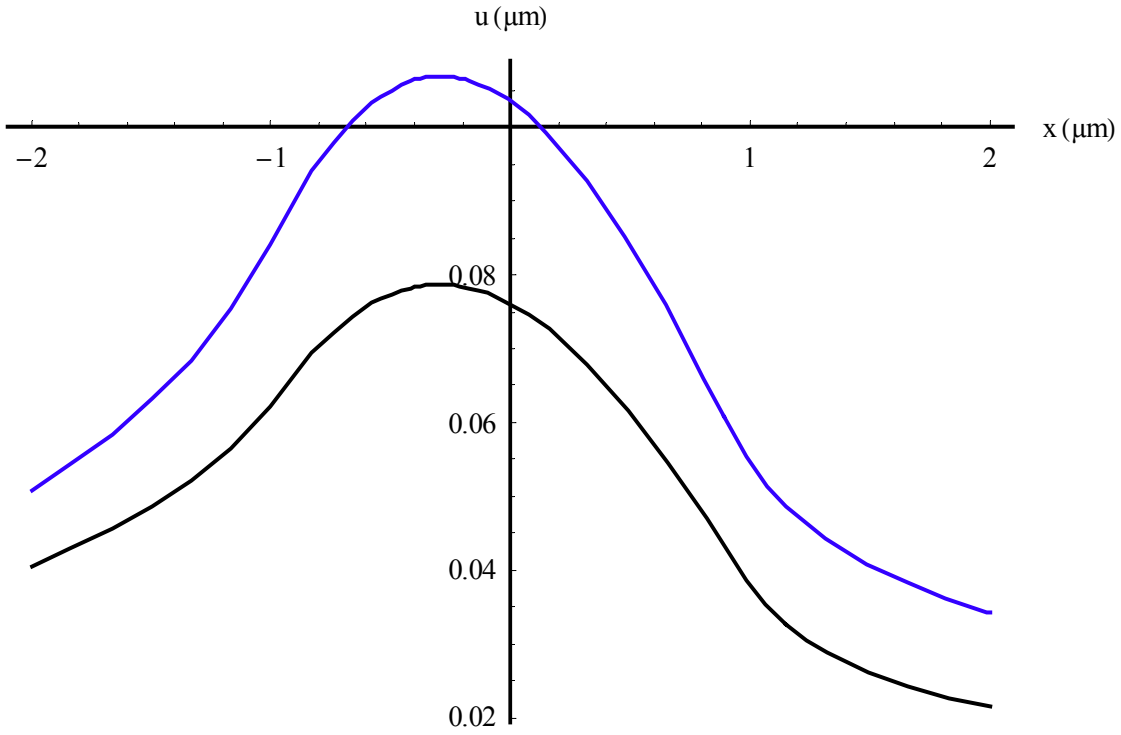

Figure 19: **Displacement in x-direction (along x-axis) for the systems 7 (black) and 10 (blue)**

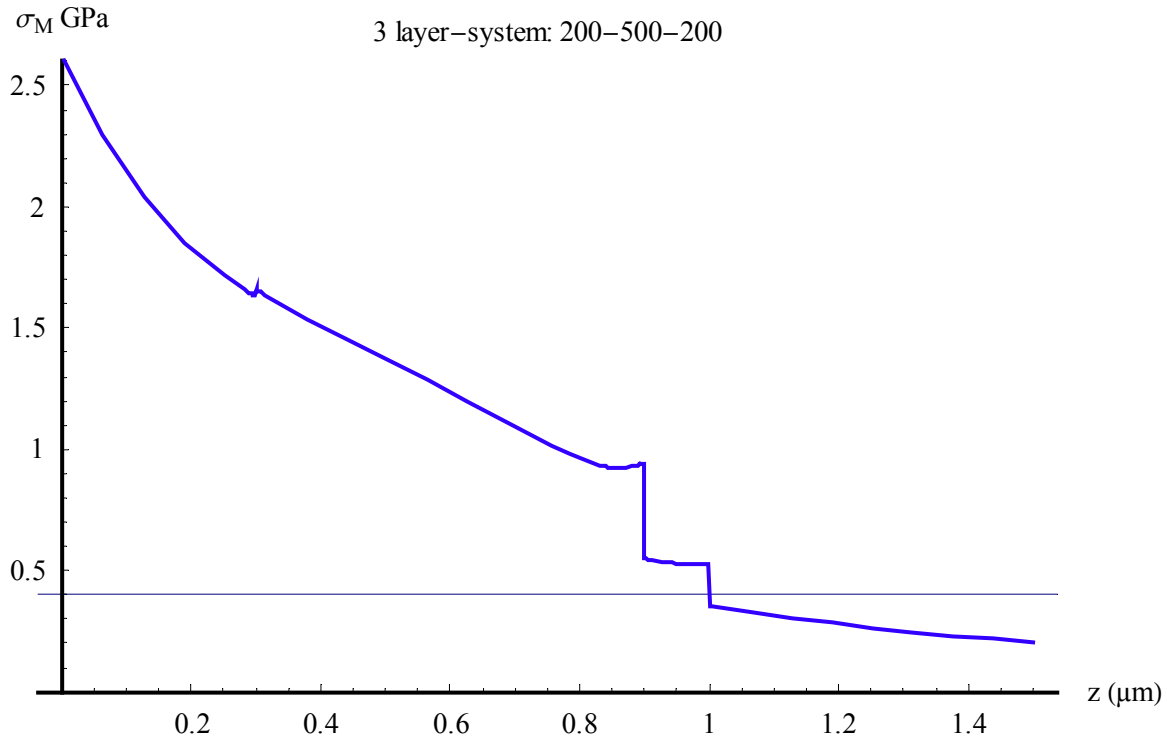

Figure 20: **Maximum values of the v. Mises stress at different depths for system 11. The thin horizontal „grid-line“ at 400MPa marks the yield strength of the Al-alloy.**

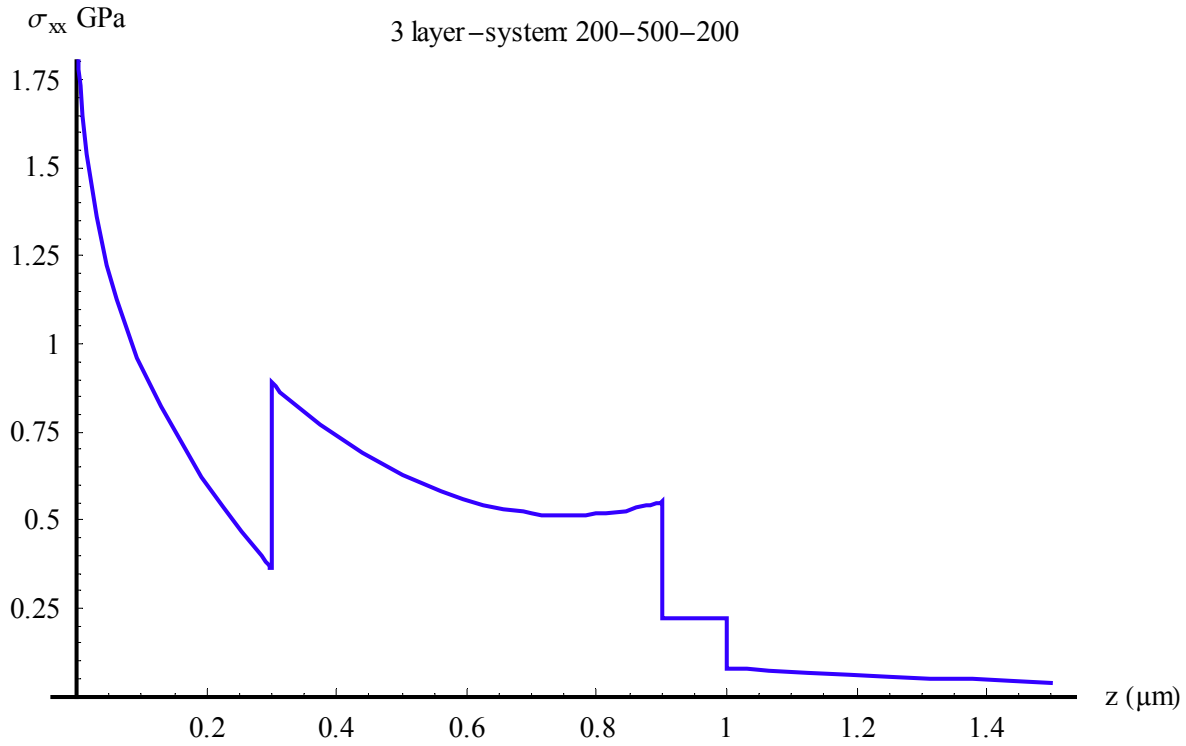

Figure 21: Maximum values of the σ_{xx} stress at different depths for system 11.

For any practical application one could state, that the systems are not well suited for asperity, especially small particle, contact. It is especially interesting that even the gradient coating with a Young's modulus function of

$$E(z) = E_{\max} - \frac{E_{\max} - E_S}{h} * z$$

does not provide a good protection. To the contrary on the surface both stresses (Mises and σ_{xx}) are far beyond their critical limits. This could be considered as some kind of "smoothed egg-shell-effect" compelling the "thin" uppermost parts (layers) of the gradient coating with the highest Young's modulus to sustain relatively large deformation, which would not occur if these high-Young's-modulus-parts were thicker. We can prove this easily by calculating the displacement in x-direction (see Figure 19) and see in fact, that the surface displacement of the 500GPa-part of the gradient layer is dramatically increased compared to the monolithic-film case.

In order to find a better coating structure we again built up a three-layer-coating of the shape similar to system 6. We stipulate the Young's modulus-structure as to be: 200GPa-500GPa-200GPa. Fitting the thickness of all three layers applying our mathematical model provides us with system 11. The results for the stresses are given in the Figure 20 and Figure 21. In all components the stresses are below their critical values.

In summary, under mixed mechanical load conditions with high tangential load components, a good protective coating system should have the principal structure proposed in Figure 22. The specific parameters determining this shape must be fitted to the known substrate and coating material properties and the load problem (application) in question.

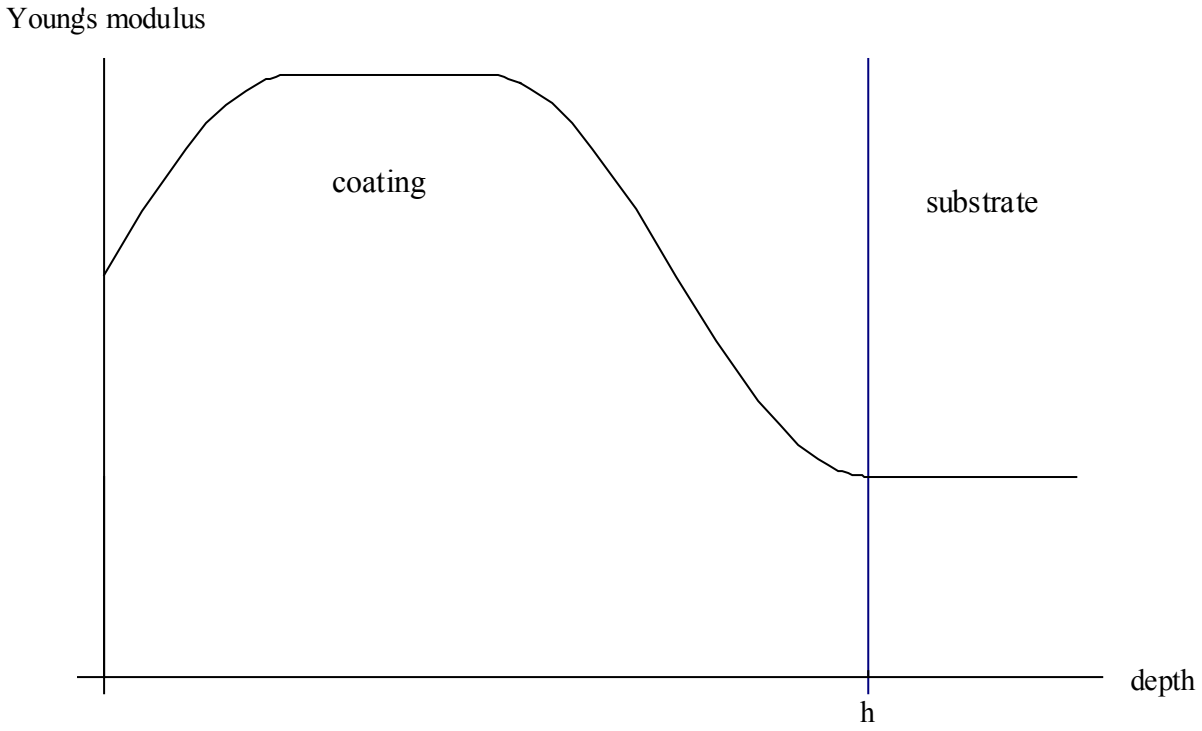

Figure 22: "Optimal" coating structure as proposed from the results of this chapter for pliant substrate materials and mixed (normal and shear) load conditions

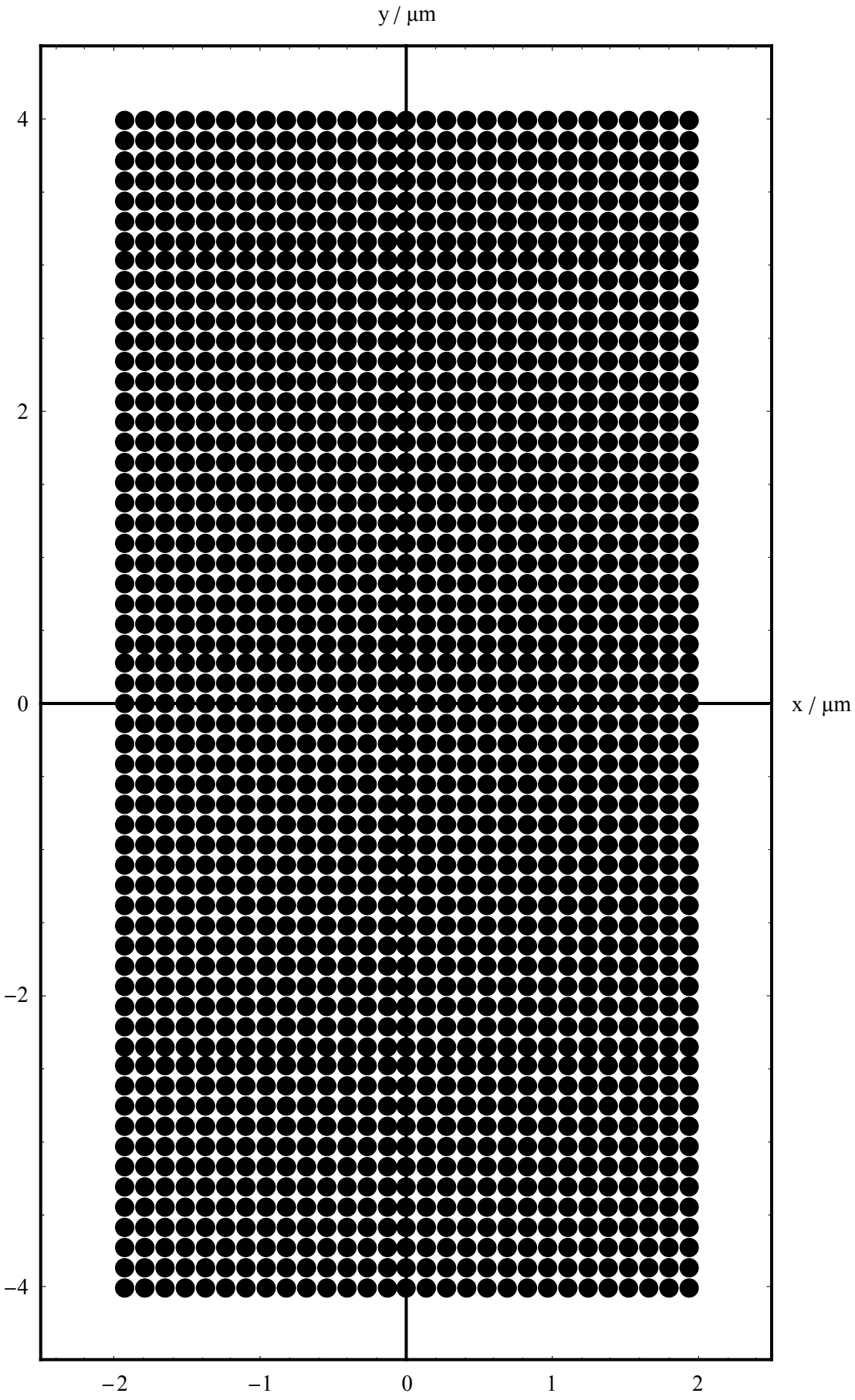

Figure 23: Rectangular array of Hertzian loads on a layered half space

3.2. Superposition of Hertzian Loads on Coating-Substrate-Compounds – Method to Treat a Variety of Contact Problems

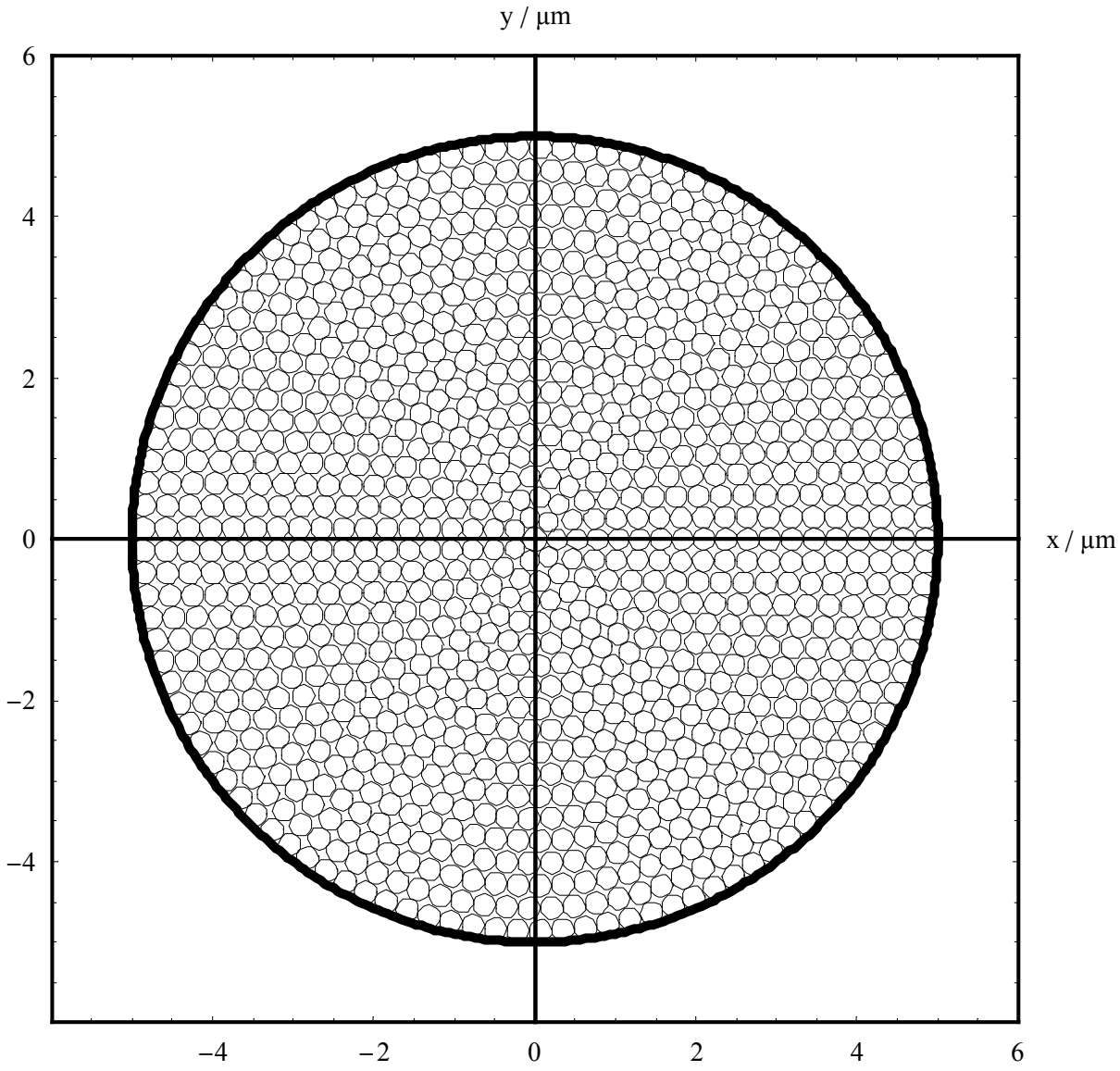

Figure 24: **Example for a circular array of load dots**

In order to investigate more complex contact problems one simply has to superpose the "basic solutions" mentioned above at as many different positions as necessary. This method, known in the literature as Boundary Element Method (BEM), provides an easy and fast running computational tool ***as long as*** the used "fundamental solution" is the correct one for the elastic space it is applied to. "Fundamental solution" here does not necessarily mean the point force solution but the solution for one single load dot (in this section for example we will only use Hertzian pressure distributions for the load dots). As long as this solution is complete and correct for the elastic body in question the pre-processing is a simple combination of these

fundamental solutions in suitable arrays. In general, BEM is not restricted to this simplicity (see e.g. [12]). There, because of the lack of correct solutions for the geometries one wants to investigate, "ill-adapted" fundamental solutions are applied and this requires cumbersome pre-processing and results very often in numerical instabilities and uncertainties. So it should be pointed out again, that within this section due to the combination of the method of image loads and superposition only correct fundamental solutions are used - even for inhomogeneous bodies. This is the principle difference to the general BEM.

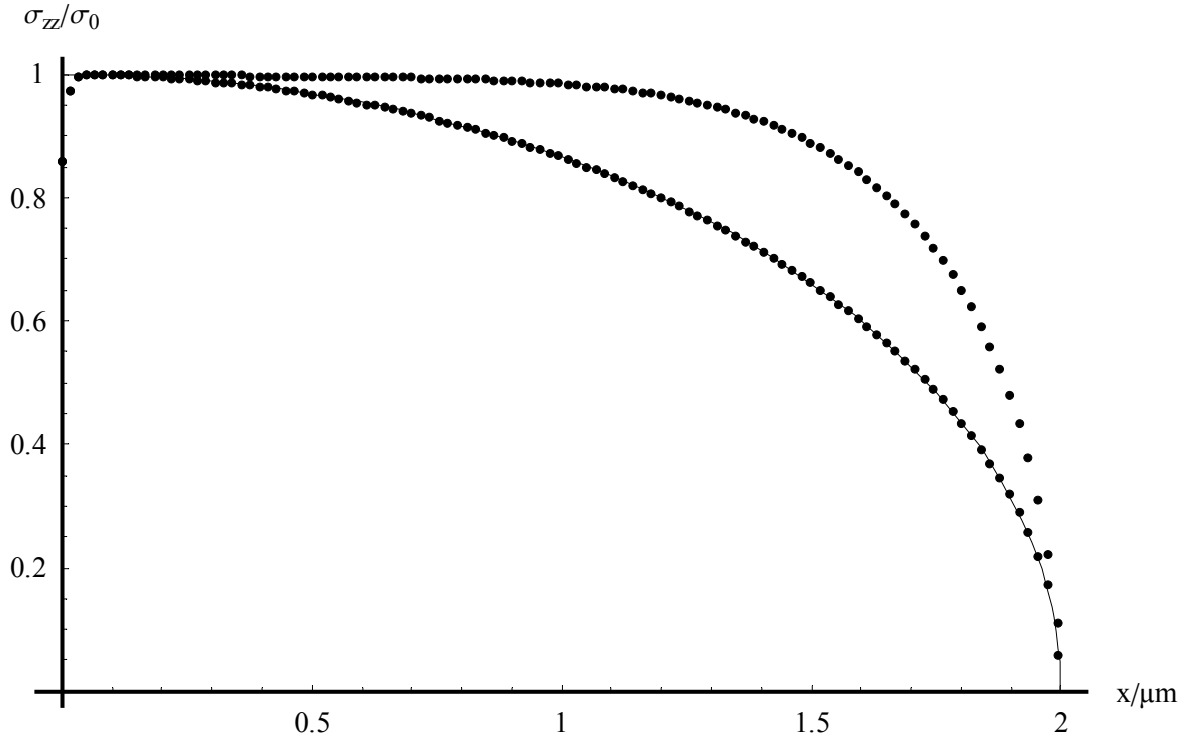

Figure 25: **σ_{zz} stress on the surface along the r-co-ordinate for a layered (according to Table 4) and a homogeneous material (lower curve of dots) loaded with a circular arrangement of load dots. The thin solid line gives the Hertzian stress distribution proportional to $\sqrt{a_{tot}^2 - r^2}$.**

Figure 23 shows one simple example. Here a rectangular array, assumed to be the contact region, is filled with a lot of small Hertzian loads. The resulting complete potential Φ has to be evaluated as a sum of all potential functions of the single loads:

$$\Phi = \sum_{\forall\ loads\ i} c_i \Phi_i = \sum_{\forall\ loads\ i} c_{kl} \Phi_{kl}\left(x - x_k, y - y_l, z\right). \tag{13}$$

This holds because the governing differential equation of linear elasticity is linear and so all its solutions are additive. In this section we will only use Hertzian loads. Its potential function P necessary to calculate the stresses and displacements are therefore given below (for more information see [8, 16] or [C1]):

$$P=\frac{\pi}{2}\left\{\begin{array}{l} z\left(2a^2+\frac{2}{3}z^2-r^2\right)\sin^{-1}\frac{a}{l_2}+\frac{1}{3}\left(a^2-l_1^{\,2}\right)^{1/2}\left(5r^2-2l_2^{\,2}-\frac{11}{3}l_1^{\,2}-\frac{10}{3}a^2\right) \\ +\frac{4}{3}a^3\ln\left[l_2+\sqrt{l_2^2-r^{\,2}}\right] \end{array}\right\}, \qquad (14)$$

3.2.1. Examples

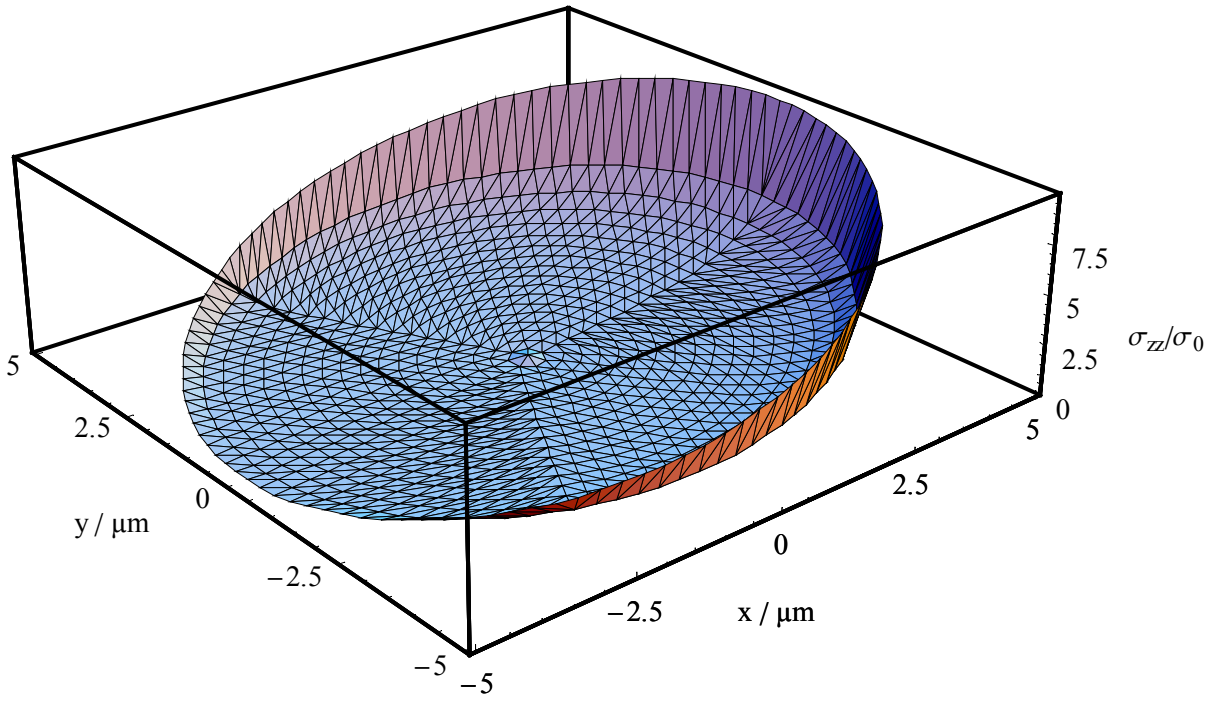

Figure 26: **σ_{zz} stress on the surface resulting from a tilted rigid flat circular punch acting on a half space**

In order to obtain a sufficiently fast evaluation process the basic calculation was done in C++ code. All calculations leading to the results presented below were performed using an "OmniBook XE_3" from Hewlett-Packard with a 850MHz Pentium III Processor and 256MB RAM. For each of the investigated contact problems none of the evaluations took longer than about 15 to 20 minutes (> 1000 load dots), even for some of the relatively complex layered half space cases and inverse calculations.

3.2.1.1. Paraboloidal indenters – circular contact areas

If one presses a rigid paraboloidal indenter into the surface of an isotropic elastic half space such, that the axis of the indenter is parallel to the surface normal, one should expect to obtain a circular contact region. We therefore construct a circular array of load dots as shown in Figure 24. Such an array may yield some geometrical artefacts resulting from the differences between the influence of dots in the centre's vicinity and those more outside on the

superposed displacement of the whole array. The character of the array should be therefore chosen very carefully and checked for agreement in the well known homogeneous half space case before it can be applied on more complex materials like layered ones.

For example we could apply an array of the following shape (c.f. Figure 24):

1. we place one single circle (n_1=1) in the centre,
2. we surround the centre circle by a proper amount n_2 of new equally sized circles such that they exactly fill the band around the centre circle,
3. we surround the band of circles by a proper amount n_3 of new equally sized circles such that they exactly fill the band around the already placed circles, a.s.o..

Calculating the number of circles for each band from:

$$n_i = const*(i-1)+1; \quad i=1,2,3,...,k \tag{15}$$

we have to evaluate the resulting radii a_i of the series of circles from:

$$\begin{aligned} a_1 &= a_{start} \\ a_i &= a_1 + \frac{\pi}{n_i - \pi}\sum_{j=2}^{i-1} 2\,a_j \end{aligned} \tag{16}$$

Setting const=6 and a_{start}=0.151321µm Figure 24 gives one example of such an array.

Table 4: Coating substrate system with relatively big Young's modulus ratio E_f/E_s=4

	Young's modulus	Poisson's ratio	Thickness
coating	200 GPa	0.25	1µm
substrate	50 Gpa	0.23	∞

Because of the symmetry of revolution the fit process can be simplified dramatically compared to the rectangular case (for the detailed description of the process in the case of a circular contact area see [50]). Applying now a rigid paraboloidal indenter with the surface shape given due to $w(r \le a_{tot}) \sim w_0 - r^2$ ($r^2=x^2+y^2$, a_{tot}=radius of the over all contact zone) we fit an array of k=110 which corresponds to a total number of 36.080 Hertzian load dots. If we set a_{start}=0.0094765µm we obtain the total radius of the whole array to a_{tot}=2µm. Figure 25 shows the result for the σ_{zz} stress (stress component normal to the surface) distribution for a homogeneous material and a composite with the parameters given in Table 4. Except for a few points in the very centre of the contact area the agreement of the fit for the homogeneous material with the Hertzian load function $\sigma_{zz}\big|_{z=0} \sim \sqrt{a_{tot}^2 - r^2}$ (thin solid line in Figure 25) is

very good. The fit for the layered material however shows a strong deviation from the Hertzian load.

Because of its importance on thin film measurement using spherical indenters the circular contact area case will be discussed in more detail elsewhere [50].

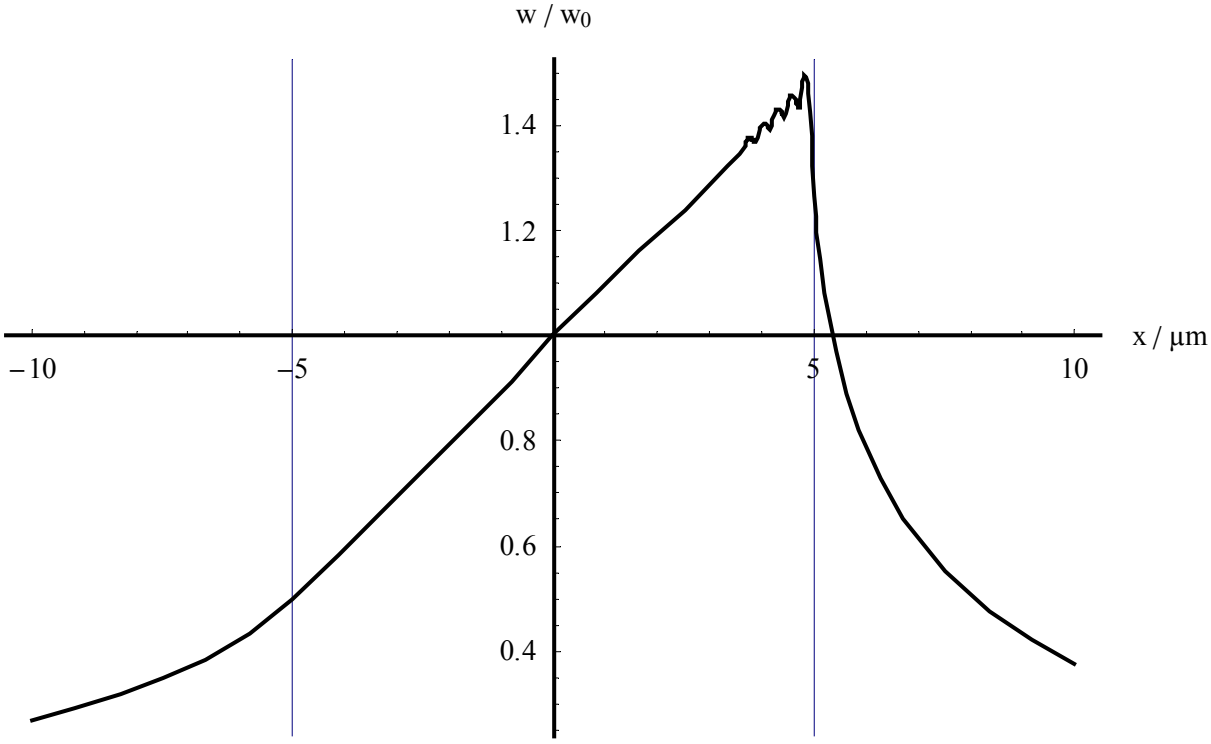

Figure 27: Displacement w normal to the surface resulting from a tilted rigid flat circular punch acting on a half space (see text)

3.2.1.2. Flat circular tilted punch with rounded edges

We now consider the following contact problem. A homogeneous half space is loaded with a rigid flat circular punch such, that the punch is tilted along the x axis. Figure 24 shows the geometrical conditions and the array of load dots applied in the BE-Model in order to solve the contact problem. Because of the tilting moment the symmetry is broken compared to the paraboloidal indenter case and so we have to consider all load dots[2]. Thus, we use a total number of 1045 dots with a Hertzian stress distribution for each of them. The resulting stress distribution (Figure 26) shows apart from a strong asymmetry the typical high stresses at the

[2] In fact there is one symmetry plane left (the y-axis) and this would allow one to reduce the size of the system of equations by a factor ½.

contact rim[3] except in the vicinity of the "raised" side, where it does not significantly exceed the stress in the centre of the contact. The rounded edge effect simply comes from the non singular stress distribution of the Hertzian load dots. We can see their individual influence particularly clear at the lowered side of the tilted indenter within the presentation of the displacement w in direction normal to the undeformed surface as presented in Figure 27.

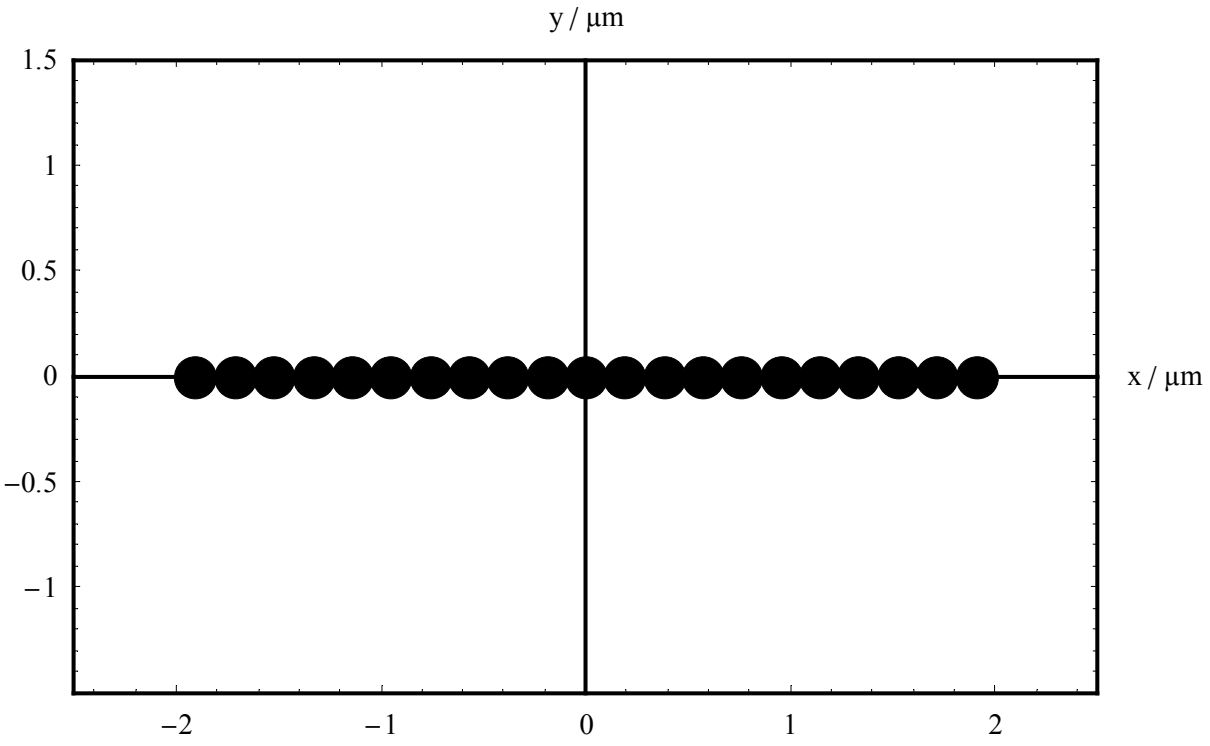

Figure 28: Linear arrangement of Hertzian loads on a layered half space

3.2.1.3. Contacts along one line

The next contact problem to be considered shall be an arrangement of load dots along a single line as shown in Figure 28. Assuming a parabolic displacement $w \sim w_0 - x^2$ along this line and setting as additional boundary conditions:

1. all load dots act with compressive normal stresses towards the surface,
2. at the contact rim the stress shall vanish,

we obtain the value of the constant w_0 (Figure 29) and the coefficients of our load dots array. We apply the method on the compound given in Table 5. The stress distribution along the line shows in contrary to the rectangular case - we discuss below - with an aspect ratio $a_y/a_x > 1$ a

[3] A real flat punch would produce a stress singularity at the rim but because we are working with an approach of Hertzian loads we rather investigating the problem of a punch with a rounded and not a sharp edge.

slightly sharper maximum at the contact centre compared to the Hertzian distribution (Figure 30).

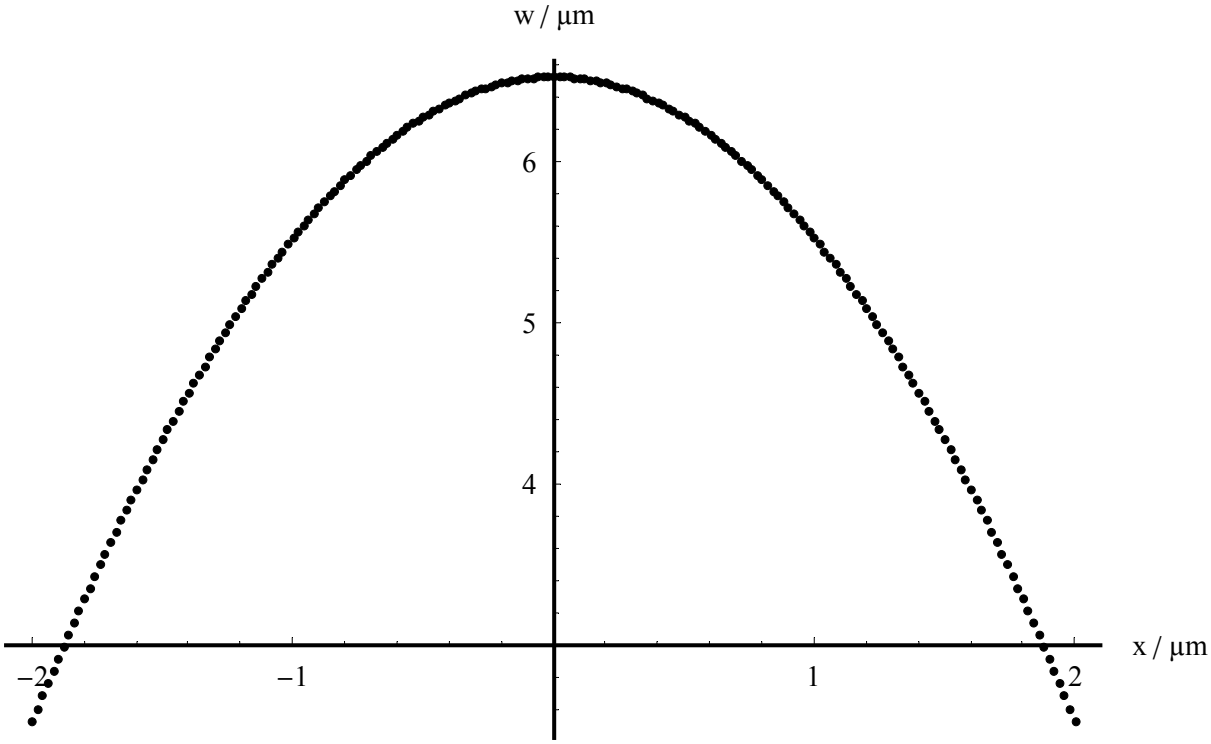

Figure 29: **Resulting displacement w for a linear arrangement of Hertzian loads on a layered half space**

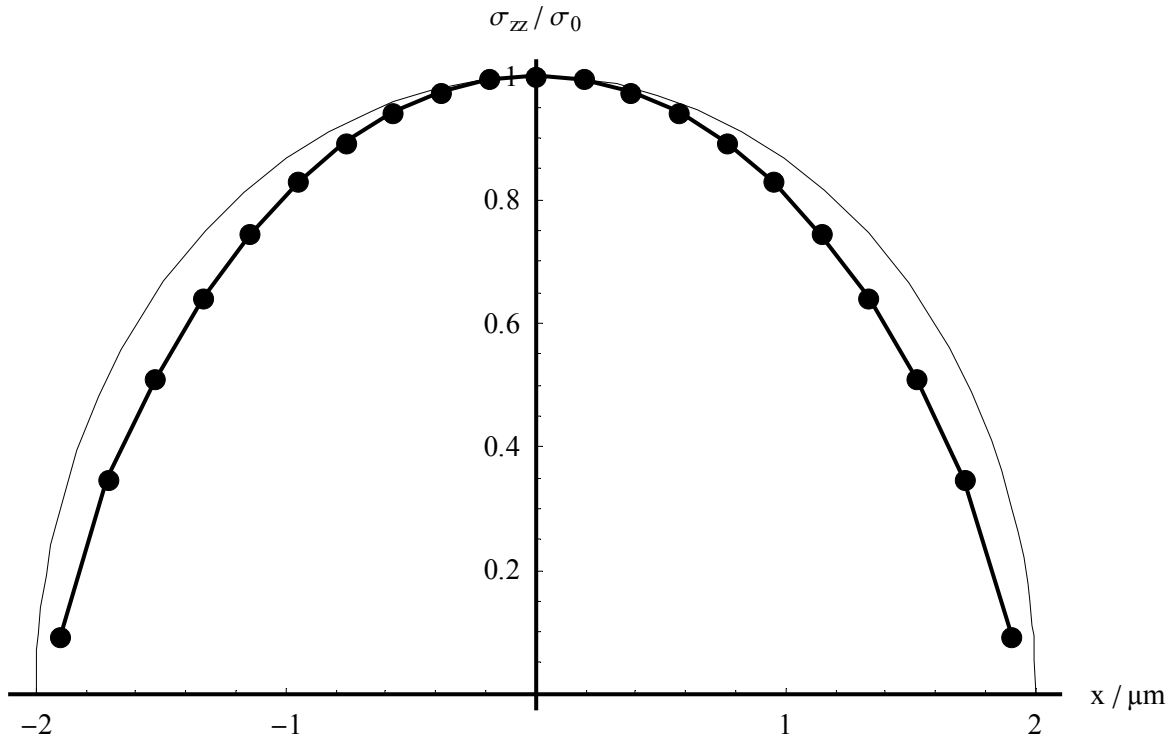

Figure 30: **σ_{zz} stress on the surface along the x-axis for a layered material according to Table 5 loaded with a linear arrangement of load dots (dotted line). The thin solid line gives the Hertzian stress distribution proportional to $\sqrt{a_x^2 - x^2}$.**

Table 5: Coating substrate system with huge Young's modulus ratio of E_f/E_s=16

	Young's modulus	Poisson's ratio	Thickness
coating	800 GPa	0.22	1µm
substrate	50 Gpa	0.25	∞

3.2.1.4. Rectangular Array of Hertzian loads

As an other application of the new fundamental solutions we superpose several Hertzian loads within a square and solve the contact problem for a rigid indenter of the shape given due to the equation $s=w_0-x^2$ (see Figure 31). The contact shall be without friction. Within the contact zone $-a_x \le x \le a_x$; $-a_y \le y \le a_y$ the coefficients c_i have to be determined by fitting the displacement in z direction w to the shape of the indenter, which yields:

$$\begin{pmatrix} \left[w_0 - x^2 \right]_{\substack{-a_x \le x \le a_x \\ -a_y \le y \le a_y}} \\ 0 \end{pmatrix} = \begin{pmatrix} \left[\sum_{\forall\ loads\ inside} c_i \frac{\partial \Phi_i}{\partial z} \right]_{\substack{-a_x \le x \le a_x \\ -a_y \le y \le a_y}} \\ c_i \mid \forall\ loads\ outside \end{pmatrix} \tag{17}$$

The fit has to be performed such that at first all surface stresses should be compressive and second that all coefficients making loads outside the contact area should vanish.

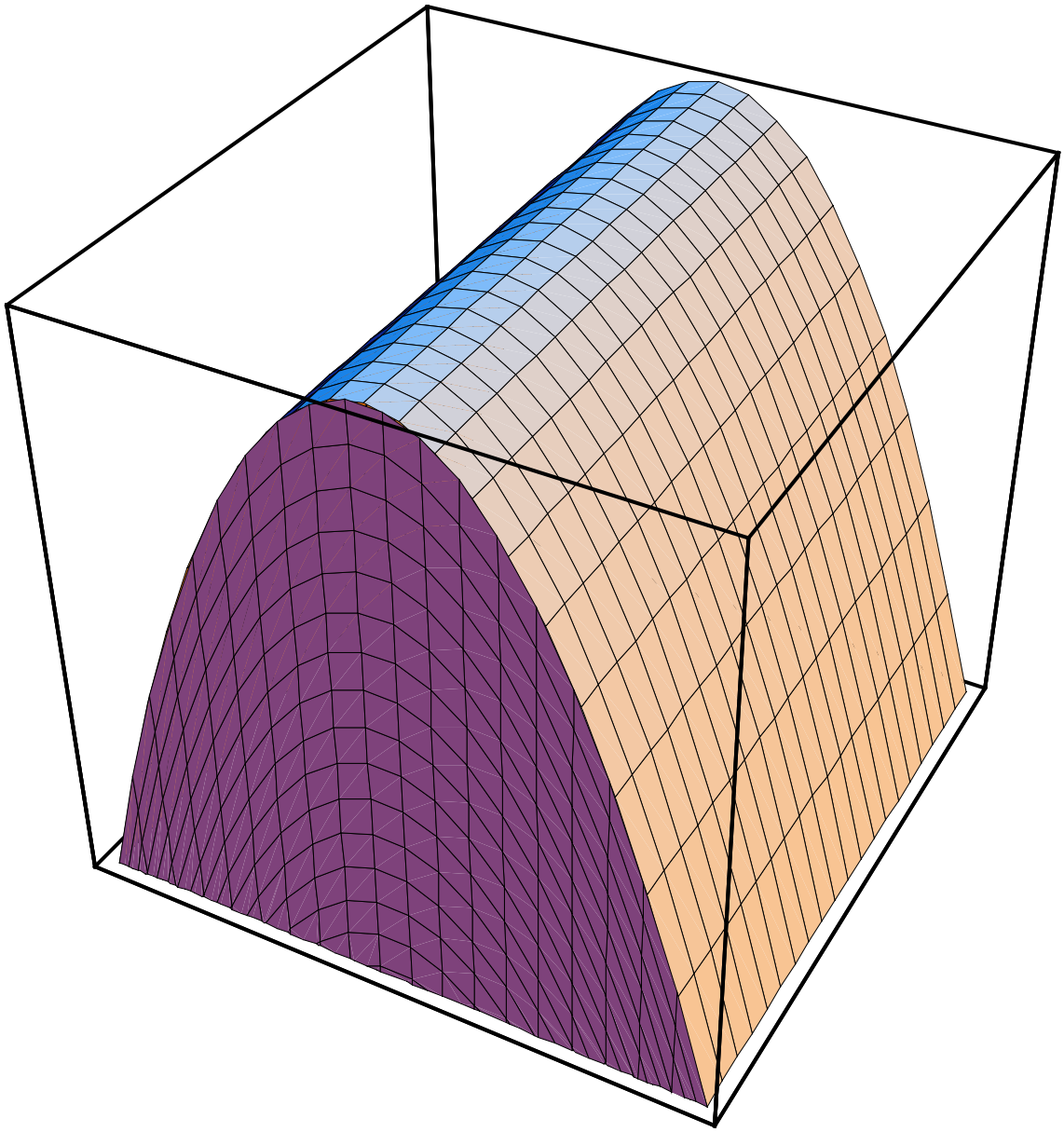

Figure 31: Shape of the indenter used in the examples with an rectangular contact area

These conditions provide the value of the so far unknown constant w_0. The fitting process can be separated into the following steps:

1. The array of load dots is built with suitable radii a_s according to the necessity of filling the whole contact region sufficiently dense with "contact elements". The co-ordinates of the load dot's centre are calculated from:

$$\begin{aligned} &k_{ij} = \left(x_i, y_j\right), \\ &x_i = a_s - a_x + i * \Delta x; \quad i = 1,2,...n_x; \quad \Delta x = 2a_s, \\ &y_j = a_s - a_y + j * \Delta y; \quad j = 1,2,...n_y; \quad \Delta y = 2a_s. \end{aligned} \tag{18}$$

2. We built a linear system of equations by giving w_0 a starting point and calculating equation (17) at as many points as coefficients c_i of load dots laying within the contact

zone have to be determined (one can use for example the co-ordinates of the load dot's centres).

3. The resulting system of equations has to be solved with respect to the c_i.
4. The process has to be repeated by successively seeking for a proper w_0 in order to fulfil the requirements of the above mentioned contact boundary conditions.

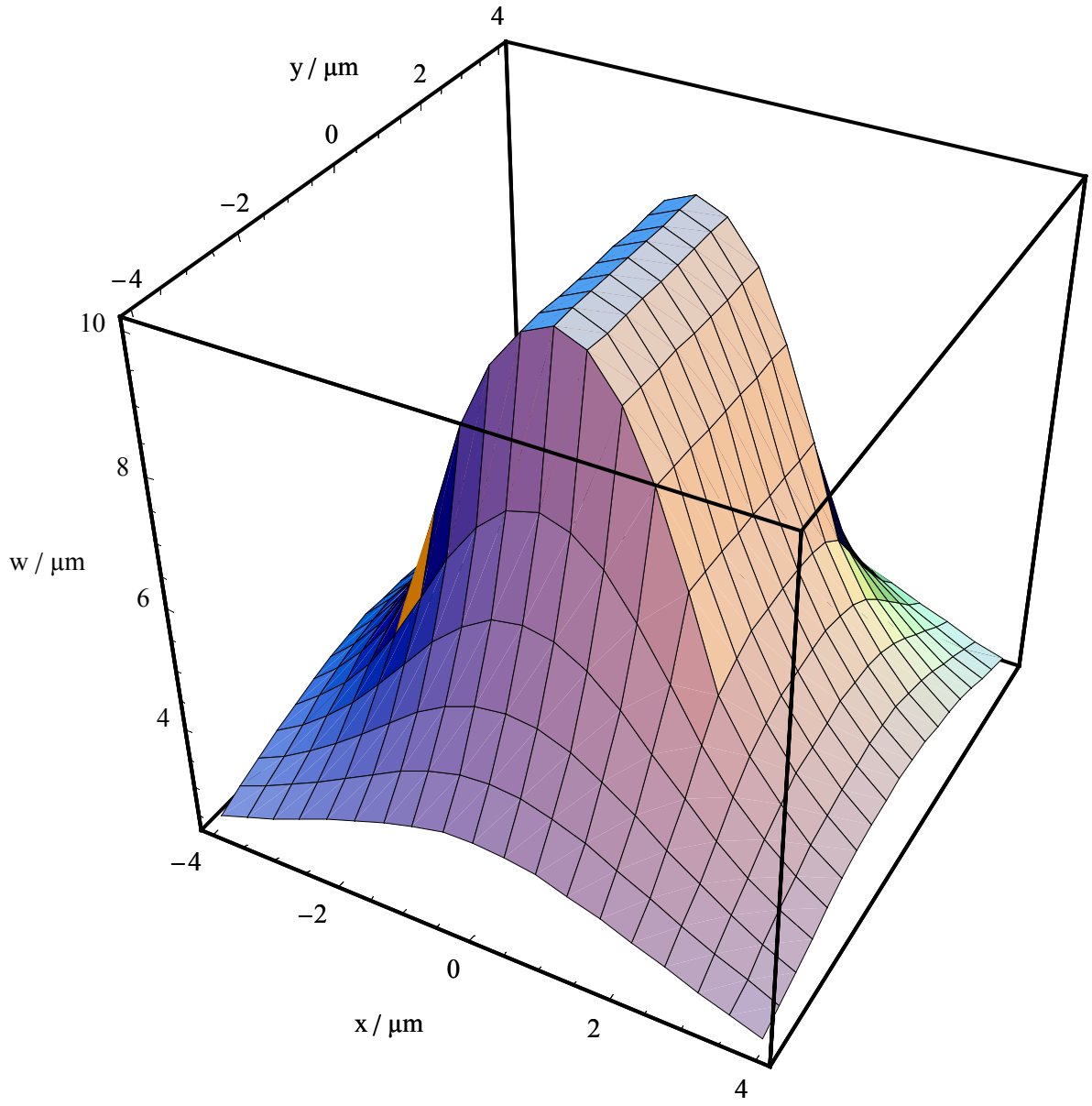

Figure 32: Surface displacement resulting from an indenter of the shape given in the figure above with the contact area $a_x=a_y=2\mu m$

In the case of a homogeneous material (half space) the potentials Φ_i can be given due to equation (14). Here however we again want to apply the method on a simple layered material with the parameters given in Table 5.

The fit performed according to equation (17) yields all loads' coefficients and thus gives us an approximation of the whole elastic field which is as correct as good the resolution of our loads array has been. Choosing now a concrete example, namely $a_x=a_y=2\mu m$ Figure 32 gives the surface displacement in the vicinity of the contact area. The absolute height of the displacement w may be considered as arbitrary because it can be changed easily by applying a constant factor to all c_i which coincides with changing the total force resulting from all load dots.

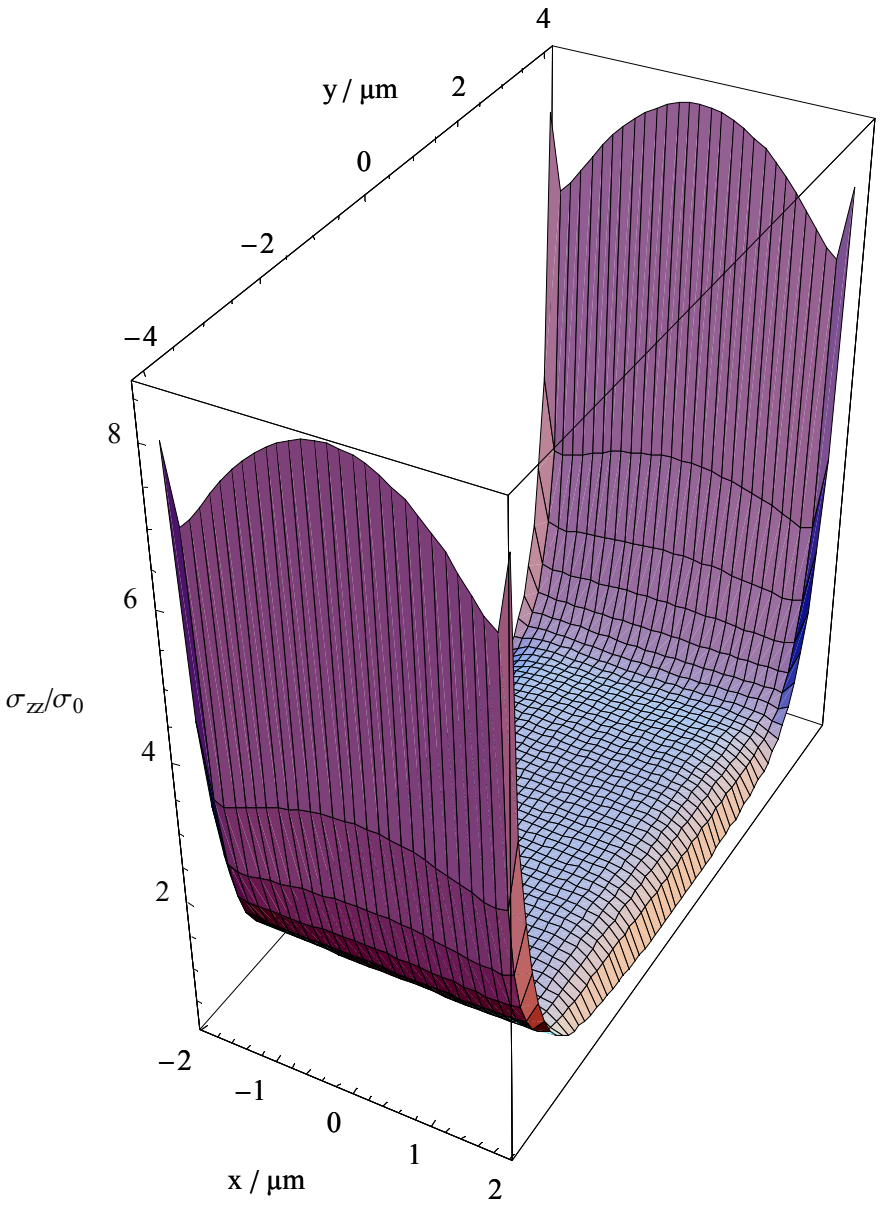

Figure 33: **σ_{zz} stress on the surface within the contact area for a layered material according to Table 5 loaded with a rectangular array of load dots**

Figure 33 shows the surface stress distribution of an rectangular array with the aspect ratio $2*a_x=a_y=4\mu m$ (Figure 23) below the indenter. The array has a resolution of 29 x 59 load dots in x and y direction, respectively (1711 dots in total). The stress is shown normalised to the

stress in the centre σ_0 at x=y=0. At the sharp edges of the indenter (y=-4µm and y=4µm) the fit provides "singular" stresses similar to those known from the flat punch [8]. But according to the discussion of the flat tilted punch above we here do not have sharp edges. In fact because of the usage of singular Hertzian loads our edges could be considered as rounded and slightly perforated like the rim of a stamp. In order to obtain sharper edges one simply has to increase the amount of Hertzian load dots at the contact's rim. The stress distribution along the y-axis in the layered case (Figure 34) shows a distinct deviation from the Hertzian load distribution we have obtained for the homogeneous case (Figure 35). In tendency this deviation agrees with the results known from Gupta and Walowit who have investigated two dimensional contact problems for layered materials [3]. However, their results for the stress distribution were a bit more "peculiar" (as they called the deviation from the Hertzian shape) then ours, but of course we can not expect to obtain a complete quantitative agreement because we are neither considering infinite line contacts nor can we arbitrarily increase the aspect ratio a_y/a_x and thereby maintaining a sufficiently high density of load dots.

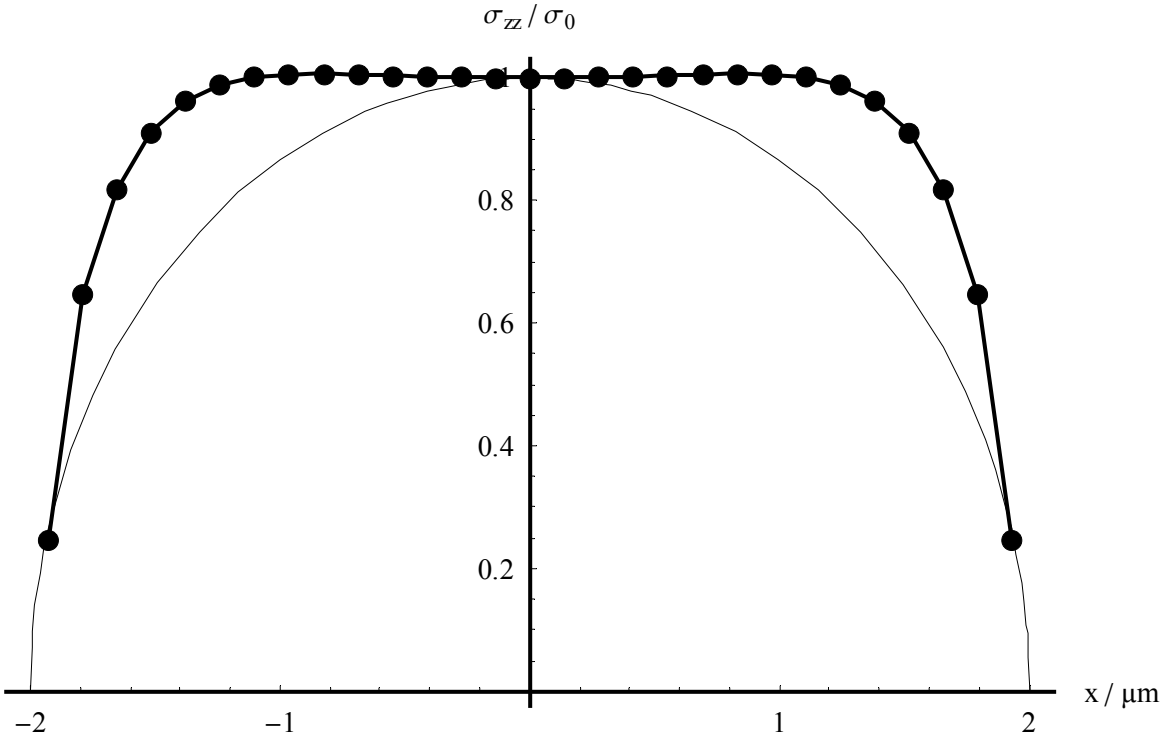

Figure 34: **σ_{zz} stress on the surface along the x-axis for a layered material according to Table 5 loaded with a rectangular array of load dots (dotted line). The thin solid line gives the Hertzian stress distribution proportional to $\sqrt{a_x^2 - x^2}$.**

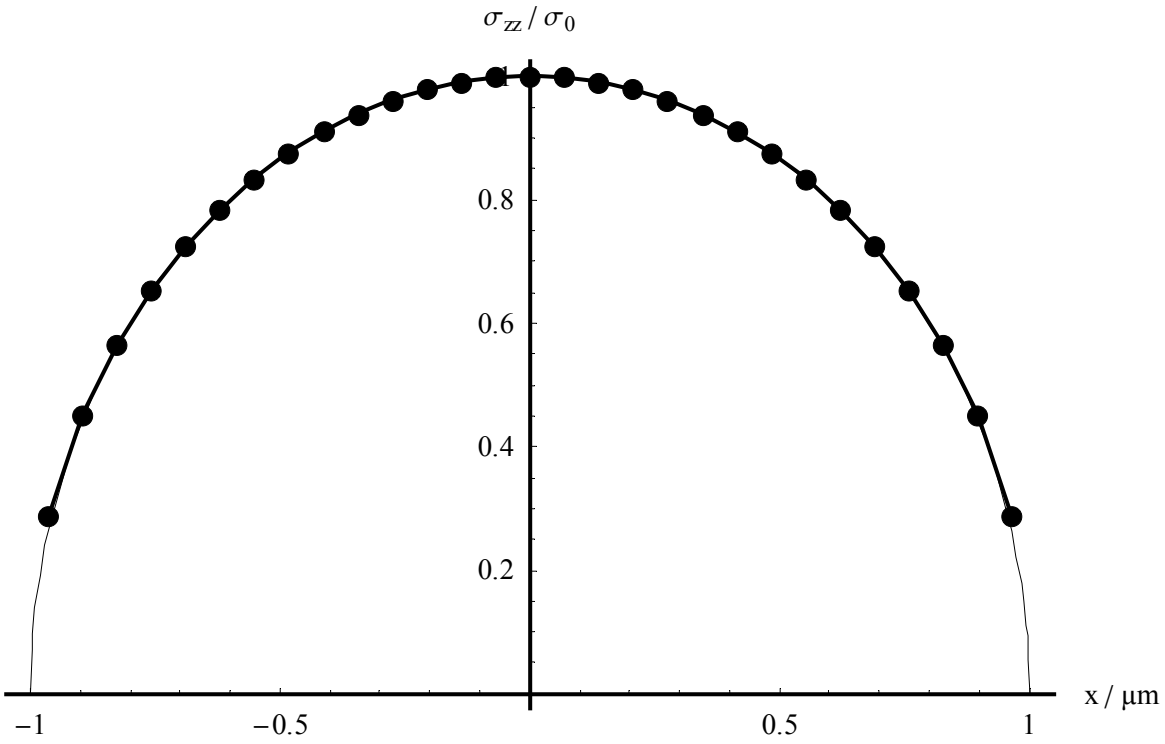

Figure 35: **σ_{zz} stress on the surface along the x-axis for a homogeneous material loaded with a rectangular array of load dots (dotted line). The thin solid line gives the Hertzian stress distribution proportional to $\sqrt{a_x^2 - x^2}$.**

3.3. A Method of determining intrinsic stresses in layered materials via nanoindentation – the question of in principle feasibility

The problem of measuring intrinsic stresses in monolithic materials using nano-indentation techniques has been proved experimentally possible by Swadener, Taljat and Pharr ([44] and 45]). Here we discuss the possible application of this method on the measurement of intrinsic thin-film-stresses.

3.3.1. Pure normal loading with spherical indenters

3.3.1.1. Taking the substrate as indicator

We propose the following 5-step procedure:

1. The mechanical parameters of the – uncoated - substrate including the critical v. Mises stress for the beginning plastic flow are determined using for example spherical tip nanoindentation (see e.g. [23]),

2. After deposition of the coating: Determination of the elastic properties of the coating (Young's modulus) using again spherical tip nanoindentation (instrinsic stresses do not influence this value) and its thickness,

3. Chosing an indenter tip radius big enough to ensure that plastic deformation will first occur only within the substrate,

4. Determination of the beginning of plastic flow in the substrate due to periodic loading and unloading as proposed by Swain (see e.g. [23]),

5. Now we have to add the two elastic fields resulting from the intrinsic stresses σ_{ij}^{I} and the nanoindenter loading σ_{ij}^{L}. The von Mises stress can be written in the following from:

$$\sigma_M = \sqrt{\frac{1}{2}\left(\left(\sigma_{xx}-\sigma_{yy}\right)^2+\left(\sigma_{zz}-\sigma_{yy}\right)^2+\left(\sigma_{xx}-\sigma_{zz}\right)^2+6*\left(\tau_{xy}^2+\tau_{xz}^2+\tau_{zy}^2\right)\right)}$$

with $\sigma_{ij}=\sigma_{ij}^{I}+\sigma_{ij}^{L}$. Because according to our approach (12) for the intrinsic stresses we can write the intrinsic stress field as $\sigma_{ij}^{I}=\sigma_{rr}^{f}*f_{ij}^{I}\left(x,y,z\right)\equiv\sigma_{rr}^{f}*f_{ij}^{I}$ with a suitable function f(x,y,z) we result in the following equation for the measured critical von Mises stress:

$$\sigma_M^{crit} = \sqrt{\frac{1}{2}\begin{pmatrix}\left(\sigma_{xx}^{L}-\sigma_{yy}^{L}+\sigma_{rr}^{f}\left(f_{xx}^{I}-f_{yy}^{I}\right)\right)^2+\left(\sigma_{zz}^{L}-\sigma_{yy}^{L}+\sigma_{rr}^{f}\left(f_{zz}^{I}-f_{yy}^{I}\right)\right)^2\\+\left(\sigma_{xx}^{L}-\sigma_{zz}^{L}+\sigma_{rr}^{f}\left(f_{xx}^{I}-f_{zz}^{I}\right)\right)^2\\+6*\left((\tau_{xy}^{L}+\sigma_{rr}^{f}f_{xy}^{I})^2+(\tau_{xz}^{L}+\sigma_{rr}^{f}f_{xz}^{I})^2+(\tau_{zy}^{L}+\sigma_{rr}^{f}f_{zy}^{I})^2\right)\end{pmatrix}}.$$

From this we can easily obtain a formula for the intrinsic film stress σ_{rr}^{f}:

$$\sigma_{rr}^{f} = \frac{\begin{pmatrix}-6\left(f_{xy}^{I}\tau_{xy}^{L}+f_{xz}^{I}\tau_{xz}^{L}+f_{yz}^{I}\tau_{yz}^{L}\right)+f_{xx}^{I}\left(-2\sigma_{xx}^{L}+\sigma_{yy}^{L}+\sigma_{zz}^{L}\right)\\+f_{yy}^{I}\left(-2\sigma_{yy}^{L}+\sigma_{xx}^{L}+\sigma_{zz}^{L}\right)+f_{zz}^{I}\left(-2\sigma_{zz}^{L}+\sigma_{yy}^{L}+\sigma_{xx}^{L}\right)\end{pmatrix}}{\pm\sqrt{\begin{pmatrix}4\begin{pmatrix}f_{xx}^{I\,2}+f_{yy}^{I\,2}+3\left(f_{xy}^{I\,2}+f_{xz}^{I\,2}+f_{yz}^{I\,2}\right)\\-f_{yy}^{I}f_{zz}^{I}+f_{zz}^{I\,2}-f_{xx}^{I}\left(f_{yy}^{I}+f_{zz}^{I}\right)\end{pmatrix}\\*\begin{pmatrix}\sigma_M^{crit\,2}-\sigma_{xx}^{L\,2}-\sigma_{yy}^{L\,2}-3\left(\tau_{xy}^{L\,2}+\tau_{xz}^{L\,2}+\tau_{yz}^{L\,2}\right)\\+\sigma_{yy}^{L}\sigma_{zz}^{L}-\sigma_{zz}^{L\,2}+\sigma_{xx}^{L}\left(\sigma_{yy}^{L}+\sigma_{zz}^{L}\right)\end{pmatrix}\\+\begin{pmatrix}-6\left(f_{xy}^{I}\tau_{xy}^{L}+f_{xz}^{I}\tau_{xz}^{L}+f_{yz}^{I}\tau_{yz}^{L}\right)+f_{xx}^{I}\left(-2\sigma_{xx}^{L}+\sigma_{yy}^{L}+\sigma_{zz}^{L}\right)\\+f_{yy}^{I}\left(-2\sigma_{yy}^{L}+\sigma_{xx}^{L}+\sigma_{zz}^{L}\right)+f_{zz}^{I}\left(-2\sigma_{zz}^{L}+\sigma_{yy}^{L}+\sigma_{xx}^{L}\right)\end{pmatrix}^2\end{pmatrix}}}{2\begin{pmatrix}f_{xx}^{I\,2}+f_{yy}^{I\,2}+3\left(f_{xy}^{I\,2}+f_{xz}^{I\,2}+f_{yz}^{I\,2}\right)\\-f_{yy}^{I}f_{zz}^{I}+f_{zz}^{I\,2}-f_{xx}^{I}\left(f_{yy}^{I}+f_{zz}^{I}\right)\end{pmatrix}}. \qquad (19)$$

In order to estimate the accuracy necessary to measure σ_{rr}^{f} via nano-indentation we again use the parameters of Table 1 and assume a very plate-like substrate with a side length of 10mm.

Now we apply our approach (12) and use a Fourier series in order to describe constant shear loading $\sigma_{xz} = \sigma_{yz} = const$ on the substrate surface. We find, that a relatively high σ_{rr}^{f} value of –10GPa would produce a maximum von Mises stress of about 0,2GPa directly at the interface under the coating. The elastic substrate parameters given in Table 1 are those from silicon. From publications concerning spherical indentation of coated Si substrates [25] we know that Si suffers plastic deformation at a von Mises stress of 11.3 GPa. This corresponds approximately to the hardness of Si [25]. Because we need to chose the indenter such that the maximum of the von Mises stress occurs close to the interface (biggest influence of the intrinsic stresses) we could apply a 25µm diamond indenter pressed into the compound with about 370mN in the intrinsic-stress-free case and about 345mN in the pre-stressed case to reach plastic deformation. The coating which we assume to be TiN with a critical von Mises value of about 15GPa will behave completely elastically during the indentation. Exact calculation of the combined stress fields and applying equation (19) yields an accuracy of the depth measurement of at least 20nm (The difference between both cases is about 25nm). But because this does not simply mean the absolute position of the indenter tip but the detection of the depth of beginning plastic flow due to periodic loading partial unloading this seems very difficult to be achievable. However, perhaps if the substrate material would have a much lower critical von Mises stress being in the order of the intrinsic stress it might be possible to measure this influence. We therefore repeat the calculation with the following (academic) substrate: Al-alloy with 70GPa Young's modulus and 400MPa critical von Mises stress (c.f. Table 3). All other parameters are the same as in the example above. The maximum intrinsic stress below the coating would now be approximately 90MPa. Now we would use a 5µm diamond indenter and apply a force of about 2mN. The minimum accuracy with which the critical depth of beginning plastic flow should be detected would be approximately 4nm (at a total penetration depth of 20 to 25 nm). This is again an accuracy which can not be achieved using standard nano-indenter equipment not to mention the other error sources like surface roughness, non spherical tip-shape, etc.. Thus, it has to be concluded, that normal indentation and using the substrate as the "indicator" does not seem to be a suitable method to determine intrinsic coating stresses except for a few "academic" examples.

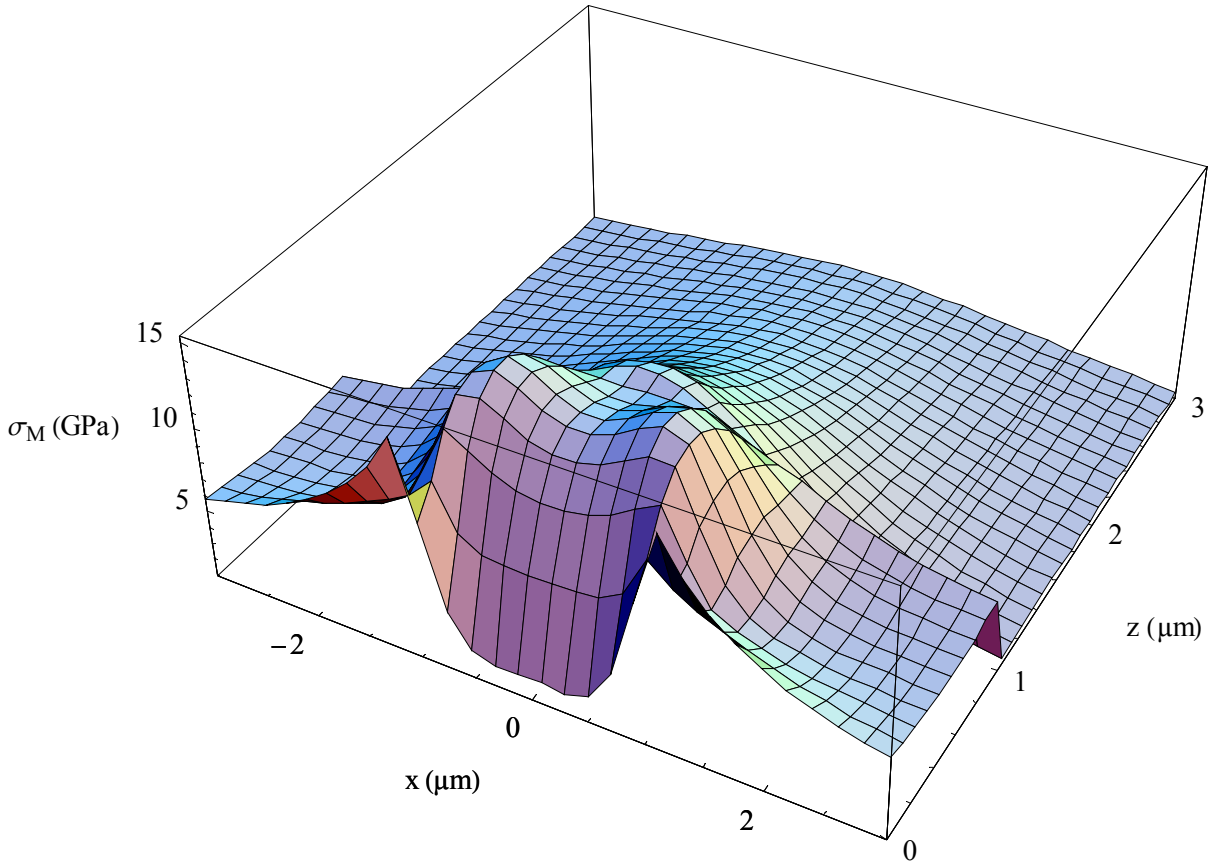

Figure 36: **von Mises stress for the system given in Table 1 at a load of 72mN with a contact radius of 1μm and an intrinsic film stress of $\sigma_{rr}^{f} = -10GPa$.**

3.3.1.2. Taking the coating as indicator

However the relatively small effect of the intrinsic film stress on the substrate does not mean that its effect would be completely insignificant. On the example of the von Mises stress distribution one can see (Figure 36 and Figure 37) that the influence is quite dramatic but simply more on the shape of the distribution of the von Mises stress rather than their absolute values. The figures show for both cases the situation “around” the yield point (a critical value of 15GPa is assumed for the coating) and regarding them it becomes clear, that the plastic regions would also take completely different shapes. The value of the total force has been chosen such that the three dimensional presentation shows clearly v. Mises stresses above the assumed yield point of 15GPa within the coating. This is motivated by the discussion of the probable shape of the plastic zone. Absolute values of the moment of beginning plastic flow will be considered later. Assuming the substrate material to be silicon with a critical v. Mises

stress of about 11.3GPa no plastic flow should occur there in the contact situations considered here.

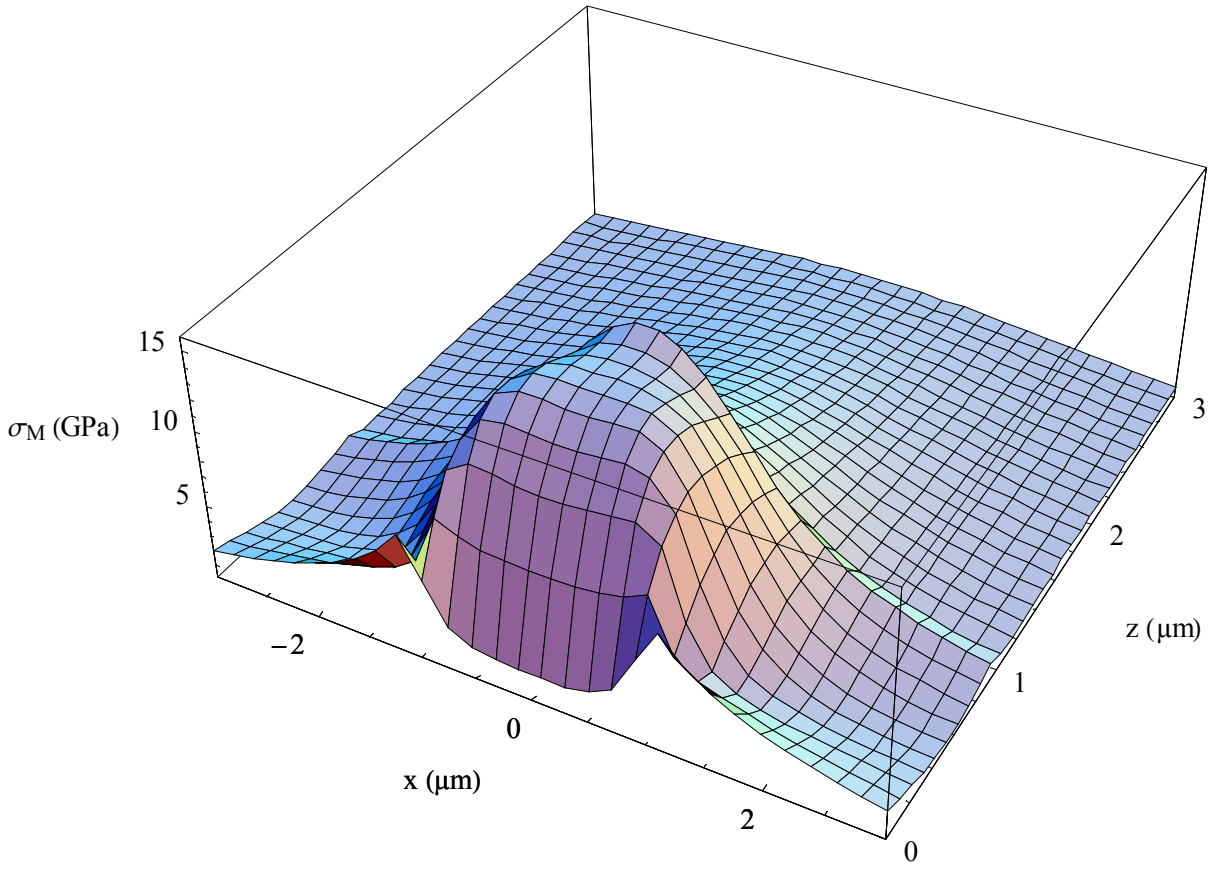

Figure 37: **von Mises stress for the system given in Table 1 at a load of 54mN with a contact radius of 1µm ($\sigma_{rr}^{f} = 0$)**

Despite the fact that we here consider layered materials the difference in the shape agrees principally with the results given in [44] and [45] where "the location of first yielding is expected to switch from beneath the surface on the axis of symmetry to the contact periphery at the surface". Finite Element calculations have been used in [44] to examine this effect. In fact, a strongly increased maximum at the surface can be detected in the intrinsic-stress case comparing Figure 36 and Figure 37, but caused by the layered structure we observe a torus-like maximum also at the interface. This deviation from the non-intrinsic stress state should be visible in the load-depth-curves. One can deduce this especially because the normal stress distribution below the indenter is of course different for different shapes of plastic zones and the propagation of their boundary (c.f. [46]). A piece of circumstantial evidence can be obtained from purely elastic considerations. Such a consideration should be valid as long as

the elastic strains are large compared to the plastic strains. During nano-indentation the mean or average pressure p_m (c.f. [45]) is measured indirectly via the total Force F. The latter determines in addition the factor of normalization for the elastic field due to the following equation:

$$F = 2\pi \int_0^a \sigma_{zz}\big|_{z=0} r dr; \quad p_m = \frac{F}{\pi a^2}, \tag{20}$$

where we have assumed a contact region of symmetry of revolution with the radius a. This determines also the field of displacements. In order to see the effect of different surface stress distributions we chose the following - somewhat extreme - example: In the elastic regime the two stress distributions $\sigma_{zz}\big|_{z=0} \sim \sqrt{a^2 - r^2}$ and $\sigma_{zz}\big|_{z=0} \sim r^2\sqrt{a^2 - r^2}$ would result in a displacement at the contact center of $w = \frac{3\pi F}{4a} H$ and $w = \frac{15\pi F}{32a} H$, respectively (H is a constant). This shows that one could in fact expect a relatively strong influence on the measured displacement if the stress distribution below the indenter changes. Staying completely in the elastic regime this could only happen in such peculiar situations where the indenter suddenly changes its shape or material anywhere below the indenter starts to disappear or being moved. But the latter definitively is the case at the moment of plastic flow initiation. Thus, different shapes of plastic zones (resulting from different intrinsic stresses) should effect the load-depth-curves in a measurable manner but analyzing this correctly and quantitatively would require an elastic-plastic approach, which is not available yet in a closed form model. However, in [45] half empirical combined with FE methods have been applied with great success on pre-stressed monolithic Al-alloy specimens. There the effect of the changed load-depth-curves has been measured due to comparing the results of the stressed specimen with unstressed reference samples. So, one could suggest to use reference samples with well defined stress states also in the case of coating-substrate-compounds. But in practice this could only mean deposition of thin bendable substrates parallel to the substrates one is interested. Apart from the fact that this is simply not possible because not all substrate materials are available in a plate like shape this would mean an additional inconvenient step of investigation. In order to avoid this we suggest an other experimental approach.

3.3.2. Mixed normal and tangential loading

The reader may find a relatively comprehensive consideration of “mixed” loading on layered materials in [C3].

Assuming that we posses a lateral force nano-indenter allowing us to measure normal and tangential forces and displacements as accurate as the normal loads and displacements alone with the standard nano-indenters the author proposes the measurement of intrinsic stresses as follows.

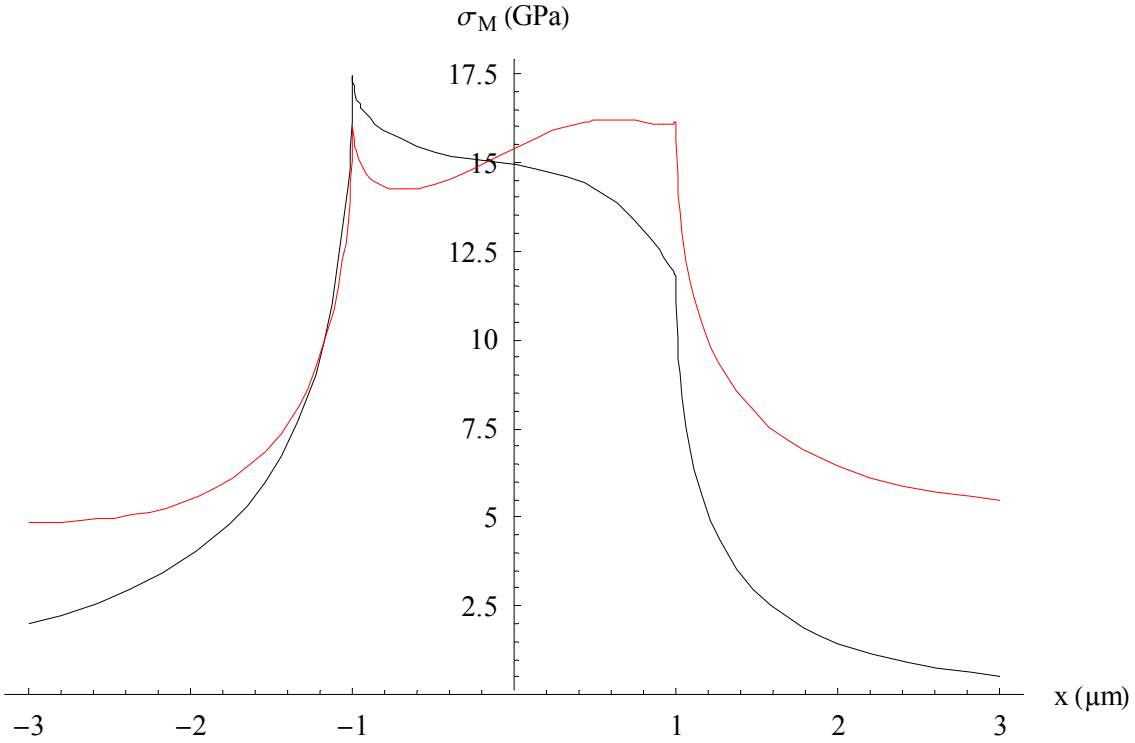

Figure 38: von Mises stress for the system given in Table 1 at a normal load of 30mN (friction coefficient 0.6) with a contact radius of 1μm (black: $\sigma_{rr}^f = 0$, red: $\sigma_{rr}^f = -10$)

- At first the critical v. Mises stress is determined using only normal loading. The indenter has to be chosen such, that the radius of the contact region is approximately equal to the film thickness. From Figure 36 and Figure 37 we see that we would obtain plastic flow at 72mN for the intrinsic-stress-case and at only 54mN for the non-intrinsic-stress case. So, a relatively big difference occurs between the two cases for pure normal loading.
- But if we add a tangential force component (more than 1/2 of the normal force) the maximum of the v. Mises stress moves to the surface and we reach the critical value at almost the same force for both the stressed and the unstressed case.

This means determination the critical v. Mises stress due to mixed loading with sufficient high portions of tangential loads gives us a yield stress almost independent on the σ_{rr}^f provided we have chosen the correct geometrical contact conditions (contact radius a being in the order of the coating thickness). Figure 39 gives proof to this fact for different friction coefficients

varied from μ=0.3 to μ=0.6 (strictly speaking, this only holds for the example considered here, but especially in the practical interesting case of hard coatings on pliant materials similar results would be obtained). Figure 40 on the contrary presents the same calculation for pure normal loading, which shows a much bigger dependence on the intrinsic stresses (only compressive intrinsic stresses are considered here).

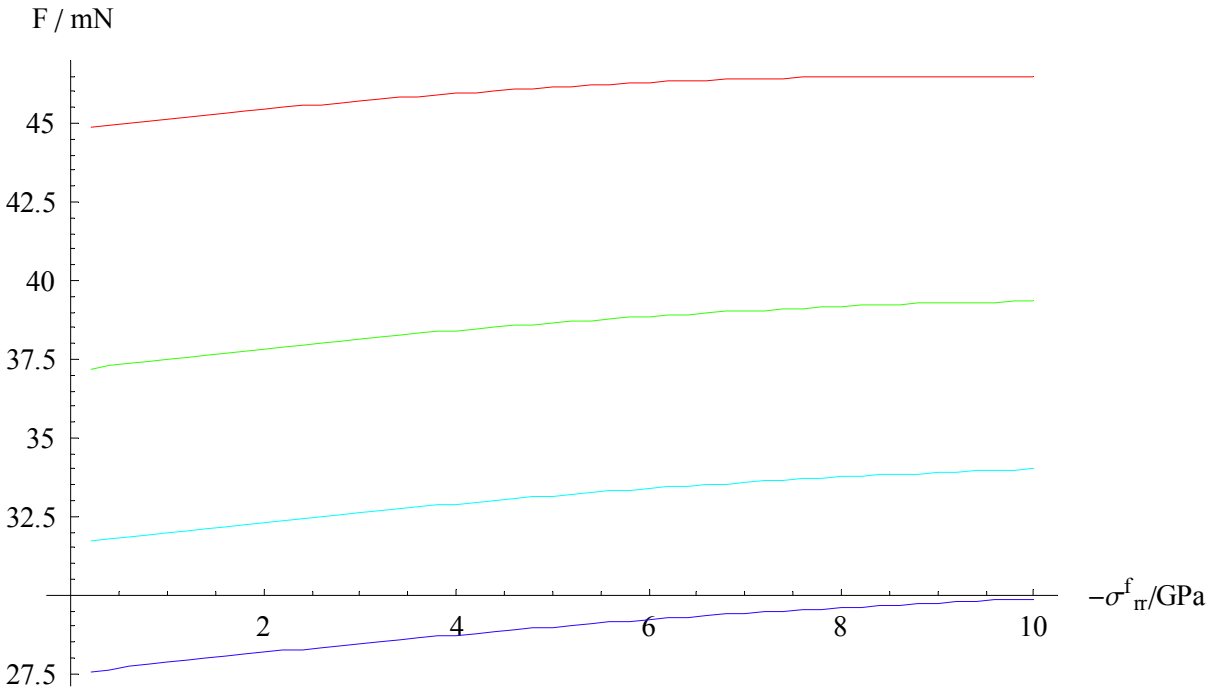

Figure 39: **The influence of compressive intrinsic stresses on the force F necessary to generate plastic deformation for the system given in Table 1 with a contact radius of 1μm and a variety of friction coefficients μ: 0.3 (red), 0.4 (green), 0.5 (light blue), 0.6 (dark blue)**

Applying now only normal loading one simply has to compare the expected value for the unstressed case with the measured one σ_M^{crit} and could evaluate σ_{rr}^f using equation (19), which can be dramatically simplified due to the fact that within the coating $f_{xx}^I = f_{yy}^I = 1$ and all other $f_{ij}^I = 0$.

$$\sigma_{rr}^f = \frac{-\sigma_{xx}^L - \sigma_{yy}^L + 2\sigma_{zz}^L \pm \sqrt{4\sigma_M^{crit\,2} - 3\left(\left(\sigma_{xx}^L - \sigma_{yy}^L\right)^2 + 3\left(\tau_{xy}^{L\,2} + \tau_{xz}^{L\,2} + \tau_{yz}^{L\,2}\right)\right)}}{2}. \qquad (21)$$

The calculation can be repeated for other examples and one finds that the geometrical conditions of a contact radius close to the coating thickness and a relatively big tangential force component (friction coefficient: μ≥0.5) are necessary to get the critical values of the v. Mises stress sufficiently independent from the σ_{rr}^f - value. But even for smaller μ the method

is at least theoretically still applicable because of the principle non linear dependency of the two measurements “pure normal” and “mixed” on the value of σ_{rr}^{f}.

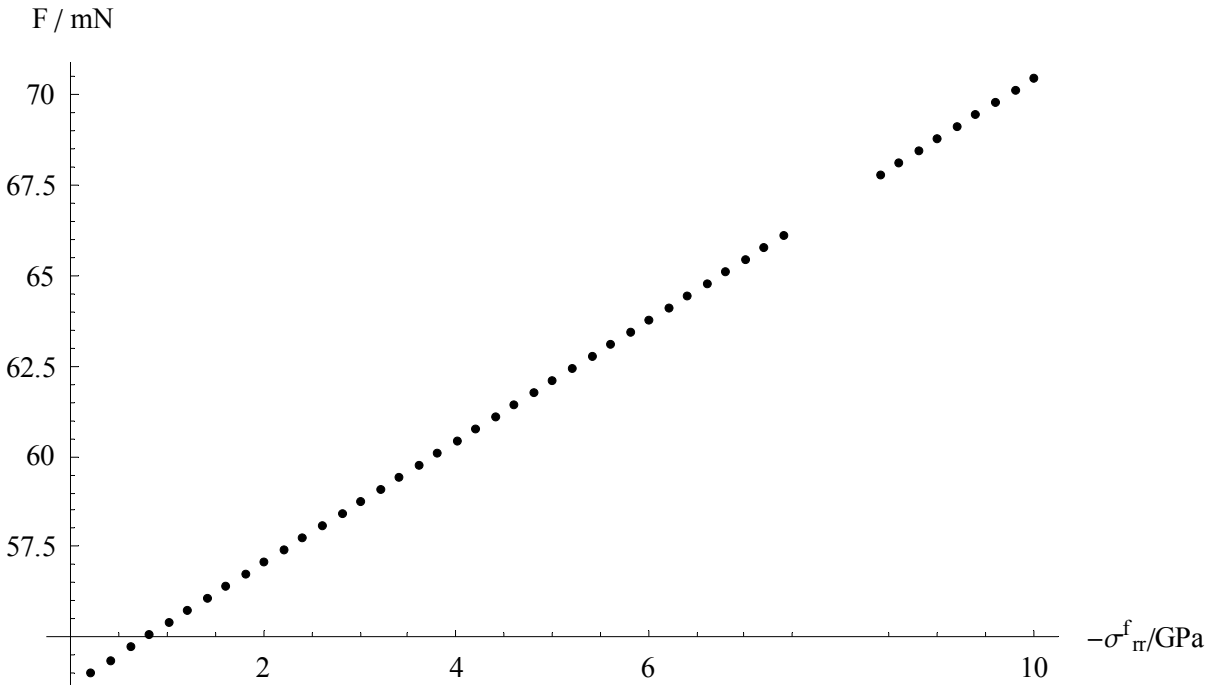

Figure 40: **The influence of compressive intrinsic stresses on the force F necessary to generate plastic deformation for the system given in Table 1 with a contact radius of 1µm under pure normal loading**

The two measurements provide us with two linear independent results of the two interesting parameters σ_{rr}^{f} and $\sigma_{M}^{crit}\left(\sigma_{rr}^{f}=0\right)$ and principally gives a system of two equations we can solve:

$$\sigma_{rr}^{f}=\frac{-\sigma_{xx}^{m}-\sigma_{yy}^{m}+2\sigma_{zz}^{m}\pm\sqrt{4\sigma_{M}^{crit\,2}-3\left(\left(\sigma_{xx}^{m}-\sigma_{yy}^{m}\right)^{2}+3\left(\tau_{xy}^{m\,2}+\tau_{xz}^{m\,2}+\tau_{yz}^{m\,2}\right)\right)}}{2}, \tag{22}$$

$$\sigma_{rr}^{f}=\frac{-\sigma_{xx}^{pn}-\sigma_{yy}^{pn}+2\sigma_{zz}^{pn}\pm\sqrt{4\sigma_{M}^{crit\,2}-3\left(\left(\sigma_{xx}^{pn}-\sigma_{yy}^{pn}\right)^{2}+3\left(\tau_{xy}^{pn2}+\tau_{xz}^{pn2}+\tau_{yz}^{pn2}\right)\right)}}{2}, \tag{23}$$

where the $\sigma_{ij}^{m}=\sigma_{ij}^{n}+\sigma_{ij}^{t}$ and the σ_{ij}^{pn} are giving the components of the mixed and the pure normal loading, respectively at the maximum point of the v. Mises stress, which has exactly the value σ_{M}^{crit}. The solution is given in the appendix. Thus, theoretically using mixed loading with two different portions of the tangential load offers the opportunity to determine the critical v. Mises stress of the unstressed state and the residual stress due to two indenter

measurements. It only depends on the accuracy of the measurement whether also lower μ (small differences of the tangential loadings) provide a sufficient linear independence of the two equations. The critical value to measure is the difference of the force at the point of beginning plastic flow for a mixed load case and a μ=0-case.

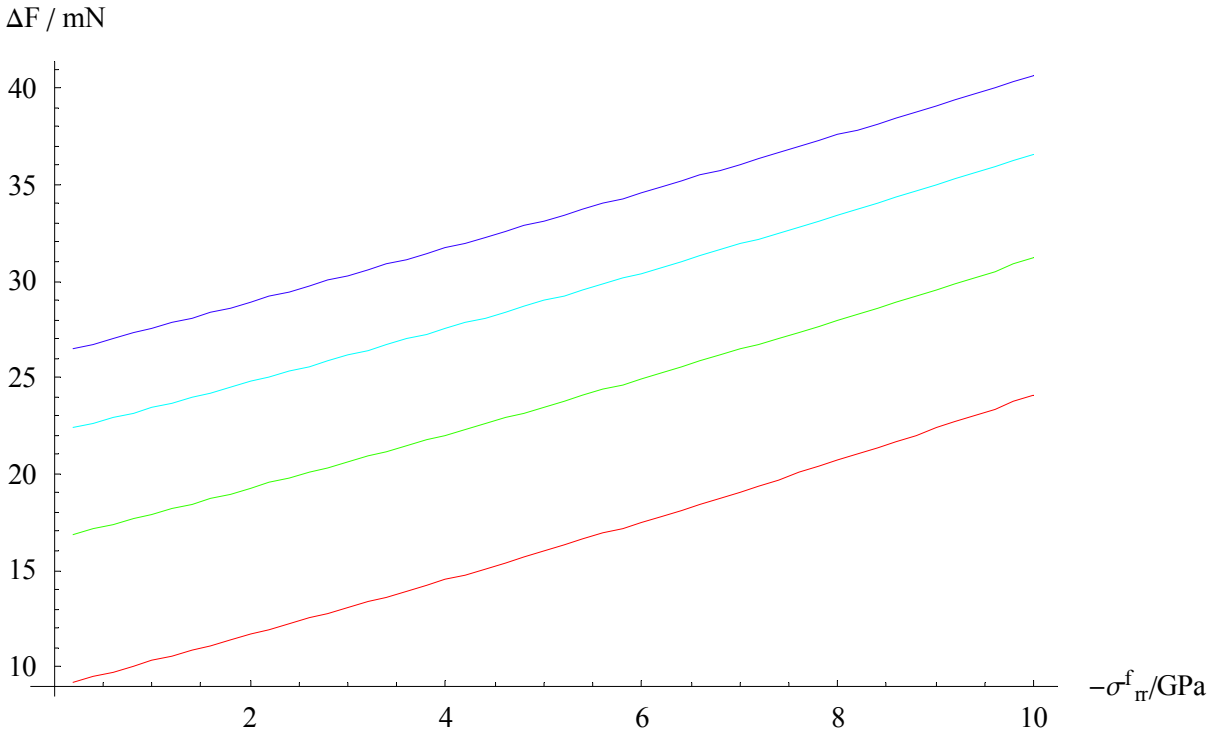

Figure 41: **Difference between the critical force values necessary to generate plastic deformation for the case of pure normal loading and mixed loading with friction coefficients μ: 0.3 (red), 0.4 (green), 0.5 (light blue), 0.6 (dark blue)**

Figure 41 shows this force-difference for our example compound given in Table 1. Now we need to estimate the error influence of the important parameter a (contact radius) on the measurement. Using our example compound we repeat the calculation of Figure 41 for different a, namely a variation of $a = 1 \pm 0.1$. In order not to overload the figure, we only consider the case μ=0.6. From Figure 42 we see, that a variation of 10% of the contact radius does not yield a deviation of the finally calculated σ_{rr}^{f} bigger than 10%-20% only in those cases where the intrinsic stress is very high ($\left|\sigma_{rr}^{f}\right| > 8GPa$). To reach the same resulting error for much smaller amounts of intrinsic stresses $\sigma_{rr}^{f} \approx -1GPa$, the contact radius must be determined with an accuracy of almost 1% (!).

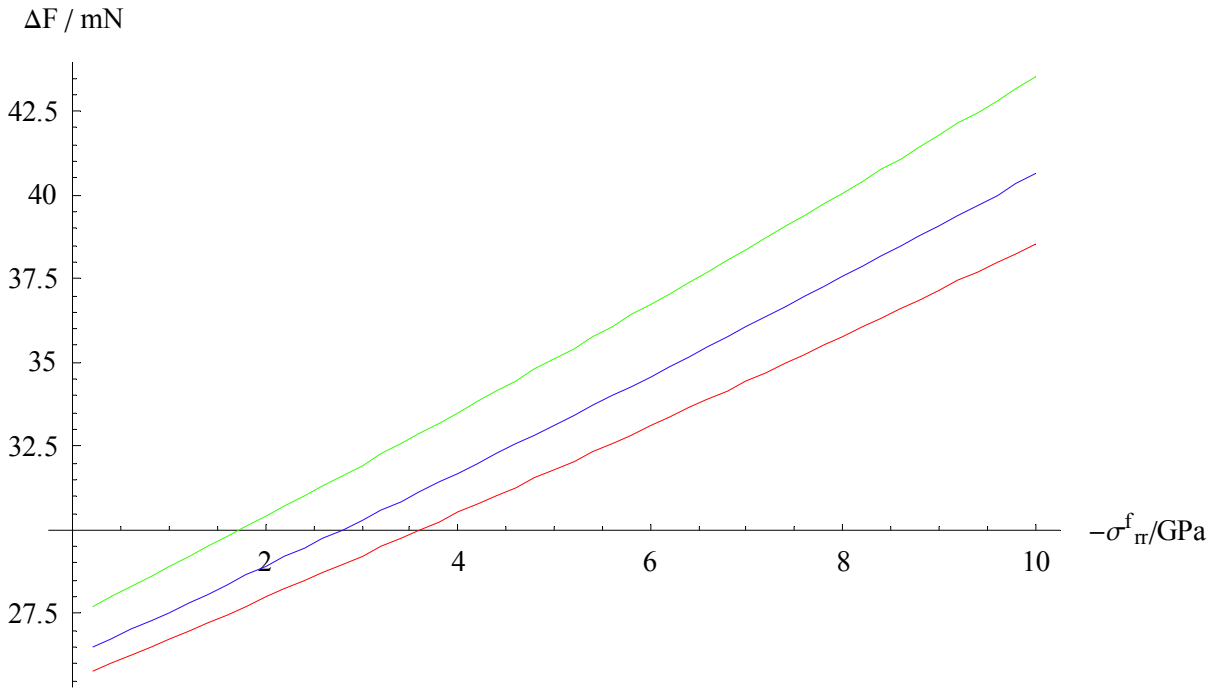

Figure 42: **Influence of the contact radius a on the difference of the critical force (see Figure 41) for a friction coefficient μ=0.6. Three different a are considered: a=0.9μm (red), a=1μm (blue), a=1.1μm (green)**

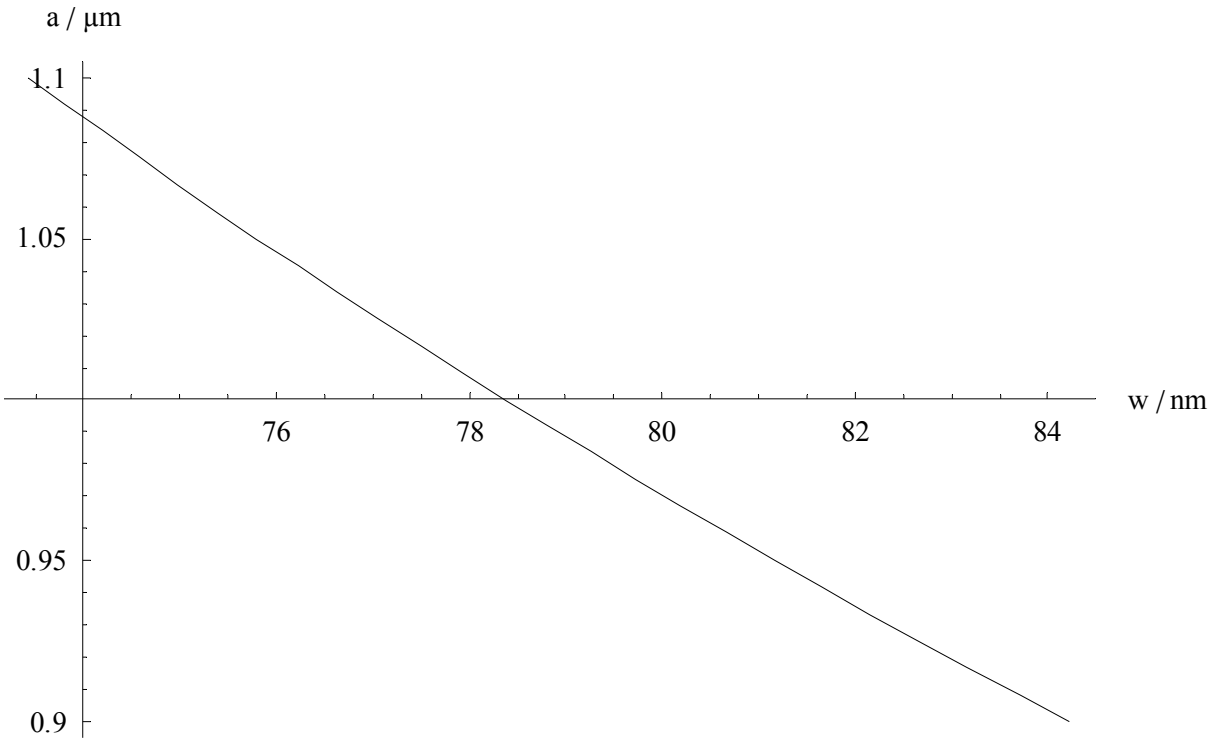

Figure 43: **Dependency of the contact radius a on the measured displacement w of the compound at the contact center for a force of F=30mN.**

On the other side the contact radius is determined by a transcendental equation (see [C2] appendix B) and depends strongly on the displacement w of the compound. Figure 43 presents this dependency between w and a, for the "worst case" of smallest critical loads being potentially possible in our example. Here we approximately have a linear dependency meaning that 1% error in the measurement of w would result in 1% error of a. Taking our example the measurement of displacement must reach an accuracy of about 1nm if one wants to detect small intrinsic stresses around 1GPa.

Even though the whole evaluation must be considered as strongly idealized[4] the values in Figure 41 and Figure 42 allow the statement, that it should be possible to realize the experimental method described above for at least relatively high amounts of intrinsic stresses of $\left|\sigma_{rr}^{f}\right| > 5GPa$ with a sufficient accuracy of the resulting values for σ_{rr}^{f} and σ_{M}^{crit}.

4. Conclusions

4.1. Linear elastic coating design - Conclusions

From the results of section 3.1 one may conclude that a gradual transition of the Young's modulus from the substrate values to that one of the hard protective coating may protect the resulting compound from plastic deformation and the so called "star cracks" in the substrate and interface area. To avoid film cracking due to tensile stresses on the surface, a final top layer with a somewhat lower Young's modulus should be added. However, it was shown that there exists neither an "optimal" coating structure which would fit all substrates and load conditions nor a simple "universal formula" to obtain it. Such an "optimal" coating structure can only be given for a specific substrate material and a distinct set of load ranges.

This means that during the search for the best possible coating design, the application has to be analysed first in order to find the typical and critical load conditions for which the coating substrate system should be designed. In this analysis part again the approaches presented in this work can be applied. So would it be sufficient to know the typical geometrical and material properties of the counterparts forming the relevant mechanical contacts and one could evaluate the complete elastic fields for any given load as long as no inelastic behaviour

[4] In the experimental situation it will be difficult to provide the variety of different spherical indenters with well defined radii of curvature necessary to realize the geometrical conditions making the effect of different influence of the intrinsic stresses on the critical force for the case of pure normal and mixed loading sufficiently visible.

does occur. Admittedly, for quite a lot of practical applications the knowledge of physical meaningful parameters like Young's modulus, anisotropy, surface topography, critical v. Mises, tensile and shear stresses or even the overall acting forces is insufficient and thus extensive measurements would be necessary first.

In a second step an "optimal" coating may be calculated utilising a fast calculation multilayer model (e.g. circular Hertzian load). This procedure can either be performed "by hand" meaning a virtual trial and error modelling is applied which leads the seeker to a successively better coating structure or the whole process is embedded into a completely automated multi-dimensional "sensitivity analysis". The latter comes in handy in all cases where the numbers of fitable parameters is higher than 2 and it is unavoidable for more than 4 different parameters or more than 2 failure mechanisms the coating has to be optimised for. For example: We only want to avoid plastic deformation within the substrate and take the thickness of the single-layer coating as the only adjustable parameter. This optimisation can easily be performed "by hand". But as soon as we are going to have 3 possible layers and must take into account also critical tensile and critical shear stresses potentially causing mode I and mode II or III fracture we would have ***at least*** 6 parameters to fit (Young's modulus and thickness for each of the three layers) and check against 4 potential failure mechanisms from which we do not yet know where they could occur. Thus, we would definitively need technical assistance in order to solve this multi-parameter optimisation problem.

Finally, the "optimal" structure should be investigated theoretically under a wider range of contact conditions (e.g. elliptical Hertzian load or superposed load dots as described in the section 3.2.) to find weak points of the structure before expensive experimental testing should be started.

Meanwhile, first results have been published [41-43] presenting an application of the modelling method on the concrete example of BCN-coating-systems.

4.2. Superposition of Hertzian loads - Conclusions

Superposition of potential fields for load problems with completely known solutions for the homogeneous and the layered half space have been shown to be a tool of great variety in order to model contact problems in an approximated manner. In section 3.2 linear, rectangular and circular contact regions have been investigated. In comparison with finite element methods where the whole body has to be built up of elements only the contact area has to be separated into an array of sufficiently dense load dots. This does not only simplify the process of constructing the model (pre-processing) but shortens in addition the evaluation time – especially in cases of layered materials. In addition the method allows inverse solutions for

any of the involved parameters. Except for the determination of the load distribution for a given normal displacement this has not been specifically treated in this paper. But the existence of this possibility is evident from the structure of the final solution of any load problem, because this consists only of completely analytical terms containing elementary functions. This structure however principally allows the application of simple optimisation procedures in order to find a solution for any parameter in question.

In this work we have only treated non-overlapping load regions, which automatically yields distinct areas completely free of load even within the assumed overall or global contact region. As a figurative understanding one could assume to have especially rough indenters forming this kind of multi contact but it should be pointed out here that, from the theoretical point of view, in general the method is of course not restricted to that kind of arrangements of load dots. So, applying overlapping arrays of Hertzian load dots one could easily come to completely filled global contact areas.

Concerning the problem of theoretically sharp contact edges or tips one even has the opportunity to mix different fundamental solutions. So could for example a clever arrangement of Hertzian and Cone dots simulate the effect of mathematically sharp Vickers, Berkowich or Knoop indenters.

Because of its flexibility and its ability concerning the built up of fast running calculation procedures the method could be valuable for the analysis of experimental data of indentation experiments for arbitrarily shaped indenters and – with some restrictions – even for rough sample surfaces.

4.3. Measurement of intrinsic stresses - Conclusions

As the considerations of section 3.3.2. have shown in principle it should be possible to measure the intrinsic film-stress using nano-indentation with “pure normal” and mixed loading. However, the demands for accuracy for intrinsic stresses below 5GPa are relatively high. In addition the method requires a great variety of well-defined spherical indenters and of course normal and tangential measurement of force and displacement. Such a highly sophisticated device is not available yet but if it will be, the method proposed here could be a practically very important application.

4.4. Outlook

Concerning industrial demands, the value of this research can only be as high as useful it is for practical applications. Thus, the author sees its first task in making the approaches

presented in this work available as easy to use and understandable tools. This can be achieved in two ways of which the author plans to follow both within the next two years.

At first the methods presented should be applied on practical cases and this way being explained and their potential being demonstrated. This mainly means paperwork where the following concrete projects are planned respectively have been already realized:

1. Experimental proof to the gradient coating approach by comparing the experimental and the theoretically evaluated load depth curve of a BCN gradient coating,
2. Contributions to the problem of arbitrarily curved interfaces,
3. Experimental proof to the problem of arbitrarily curved interfaces by comparing the experimental and the theoretically evaluated load depth curve of suitable simple examples like an inclined interface,
4. Investigation of a variety of complex contact problems with e.g. funny indenter shapes or complicated friction conditions using the BEM,
5. Investigation of contact problems on rough surfaces using the BEM.

Secondly, all mathematical procedures, models and tools will be made available as additional software packages (modules) of the program ELASTICA or derivatives of it. The following work program for the software built up (ELASTICA extensions) has been scheduled so far (MP means: programmed, but so far only available as Mathematica package):

ELASTICA-Module	**Chapter/Reference**
Load dot module (BEM)	3.2.
Intrinsic stress module	2.2.
Gradient coatings module	2.1.1.2.
Stone approach module for very thin coatings	[4] and MP
Module for impact calculation on layered materials	MP
Module for a general normal displacement	in parts as MP
Automated optimisation module	in parts as MP

In addition to this the author wishes to extend some of his approaches in contact mechanics to the case of the quarter and the eight space in order to investigate contact problems in the vicinity of edges and corners.

References:

[1] Marc Horsten (DAF Trucks N.V.): "WR/LF coatings in automotive applications", NIMR Technology roadmap workshop, Nijenrode University, 6-7 June 2002

[2] M. F. Doerner and W. D. Nix, J. Mater. Res., Vol 1 (1986) No. 4, 601-609

[3] P. K. Gupta and J. A. Walowit, ASME J. of Lubrication Technology, April 1974, 250-257

[4] D. S. Stone, J. Mater. Res., Vol. 13, No. 11, November 1998, 3207 - 3213

[5] H. Gao, Ch.-H. Chiu and J. Lee, Int. J. Solids Structures, Vol. 29 (1992) No. 20, 2471-2492

[6] H. Gao and T.-W. Wu, J. Mater. Res., Vol. 8, No. 12 (1993), 3229-3232

[7] G. Ia. Popov, Prikladnaia Mathematika i Mechanika, Vol. 37 (1973), 1109-1116

[8] V. I. Fabrikant, "Application of potential theory in mechanics: A Selection of New Results", Kluver Academic Publishers (1989), The Netherlands

[9] N. A. Rostovtsev, Prikladnaia Mathematika i Mechanika, Vol. 25 (1961), 164-168

[10] A. C. Fischer-Cripps, B. R. Lawn, A. Pajares, L. Wie, J. Am. Ceram. Soc. 79 [10] (1996), 2619-25

[11] T. A. Laursen and J. C. Simo, J. Mater. Res. Vol. 7, No. 3, March 1992, 618 - 626

[12] K. W. Man, "Contact mechanics using boundary elements. Computational Mechanics" Publications, Southhampton (1994), Hants.

[13] V. I. Fabrikant, ASME J. of Appl. Mech., Vol. 55 (1988) 604-610

[14] V. I. Fabrikant, ASME J. of Appl. Mech., Vol. 57 (1990) 596-599

[15] M. T. Hanson, ASME J. of Appl. Mechnics, Vol. 59 (1992) 123-130

[16] M. T. Hanson, ASME J. of Tribology, Vol. 114 (1992) 606-611

[17] M. T. Hanson, ASME J. of Appl. Mechnics, Vol. 60 (1993) 557-559

[18] M. T. Hanson, Int. J. Solids Structures, Vol. 31, No. 4 (1994) 567 - 586

[19] M. T. Hanson and Y. Wang, Int. J. Solids Structures, Vol. 34, No. 11 (1997) 1379 - 1418

[20] M. T. Hanson and I. W. Puja, J. of Appl. Mech., Vol. 64 (1997), 457 – 465

[21] T. Chudoba and N. Schwarzer: ELASTICA, software demonstration package, available in the internet at: http://www.asmec.de

[22] T. Chudoba, N. Schwarzer, F. Richter: "New Possibilities of Mechanical Surface Characterization with Spherical Indenters by Comparison of Experimental and Theoretical Results", San Diego Conference ICMCTF 1999, Metallurgical Coatings

and Thin Films Vol. II, Elsevier, pp. 284-289 and Thin Solid Films 355-356 (1999), 284-289

[23] T. Chudoba, N. Schwarzer, F. Richter: "Determination of Elastic Properties of Thin Films by Indentation Measurements with a Spherical Indenter", J. of Surface & Coatings Technology 127 (2000) 9-17

[24] N. Schwarzer: "Coating Design due to Analytical Modelling of Mechanical Contact Problems on Multilayer Systems", proceedings of the ICMCTF 2000, San Diego, USA, April 2000, 397 - 402, in addition: Surface and Coatings Technology 133 –134 (2000) 397 - 402

[25] T. Chdoba, N. Schwarzer, F. Richter, U. Beck: "Determination of mechanical film properties of a bilayer system due to elastic indentation measurements with a spherical indenter", proceedings of the ICMCTF 2000, San Diego, USA, April 2000, 366 – 372, in addition: Thin Solid Films 377 – 378 (2000) 366 - 372

[26] N. Schwarzer, D. Heuer, Th. Chudoba: ”Application of modern approaches in mechanics to adhesion problems in dentistry”, proceedings of the EURADH 2000, Lyon, France, September 2000, Edition SFV, 19 rue du Renard, 75004 Paris, 377-382

[27] N. Schwarzer, F. Richter: ”Adhesion Modelling in Layered Materials Using Analytical Solutions of Crack Problems”, proceedings of the EURADH 2000, Lyon, France, September 2000, Edition SFV, 19 rue du Renard, 75004 Paris, 586-591

[28] F. Richter, T. Chudoba, N. Schwarzer, G. Hecht: “Neue Möglichkeiten zur Charakterisierung dünner Schichten mit Indentermethoden - Novel Possibilities for Thin Film Characterisation Using Indentation Methods”, Materialwissenschaften und Werkstofftechnik 32 (2001) 621-627

[29] O. Wändstrand, N. Schwarzer, T. Chudoba, Å. Kassman-Rudiphi: ”Load-carrying capacitity of Ni-plated media in spherical indentation: experimental and theoretical results”, Surface Engineering Vol. 18 (2002) No. 2, 98 - 104

[30] T. Chudoba, N. Schwarzer, F. Richter: ”Steps towards a mechanical modeling of layered systems”, Surface and Coatings Technology 154 (2002) 140 - 151

[31] INDICOAT (1999): “Determination of hardness and modulus of thin films and coatings by nanoindentation”, final report (European community, project no. SMT4-CT98-2249), May 2001, ISSN 1473-2734

[32] see, for instance, C. Spaeth, M. Kuehn, T. Chudoba, F. Richter: „Mechanical properties of carbon nitride thin films prepared by ion beam assisted filtered cathodic vacuum arc deposition”, Surf. Coat. Techn. 112 (1999)140-145

[33] Anne Hoger: “The elasticità tensor of a residually stressed material”, J. of Elasticity 31 (1993), 219-237

[34] E. Suhir, J. Appl. Mech., 55 (1988) 143

[35] G. G. Stoney, Proc. Royal Soc. London, A82 (1909) 172.

[36] M. Elwenspoek and H. V. Jansen: "Silicon Micro Machining", Cambridge University Press, 1998

[37] see, for instance, M. Ohring: “The Materials Science of Thin Films”, Academic Press, San Diego, CA, 1992, pp. 413.

[38] B. S. Berry, in D. Gupta and P. S. Ho (eds.) Diffusion Phenomena in Thin Films and Microelectronic Materials, Noyes, Park Ridge, 1988, pp. 73.

[39] see, for instance, H. Ljungcrantz, L. Hultman, J.-E. Sundgren, S. Johansson, N. Kristensen, J.-A. Schweitz, C. J. Shute, J. Vac. Sci. Technol. A 11(3) May/Jun. 1993, pp. 543 or B. S. Berry and W. C. Pritchet, J. Appl. Phys. 67(8), 15 April 1990, pp. 3661.

[40] N. Schwarzer, F. Richter: Short note: On the determination of film stress from substrate bending using Stoney´s formula, Thin Solid Films, submitted January 2002

[41] F. Richter, N. Schwarzer, V. Linss, I. Hermann, T. Chudoba: “Depth-depending Young´s modulus of thin films for increased load carrying capacity”, oral presentation at the ICMCTF 2002, San Diego, USA, April/Mai 2002

[42] I. Hermann, T. Chudoba, V. Linss, N. Schwarzer, F. Richter: „Improving the load carrying capacity of a layered system due to the design of a film stack with an optimized modulus variation”, poster presentation at the ICMCTF 2002, San Diego, USA, April/Mai 2002

[43] V. Linss, N. Schwarzer, I. Hermann, U. Kreissig, F. Richter: “The B-C-N triangle - a suitable system for the production of thin films with high load carrying capacity”, proceedings of the ICMCTF 2002, San Diego, USA, April/Mai 2002

[44] B. Taljat, G. M. Pharr: “Thin Films: Stresses and Mechanical Properties VIII”, edited by R. Vinci, O. Kraft, N. Moody, E. Shaffer II (Mater. Res. Soc. Symp. Proc. 594, Warrendale, PA 2000), p. 519

[45] J. G. Swadener, B. Taljat, G. M. Pharr: „Measurement of residual stress by load and depth sensing indentation with spherical indenters”, J. of mat. Research, accepted

[46] A. Faulkner, K.C. Tang, N. Schwarzer, R.D. Arnell, F. Richter: "Comparison between an Elastic-Perfectly Plastic FE Model and a Purely Elastic Analytical Model for a Spherical Indenter on a Layered Substrate", Thin Solid Films 300 (1997) 177

[47] N. Schwarzer: „About the theory of thin coated plates", published in the internet at: http://archiv.tu-chemnitz.de/pub/2002/0006/index.html

[48] P. Heuer, N. Schwarzer, T. Chudoba: „Avoiding of plastic deformation – an ELASTICA presentation", published in the internet at: www.tu-chemnitz.de/physik/PHFK/abstracts/mechanic

[49] N. Schwarzer: "Arbitrary load distribution on inhomogeneous isotropic half spaces", Int. J. of Solids and Structures, submitted February 2002

[50] N. Schwarzer: "Justification for the use of the Hertzian load model on layered materials", J. of Surface & Coatings Technology, submitted October 2002

References available as reprints:

[C1] N. Schwarzer: "Arbitrary load distribution on a layered half space", ASME Journal of Tribology, Vol. 122, No. 4, October 2000, 672 - 681

[C2] N. Schwarzer, F. Richter, G. Hecht: "Elastic Field in a Coated Half Space under Hertzian pressure distribution", J. of Surface & Coatings Technology 114 (1999) 292-304

[C3] N. Schwarzer, Th. Chudoba, D. Billep, F. Richter: "Investigation of coating substrate compounds using inclined spherical indentation", J. of Surface & Coatings Technology 116 – 119 (1999) 244-252

Appendix of part I

The following two formulae give the solution for the system of equations (22) and (23):

$$\sigma_M^{crit} = \sqrt{\frac{1}{16}\left(\begin{array}{l} 7\sigma_{xx}^{m\,2} - 10\sigma_{xx}^{m}\sigma_{yy}^{m} + 7\sigma_{yy}^{m\,2} - 4\left(\sigma_{xx}^{m} + \sigma_{yy}^{m} - \sigma_{zz}^{m}\right)\sigma_{zz}^{m} - 2\left(\sigma_{xx}^{m} + \sigma_{yy}^{m} - 2\sigma_{zz}^{m}\right)\sigma_{xx}^{pn} \\ +7\sigma_{xx}^{pn\,2} - 2\left(\sigma_{xx}^{m} + \sigma_{yy}^{m} - 2\sigma_{zz}^{m}\right)\sigma_{yy}^{pn} - 10\sigma_{xx}^{pn}\sigma_{yy}^{pn} + 7\sigma_{yy}^{pn\,2} \\ +24\left(\sigma_{xy}^{m\,2} + \sigma_{xz}^{m\,2} + \sigma_{yz}^{m\,2} + \sigma_{xy}^{pn\,2} + \sigma_{xz}^{pn\,2} + \sigma_{yz}^{pn\,2}\right) \\ +4\left(\sigma_{xx}^{m} + \sigma_{yy}^{m} - 2\sigma_{zz}^{m} - \sigma_{xx}^{pn} - \sigma_{yy}^{pn}\right)\sigma_{zz}^{pn} + 4\sigma_{zz}^{pn\,2} \\ +\dfrac{9\left(4\left(\sigma_{xy}^{m\,2} + \sigma_{xz}^{m\,2} + \sigma_{yz}^{m\,2} - \sigma_{xy}^{pn\,2} - \sigma_{xz}^{pn\,2} - \sigma_{yz}^{pn\,2}\right) + \left(\sigma_{xx}^{m} - \sigma_{yy}^{m}\right)^2 - \left(\sigma_{xx}^{pn} - \sigma_{yy}^{pn}\right)^2\right)^2}{\left(\sigma_{xx}^{m} + \sigma_{yy}^{m} - 2\sigma_{zz}^{m} - \sigma_{xx}^{pn} - \sigma_{yy}^{pn} + 2\sigma_{zz}^{pn}\right)^2} \end{array}\right)}$$

$$\sigma_{rr}^{f} = \frac{\left(\begin{array}{l} \sigma_{xx}^{m}\left(\sigma_{yy}^{m}+\sigma_{zz}^{m}\right)+\sigma_{yy}^{m}\sigma_{zz}^{m}-{\sigma_{xx}^{m}}^{2}-{\sigma_{yy}^{m}}^{2}-{\sigma_{zz}^{m}}^{2}-3\left({\sigma_{xy}^{m}}^{2}+{\sigma_{xz}^{m}}^{2}+{\sigma_{yz}^{m}}^{2}\right) \\ +{\sigma_{xx}^{pn}}^{2}+{\sigma_{yy}^{pn}}^{2}-\sigma_{yy}^{pn}\sigma_{xx}^{pn}+3\left({\sigma_{xy}^{pn}}^{2}+{\sigma_{xz}^{pn}}^{2}+{\sigma_{yz}^{pn}}^{2}\right)-\left(\sigma_{yy}^{pn}+\sigma_{xx}^{pn}\right)\sigma_{zz}^{pn}+{\sigma_{zz}^{pn}}^{2} \end{array} \right)}{\sigma_{xx}^{m}+\sigma_{yy}^{m}-2\sigma_{zz}^{m}-\sigma_{xx}^{pn}-\sigma_{yy}^{pn}+2\sigma_{zz}^{pn}}$$

Part II

Reprints